NASA Contractor Report 165759

Development of an Orthotropic Hole Element

C. V. Smith; J. W. Markham;
J. W. Kelley; and K. Kathiresan

LOCKHEED-GEORGIA COMPANY
MARIETTA, GA 30063

CONTRACT NAS1-15840
AUGUST 1981

National Aeronautics and
Space Administration

Langley Research Center
Hampton, Virginia 23665

TABLE OF CONTENTS

TABLE OF CONTENTS (Continued)

TABLE OF CONTENTS (Concluded)

LIST OF FIGURES

LIST OF FIGURES (Concluded)

SYMBOLS

$\{a\}$	stress coefficients for the virtual stress state
n_x, n_y	x and y components of unit outer normal on the boundary
$\{\bar{q}\}$	specified generalized displacements on S_u boundary
r	polar coordinate
s	arc length
t	thickness of the finite element
x, y	cartesian coordinates
A	area of the hole element
$A_n(r)$, $B_n(r)$	radial functions in the assumed stress state
$[C]$	array of material coefficients
$[C_{xy}]$, $[C_{r\theta}]$	material coefficients in cartesian and polar coordinates, respectively
E_x, E_y	modulus of elasticity in x and y directions, respectively
F	number of degrees of freedom on S_u
G_{xy}	shear modulus
$[G]$	boundary work array
$[H]$	volume work array
$[K]$	stiffness matrix
$[KQ]$	stiffness matrix for quadrant element
$[KH]$	stiffness matrix for half element
$[KT]$	stiffness matrix for total element

SYMBOLS (Cont'd)

L	one half of the side length of the square element
N	number of stress coefficients in the assumed stress state
R	radius of the circular hole
S_τ	boundary with specified tractions
S_u	boundary with specified displacements
T_x^n, T_y^n	tractions in the x and y directions, respectively
$\{\beta\}$	stress coefficients for the real stress state
γ_{xy}, $\gamma_{r\theta}$	shear strain in cartesian and polar coordinates, respectively
ϵ_x, ϵ_y	linear strain in cartesian coordinates
ϵ_r, ϵ_θ	linear strain in polar coordinates
$[\zeta(x, y)]$	assumed displacement distribution on S_u
θ	polar coordinate
ν_{xy}, ν_{yx}	Poisson's ratios
ρ	nondimensional radial coordinates, normalized with respect to hole radius R
τ_x, τ_y, τ_{xy}	stress components in cartesian coordinates
τ_r, τ_θ, $\tau_{r\theta}$	stress components in polar coordinates
ϕ	stress function
$[\Lambda(x, y)]$	assumed stress distribution
$[\mathcal{T}(x, y)]$	traction distribution on S_u for the virtual stress state

DEVELOPMENT OF AN ORTHOTROPIC HOLE ELEMENT

by

C. V. Smith*
J. W. Markham
J. W. Kelley
K. Kathiresan

SUMMARY

The objective of this contract was to develop and implement a finite element which adequately represents the state of stress in the region around a circular hole in orthotropic material experiencing reasonably general loading. This has been achieved through a complementary virtual work formulation of the stiffness and stress matrices for a square element with center circular hole, with implementation in the NASTRAN computer program. This report discusses the theoretical foundations of the development, describes the use of NASTRAN to obtain solutions, and presents sample problem results to demonstrate the performance of the hole element.

*Consultant, Associate Professor, School of Aerospace Engineering, Georgia Institute of Technology. This report carries no endorsement by Georgia Institute of Technology.

INTRODUCTION

In present flight vehicle structures, and for some time into the future, mechanical fastening is expected to be the most used joining methed, so that connection details contain many circular holes. These connections are subjected to very general external loadings, with the additional complications of load transfer through fasteners in the holes and increasing use of nonisotropic material in the connection. The resulting local stress state in the neighborhood of each hole is very complex, with stress levels and gradients higher than those found in most regions away from the holes. Despite these complexities, the high stresses require that an accurate evaluation of the local stresses around each hole be obtained to achieve an adequate estimate of performance of the joint, as measured by fatigue and fracture mechanics analyses. As usual, the analyst is in the unenviable position of needing the best results in the regions of greatest complexity.

One method to determine the stresses, through analytical solutions, would appear to give those desired results; but this procedure can be discarded for all practical purposes. The list of available solutions is not adequate, and there is little hope that the list can ever be expanded to include all possibilities of interest.

The finite element method is a very effective way to treat problems with complex geometry, material, and loading, but the use of conventional finite elements is not efficient in applications involving fastener holes. Because of the complexity of the stress state and the high stress gradients, an excessive number of elements must be used in the neighborhood of each hole. This increases the cost of even one solution for a specified geometry and loading, and makes it very expensive to perform the multiple solutions with varying geometry and loading which are normally required in design.

What is required is an efficient special purpose finite element which provides a sufficiently accurate representation of local stresses without the need for many

conventional elements. This has previously been done for isotropic material ([8], [9], [10]*), and this report presents the extension to orthotropic material. Complementary virtual work concepts are used to develop the stiffness and stress matrices for a square element with a center circular hole. The report presents the necessary theoretical background for the development and then presents sample problem results obtained through implementation into the NASTRAN computer program.

* Numbers in brackets denote reference numbers.

SECTION 1

THEORETICAL BASIS FOR DERIVATION OF THE STIFFNESS MATRIX

1.1 STATEMENT OF THE PROBLEM

The finite element is considered to be a thin plate in a state of plane stress with displacements on the external boundary specified so as to insure displacement continuity with adjacent finite elements (see Figure 1). Conditions on the inner boundary will be specified in a later section.

The variables of primary interest are the stresses because these quantities are needed for studies in fatigue and fracture. Therefore, it was decided to seek a solution to the problem through a complementary work formulation which gives the desired stresses directly with no need for differentiations of displacements with subsequent loss of accuracy.

1.2 STATEMENT OF THE PRINCIPLE OF COMPLEMENTARY VIRTUAL WORK

The complementary virtual work (CVW) can be expressed as follows:

$$CVW = t\int_A \lfloor \delta\tau \rfloor \{\epsilon\}\, dA - t\int_A \lfloor \delta F \rfloor \{u\}\, dA - t\int_{S_u} \lfloor \delta T \rfloor \{\bar{u}\}\, ds - t\int_{S_\tau} \lfloor \delta T \rfloor \{u\}\, ds \qquad (1)$$

where t = thickness of hole element, assumed constant

A = area of hole element

S_u = that portion of the boundary over which displacements are specified, consisting of the outer boundary plus portions of the inner boundary as appropriate

S_τ = that portion of the boundary over which tractions are specified, consisting of portions of the inner boundary as appropriate

$\{\epsilon\} = \lfloor \epsilon_x \ \epsilon_y \ \gamma_{xy} \rfloor^T$ = column of strains in the real state

$\{u\} = \lfloor u_x \ u_y \rfloor^T$ = column of displacements in the real state

$\{\bar{u}\}$ = specified displacements on the S_u boundary

$\lfloor \delta\tau \rfloor = \lfloor \delta\tau_x \ \delta\tau_y \ \delta\tau_{xy} \rfloor$ = row of stresses in the virtual state

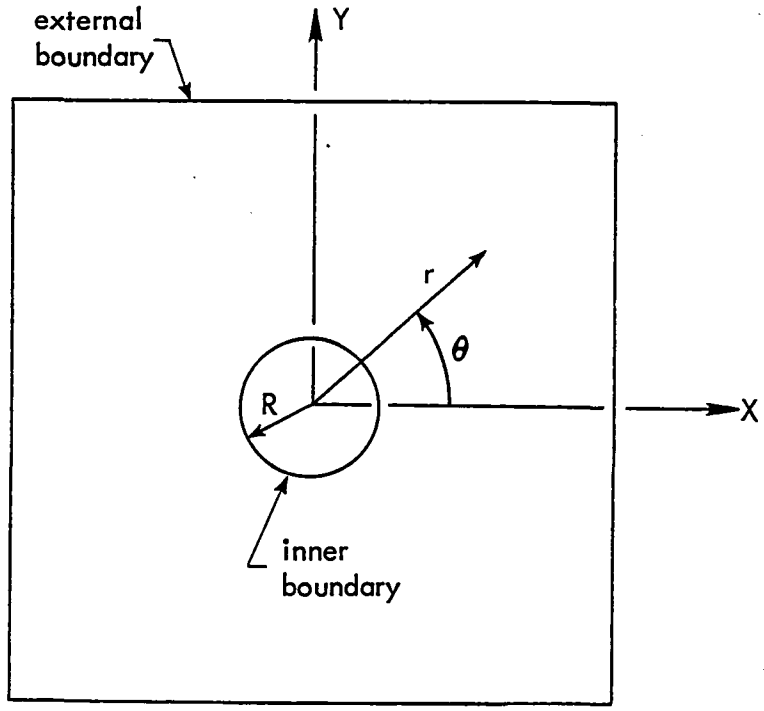

Figure 1. Finite Element

$\lfloor \delta F \rfloor = \lfloor \delta F_x \ \delta F_y \rfloor$ = row of body forces in the virtual state

$\lfloor \delta T \rfloor = \lfloor \delta \overset{n}{T}_x \ \delta \overset{n}{T}_y \rfloor$ = row of surface tractions in the virtual state, acting on element of boundary with normal $\bar{n}$.

The virtual state must satisfy the following admissibility requirements:

a) stresses and body forces satisfy the equations of equilibrium in the finite element domain:

$$\frac{\partial \delta \tau_x}{\partial x} + \frac{\partial \delta \tau_{yx}}{\partial y} + \delta F_x = 0$$

$$\frac{\partial \delta \tau_{xy}}{\partial x} + \frac{\partial \delta \tau_y}{\partial y} + \delta F_y = 0 \qquad (2)$$

$$\delta \tau_{xy} - \delta \tau_{yx} = 0$$

b) stresses and surface tractions satisfy the equations

$$\delta \overset{n}{T}_x = \delta \tau_x \ n_x + \delta \tau_{yx} \ n_y$$

$$\delta \overset{n}{T}_y = \delta \tau_{xy} \ n_x + \delta \tau_y \ n_y \qquad (3)$$

where n_x, n_y = components of unit outer normal at a point on the plate boundary.

The real state must meet the following requirements:

a) the strains and stresses are related by constitutive equations which can be written in the form

$$\{\epsilon\} = [C]\{\tau\} \qquad (4)$$

where $\{\tau\} = \lfloor \tau_x \ \tau_y \ \tau_{xy} \rfloor^T$ = column of stresses in the real state

$[C]$ = array of material coefficients

b) the stresses must satisfy equations of equilibrium in the finite element domain:

$$\frac{\partial \tau_x}{\partial x} + \frac{\partial \tau_{yx}}{\partial y} = 0$$

$$\frac{\partial \tau_{xy}}{\partial x} + \frac{\partial \tau_y}{\partial y} = 0 \qquad (5)$$

$$\tau_{xy} - \tau_{yx} = 0$$

with body forces neglected.

c) on the boundary S_τ, the stresses and the specified tractions must be related as follows:

$$\overset{n}{T}_x = \tau_x \; n_x + \tau_{yx} \, n_y$$

$$\overset{n}{T}_y = \tau_{xy} \, n_x + \tau_y \; n_y \qquad (6)$$

Note that all admissible real states can be described as stress states which satisfy equilibrium in the domain and traction boundary conditions.

The principle of complementary virtual work can be stated as follows. If a particular real state can be found for which the complementary virtual work vanishes for every admissible virtual state, then that particular real state will also satisfy compatibility requirements in the interior and displacement boundary conditions. Therefore, this particular real state satisfies all the requirements for a solution to the given problem and is, indeed, the solution.

The expression for complementary virtual work, as given in Equation (1), can be simplified by considering only those virtual states for which

$$\lfloor \delta F \rfloor = \lfloor 0 \rfloor \quad \text{in the domain}$$

and $$\lfloor \delta T \rfloor = \lfloor 0 \rfloor \quad \text{on the boundary } S_\tau .$$

These additional admissibility requirements are not necessary, but they do serve to reduce the complexity of the solution process. With these simplifications, the complementary virtual work can be calculated as follows:

$$CVW = t\int_A \lfloor \delta\tau \rfloor \{\epsilon\} dA - t\int_{S_u} \lfloor \delta T \rfloor \{\bar{u}\} ds \tag{7}$$

which is the form to be used in the derivations which follow.

For future use, note from Equation (7) that if real displacements $\{\bar{u}\}$ exist for which $\int_{S_u} \lfloor \delta T \rfloor \{\bar{u}\} ds = 0$ for every admissible $\lfloor \delta T \rfloor$, then it follows that the associated real strains $\{\epsilon\}$ must be identically zero in the domain.

1.3 USE OF COMPLEMENTARY VIRTUAL WORK IN APPROXIMATIONS

For problems with no available exact solution, the principle of complementary virtual work can be used to achieve an approximate solution. For the real state, begin with a family of admissible stresses in the form

$$\underset{3\times 1}{\{\tau(x, y)\}} = \underset{3\times 1}{\{\tau_p(x, y)\}} + \underset{3\times N}{[\Lambda(x, y)]} \underset{N\times 1}{\{\beta\}} \tag{8}$$

where $\{\tau_p\}$ denotes a stress state which satisfies the equilibrium equations (including body forces if applicable) and all nonhomogeneous boundary conditions on S_τ

$\{\beta\}$ denotes a column of N as-yet unknown coefficients

and $[\Lambda]\{\beta\}$ denotes a family of stress states which satisfy equilibrium equations with no body forces and homogeneous boundary conditions on all of S_τ.

Therefore, each column of $[\Lambda]$ represents an admissible stress state; and Equation (8) represents an admissible stress state for arbitrary values of the N coefficients $\{\beta\}$. Note that any known features of the real state stresses, such as satisfaction of symmetry conditions, can be included in the functions which constitute the elements of array $[\Lambda(x, y)]$.

The real strains are now determined by substituting into Equation (4).

$$\{\epsilon\} = [C]\{\tau_p\} + [C][\Lambda]\{\beta\} \tag{9}$$

To complete the specification of the real state, the displacements on S_u are assumed in the form

$$\underset{2\times 1}{\{\bar{u}(x, y)\}} = \underset{2\times F}{[\zeta(x, y)]}\underset{F\times 1}{\{\bar{q}\}} \tag{10}$$

where $\{\bar{q}\}$ denotes the generalized displacements on S_u; there are F degrees of freedom. Therefore, the i^{th} column of $[\zeta]$ represents boundary displacements associated with a unit value of the i^{th} degree of freedom; and by assumption, Equation (10) is a sufficiently accurate representation of the specified $\{\bar{u}\}$ on S_u.

The virtual state is specified by

$$\underset{3\times 1}{\{\delta\tau\}} = \underset{3\times N}{[\Lambda(x, y)]}\underset{N\times 1}{\{a\}} \tag{11}$$

If Equation (3) is written in the form

$$\underset{2\times 1}{\{\delta T\}} = \underset{2\times 3}{[N]}\underset{3\times 1}{\{\delta\tau\}}$$

then $$\{\delta T\} = [N][\Lambda]\{a\}$$

or $$\{\delta T\} = [T]\{a\} \tag{12}$$

Everything is now known for substitution into Equation (7) for the complementary virtual work.

$$CVW = \lfloor a \rfloor \left\{ \left\{ t\int_A [\Lambda]^T [C] \{\tau_p\} dA \right\} + \left[t\int_A [\Lambda]^T [C][\Lambda] dA \right] \{\beta\} - \left[t\int_{S_u} [\mathcal{T}]^T [\zeta] ds \right] \{\bar{q}\} \right\}$$

Define
$$\underset{N\times 1}{\{\beta_p\}} = t\int_A \underset{N\times 3}{[\Lambda]^T} \underset{3\times 3}{[C]} \underset{3\times 1}{\{\tau_p\}} dA \tag{13}$$

$$\underset{N\times N}{[H]} = t\int_A \underset{N\times 3}{[\Lambda]^T} \underset{3\times 3}{[C]} \underset{3\times N}{[\Lambda]} dA \tag{14}$$

$$\underset{N\times F}{[G]} = t\int_{S_u} \underset{N\times 2}{[\mathcal{T}]^T} \underset{2\times F}{[\zeta]} ds \tag{15}$$

Therefore, $$CVW = \lfloor a \rfloor \left\{ \{\beta_p\} + [H]\{\beta\} - [G]\{\bar{q}\} \right\} \tag{16}$$

Now, within the approximation of Equation (11), every virtual state is described by a set of values for coefficients $\{a\}$. Therefore, if the CVW is to vanish for every admissible virtual state, it follows that

$$\{\beta_p\} + [H]\{\beta\} - [G]\{\bar{q}\} = \{0\} \tag{17}$$

The values of β are determined from

$$\{\beta\} = [H]^{-1}[G]\{\bar{q}\} - [H]^{-1}\{\beta_p\} \tag{18}$$

With $\{\beta\}$ known from Equation (18), the solution for the real stress state is found from substitution into Equation (8).

Note that when the material constant matrix $[C]$ is positive definite, then in the real state

$$[\tau][C]\{\tau\} \geq 0 \text{ for every } \{\tau\} .$$

If the stress state is chosen as $\{\tau\} = [\Lambda]\{\beta\}$, then it follows that

$$[\beta][\Lambda]^T[C][\Lambda]\{\beta\} \geq 0 \text{ for every } \{\beta\} .$$

Therefore, the integrand in Equation (14) is positive definite, which means that the array $[H]$ is positive definite. This guarantees the existence of $[H]^{-1}$, so that the solution in Equation (18) exists.

1.4 OBSERVATIONS ON THE ARRAY G

In Equation (11), it was not necessary to assume that the virtual stress state $\{\delta\tau\}$ has the same spatial distribution $[\Lambda(x, y)]$ as was assumed for the homogeneous real stress state. Furthermore, it was not necessary to assume that the number of coefficients $\{a\}$ equals the number of coefficients $\{\beta\}$ in the real state. However, if the CVW is expressed by the simplified form in Equation (7), then the number of coefficients $\{a\}$ must equal the number of coefficients $\{\beta\}$. Also, the virtual state stresses must satisfy homogeneous equilibrium equations and give zero traction values on the boundary S_τ; but these are exactly the admissibility requirements for the homogeneous real stresses, so the virtual and homogeneous real stresses might as well be assumed to have the same spatial distribution.

The external work, δW_e, done by the virtual state surface tractions moving through the real state boundary displacements is given by

$$\delta W_e = t\int_{S_u} [\delta T]\{\bar{u}\}\, ds \tag{19}$$

where there is no contribution from S_τ because $\lfloor \delta T \rfloor = \lfloor 0 \rfloor$ on S_τ. Substitute Equations (10) and (12) into Equation (19):

$$\delta W_e = \lfloor a \rfloor \left[t \int_{S_u} [T]^T [\zeta] ds \right] \{\bar{q}\}$$

Then substitute Equation (15) to conclude

$$\delta W_e = \lfloor a \rfloor [G] \{\bar{q}\} \tag{20}$$

From Equation (20) it follows that the G_{ij} element in array $[G]$ (the element in the i^{th} row and j^{th} column) represents the boundary work done by the virtual tractions associated with coefficient a_i moving through the real displacements associated with $\bar{q}_j$. Array $[G]$ will be called the boundary work array.

Because the virtual state stresses satisfy homogeneous equations of equilibrium, it follows that the virtual boundary tractions evaluated from Equation (3) will be self-equilibrating. Furthermore, because the virtual stresses satisfy homogeneous traction boundary conditions on S_τ, it follows that the non-zero virtual tractions on S_u must be self-equilibrating. Therefore, the external work δW_e, as expressed in Equation (20), should be zero if and only if the real displacements $\{\bar{q}\}$ represent a rigid body motion of the S_u boundary; and this must be true for every admissible virtual stress state (for every $\lfloor a \rfloor$). These requirements provide checks on the formation of the $[G]$ array and provide guidance in the selection of the arrays $[T]$ and $[\zeta]$ which are used to derive $[G]$ through Equation (15).

1.5 REQUIREMENTS ON THE ASSUMED BOUNDARY DISPLACEMENTS

Equation (10) expresses the displacements $\{\bar{u}\}$ at any point on the boundary S_u in terms of the specified degrees of freedom $\{\bar{q}\}$. If the external work δW_e is to vanish for a rigid body motion, then obviously there is a requirement that Equation (10) must include rigid body motion. Let $\{\bar{q}\}_{RB}$ denote rigid body generalized displacements of S_u. Then if $\{\bar{q}\} = \{\bar{q}\}_{RB}$ is substituted into Equation (10), the resulting $\{\bar{u}\}$ must represent rigid body motion everywhere on S_u. That is,

$$\left\{\bar{u}\,(x, y)\right\}_{RB} = \left[\zeta\,(x, y)\right] \left\{\bar{q}\right\}_{RB} \tag{21}$$

which places requirements on the elements in the array $\left[\zeta\right]$.

1.6 REQUIREMENTS ON THE NUMBER OF STRESS COEFFICIENTS

Because the work δW_e, as given in Equation (20), must vanish for every virtual stress state moving through real state rigid body motions, it follows that as a necessary condition

$$\underset{NxF}{\left[G\right]} \quad \underset{Fx1}{\left\{\bar{q}\right\}} = \underset{Nx1}{\left\{0\right\}} \tag{22}$$

should be satisfied only by displacements $\left\{\bar{q}\right\}_{RB}$ which are derived from true rigid body motions of the boundary S_u. That is, Equation (22) should be satisfied by rigid body $\left\{\bar{q}\right\}$ and should not be satisfied by any non-rigid body $\left\{\bar{q}\right\}$.

Equation (15) shows that the array $\left[G\right]$ has N rows and F columns, where N is the number of stress coefficients and F is the number of S_u boundary degrees of freedom in Equation (10). Let $\bar{R}$ denote the number of rigid body degrees of freedom which are consistent with any special features (such as symmetry conditions) included in the elements of array $\left[\zeta\,(x, y)\right]$ and which cause non-zero displacements on S_u. (Note that there might be a rigid body degree of freedom which causes zero displacements on S_u. The resulting $\left\{\bar{q}\right\}_{RB} \equiv \left\{0\right\}$ will certainly give $\delta W_e = 0$ from Equation (20) but this provides very little information as a check on the array $\left[G\right]$.)

Now, because there exist only $\bar{R}$ true rigid body motions, it follows that the most general nontrivial solution for $\left\{\bar{q}\right\}$ in Equation (22) must contain $\bar{R}$ independent constants. If the $\bar{R}$ constants are selected to be $\bar{R}$ components of $\left\{\bar{q}\right\}$, it follows that it must be possible to solve Equation (22) for the remaining $(F-\bar{R})$ components in terms of the $\bar{R}$ rigid body components. From this it follows that the rank of $\left[G\right]$, denoted by rank $\left[G\right]$, must be equal to $(F-\bar{R})$.

If rank $[G] > (F-\bar{R})$, then it would be possible to solve Equation (22) for more than $(F-\bar{R})$ components expressed in terms of less than $\bar{R}$ independent constants. This would mean fewer than $\bar{R}$ rigid body motions, which means that some of the true rigid body modes have been suppressed. If the structure were to experience the suppressed rigid body motion, there would be non-zero δW_e and non-zero stresses from Equation (18). This possibility will not occur with self-equilibrating tractions.

If rank $[G] < (F-\bar{R})$, then it would be possible to solve Equation (22) for less than $(F-\bar{R})$ components expressed in terms of more than $\bar{R}$ independent constants. This would mean more than $\bar{R}$ rigid body motions, which means that spurious rigid body modes have been introduced into the system. If the structure experiences a spurious rigid body motion, there will be zero δW_e and zero stresses even though the imposed displacements are actually not rigid body. This is bad and should be avoided.

The requirement that rank $[G] = (F-\bar{R})$ imposes the obvious requirement that $N \geq (F-\bar{R})$, for if $N < (F-\bar{R})$ then it is impossible to have rank $[G] = (F-\bar{R})$. Note that there is no theoretical objection to $N > (F-\bar{R})$ provided that all N equations in Equation (22) are satisfied by the rigid body displacements $\{\bar{q}\}_{RB}$ (this is guaranteed since the virtual stress states are self-equilibrating).

In order to develop additional requirements on the choice of stress coefficients, consider the array $[\bar{q}]$ in the partitioned form

$$\underset{1 \times F}{[\bar{q}]} = \underset{1 \times (F-S)}{[\bar{q}_1 \;\vdots\;} \underset{1 \times S}{\bar{q}_{RB}]} \tag{23}$$

where $[\bar{q}_{RB}]$ now denotes any set of generalized displacements on S_u selected so that $[\bar{q}_{RB}] \equiv [0]$ is sufficient to suppress all true rigid body motion. Clearly, there is a requirement that $S \geq \bar{R}$; but the choice of elements in the $[\bar{q}_{RB}]$ array is not unique. Consistent with the partitioning of $[\bar{q}]$, partition array $[G]$ in the form

$$\underset{N \times F}{[G]} = \underset{N \times (F-S)}{[G_1 \;\vdots\;} \underset{N \times S}{G_{RB}]} \tag{24}$$

Then $\delta W_e = \lfloor a \rfloor \left[G_1\right] \left\{\bar{q}_1\right\} + \lfloor a \rfloor \left[G_{RB}\right] \left\{\bar{q}_{RB}\right\}$;

and if the true rigid body motions are suppressed by setting $\left\lfloor \bar{q}_{RB} \right\rfloor \equiv \lfloor 0 \rfloor$, then the external work δW_e should vanish.

$$\delta W_e = \lfloor a \rfloor \left[G_1\right] \left\{\bar{q}_1\right\} = 0$$

This must be true for every $\lfloor a \rfloor$, which requires

$$\underset{N \times (F-S)}{\left[G_1\right]} \quad \underset{(F-S) \times 1}{\left\{\bar{q}_1\right\}} = \underset{N \times 1}{\{0\}} , \tag{25}$$

Because true rigid body motion has been suppressed, Equation (25) should be satisfied only by the trivial solution $\left\{\bar{q}_1\right\} = \{0\}$. Therefore, it follows that the rank of array $\left[G_1\right]$ must equal to (F-S), for suppose rank $\left[G_1\right] <$ (F-S); say rank $\left[G_1\right] = M$. Then it would be possible to consider a virtual stress state consisting of the proper choice of M independent stress states, denoted by $\lfloor a_1 \rfloor$, such that

$$\delta W_e = \underset{1 \times M}{\lfloor a_1 \rfloor} \quad \underset{M \times (F-S)}{\left[G_1\right]} \quad \underset{(F-S) \times 1}{\left\{\bar{q}_1\right\}}$$

would vanish for arbitrary $\lfloor a_1 \rfloor$ and nontrivial $\left\{\bar{q}_1\right\}$. This indicates existence of a spurious rigid body motion, which is to be avoided.

In summary, the number of independent stress states in the virtual stress state must first be sufficient to give $N \geq (F-\bar{R})$. Then it is necessary to insure that rank $\left[G\right] = (F-\bar{R})$. Finally, it is necessary to insure rank $\left[G_1\right]$ = (F-S), and this must be true for every choice of $\left\lfloor \bar{q}_{RB} \right\rfloor$ in Equation (23).

1.7 TREATMENT OF BOUNDARY CONDITIONS

As described earlier, the domain boundary consists of two parts - an S_u portion over which displacements are specified and an S_T portion over which tractions are specified. In a complementary virtual work formulation, the requirements on the S_T boundary, Equation (6), impose requirements on the admissible stress states, Equation (8). If these requirements can be exactly satisfied, then a true complementary virtual work approximate solution can be achieved.

However, there may be problems for which it is too difficult to achieve satisfaction of all the S_T constraints. Or it might be desired to generalize the formulation in order to achieve results which could be adapted to different sets of S_T conditions. For whatever the reason, in Equation (1), all or part of the S_T boundary can be converted to S_u boundary. The effect of this is to increase the number of displacement degrees of freedom on S_u; that is, the magnitude of F in Equation (10) is increased. This modified problem can then be solved by complementary virtual work. The final stresses for the modified problem will be functions of the additional degrees of freedom, and these additional freedoms can finally be selected to impose some measure of satisfaction of the original requirements on the original S_T surface.

SECTION 2

DEVELOPMENT OF THE ASSUMED STRESS STATES

2.1 INTRODUCTION

In Section 1 it is shown that a complementary virtual work solution requires a stress state which satisfies equations of equilibrium in the domain and traction boundary conditions on the S_T portion of the boundary. For the finite element shown in Figure 1, the exterior boundary is an S_U boundary because all displacements are specified to guarantee adjacent element continuity; therefore, there are no requirements on the stress state evaluated at the exterior boundary.

The nature of the inner, or hole, boundary will depend upon the particular problem of interest. The inner boundary will be completely S_T for an open hole. If the hole is to be filled with other finite elements and complete adjacent element continuity is required, then the inner boundary will be completely S_U in the complementary work solution for the hole element. If the hole is to be filled with a fastener and if there is load transfer with separation between fastener and hole boundary, then part of the boundary might be completely S_U and part will be completely S_T. Or if the hole is to be filled with a fastener and if friction between fastener and hole boundary is ignored, then all or part of the boundary will be S_U with respect to the radial direction (continuity of radial displacement between hole boundary and fastener) but S_T with respect to tangential direction (zero shear stress on the hole boundary).

The most general hole boundary conditions would be completely S_U. Then any S_T conditions could be satisfied by using the procedure discussed in Section 1.7. However, all intended applications of this finite element will have zero shear stress on the hole boundary (either open hole or friction free fastener); and for these problems, a more accurate approximate solution should be obtained by requiring that the assumed stress states give exactly zero shear on the inner boundary. Therefore, this S_T boundary condition is imposed on the solution which follows.

Because the hole boundary is circular, the S_T boundary condition can be most easily expressed through the use of polar coordinates. Therefore, in what follows, the domain

will be described by polar coordinates with origin at the center of the circular hole boundary (see Figure 1); and the stress state will be expressed in polar components.

2.2 THE MOST GENERAL PERIODIC STRESS STATE

In polar coordinates, the equations of equilibrium for plane stress and no body forces are [1,p.66]

$$\frac{\partial \tau_r}{\partial r} + \frac{1}{r}\frac{\partial \tau_{r\theta}}{\partial \theta} + \frac{1}{r}(\tau_r - \tau_\theta) = 0$$

$$\frac{1}{r}\frac{\partial \tau_\theta}{\partial \theta} + \frac{\partial \tau_{r\theta}}{\partial r} + \frac{2\tau_{r\theta}}{r} = 0 \qquad (26)$$

These equations are satisfied if the stress components are defined as follows in terms of a stress function ϕ:

$$\tau_r = \frac{1}{r}\frac{\partial \phi}{\partial r} + \frac{1}{r^2}\frac{\partial^2 \phi}{\partial \theta^2}$$

$$\tau_\theta = \frac{\partial^2 \phi}{\partial r^2} \qquad (27)$$

$$\tau_{r\theta} = -\frac{\partial}{\partial r}\left(\frac{1}{r}\frac{\partial \phi}{\partial \theta}\right)$$

Begin the development of the assumed stress state by recognizing that the stresses must be periodic in θ in order to provide traction continuity across interior surfaces in the domain. Since any periodic function can be expanded in a Fourier series, it follows that the shear stress, $\tau_{r\theta}$, can be written in the form

$$\tau_{r\theta}(r,\theta) = f(r) + \sum_{n=1}^{\infty}\left[a_n(r)\cos n\theta + b_n(r)\sin n\theta\right]$$

From this it follows that the stress function, ϕ, has the form

$$\phi(r,\theta) = \left[rF(r)\right]\theta + rG(\theta) + H(r) + \sum_{n=1}^{\infty}\left[A_n(r)\cos n\theta + B_n(r)\sin n\theta\right]$$

Then $$\tau_\theta = \theta\frac{d^2}{dr^2}(rF) + (\text{periodic terms})$$

and since τ_θ must be periodic, it follows that

$$\frac{d^2}{dr^2}(rF) = 0$$

which gives $$F(r) = C_1 + C_2\frac{1}{r}$$

Now $\tau_r = \frac{1}{r}\left(\frac{d^2G}{d\theta^2} + G + C_1\theta\right) + (\text{periodic terms})$, from which it can be concluded that

$$\frac{d^2G(\theta)}{d\theta^2} + G(\theta) + C_1\theta = C_3 + \sum_{n=1}^{\infty}(a_n\cos n\theta + b_n\sin n\theta)$$

From this it can be shown that

$$G(\theta) = -C_1\theta + C_3 + C_4\cos\theta + C_5\sin\theta + \frac{1}{2}a_1\theta\sin\theta - \frac{1}{2}b_1\theta\cos\theta$$

$$-\sum_{n=2}^{\infty}\frac{1}{n^2-1}(a_n\cos n\theta + b_n\sin n\theta)$$

Finally, it can be shown that the most general stress function which provides periodic stresses can be written as

$$\phi(r,\theta) = H(r) + D_1\theta + D_2 r\theta\sin\theta + D_3 r\theta\cos\theta$$

$$+ \sum_{n=1}^{\infty} \left[A_n(r)\cos n\theta + B_n(r)\sin n\theta\right] \tag{28}$$

Note that this stress function is valid for any material because the expression has been derived only from equilibrium considerations.

2.3 RESULTANT FORCES ON THE CIRCULAR BOUNDARY

Based on Equations (27) and (28), the stress components τ_r and $\tau_{r\theta}$ are

$$\tau_r = \frac{1}{r}\frac{dH}{dr} + D_2\frac{2\cos\theta}{r} - D_3\frac{2\sin\theta}{r}$$

$$+ \sum_{n=1}^{\infty} \left[\left(\frac{1}{r}\frac{dA_n}{dr} - \frac{n^2}{r^2}A_n\right)\cos n\theta + \left(\frac{1}{r}\frac{dB_n}{dr} - \frac{n^2}{r^2}B_n\right)\sin n\theta\right] \tag{29}$$

$$\tau_{r\theta} = D_1\frac{1}{r^2} + \sum_{n=1}^{\infty} n\left[\frac{d}{dr}\left(\frac{1}{r}A_n\right)\sin n\theta - \frac{d}{dr}\left(\frac{1}{r}B_n\right)\cos n\theta\right] \tag{30}$$

These stresses, acting on the hole boundary with radius of R, have a resultant force with components as follows (see Figure 2)

$$F_x = \int_0^{2\pi} (\tau_{r\theta}\sin\theta - \tau_r\cos\theta)\, R\, d\theta$$

$$F_y = -\int_0^{2\pi} (\tau_r\sin\theta + \tau_{r\theta}\cos\theta)\, R\, d\theta \tag{31}$$

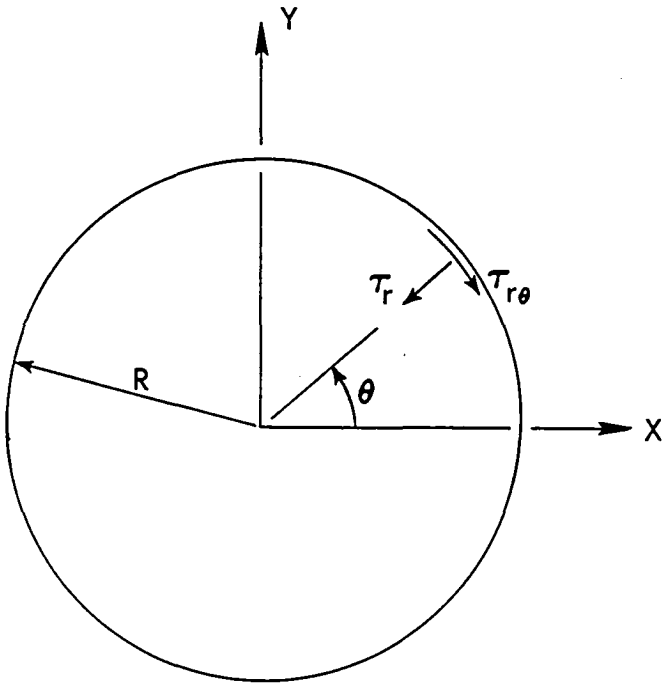

Figure 2. Tractions on the Hole Boundary

Substituting Equations (29) and (30) into Equation (31) gives the results

$$F_x = -2\pi D_2 , \qquad F_y = 2\pi D_3 \tag{32}$$

Note that the results shown in Equation (32) are independent of the magnitude of R.

2.4 SATISFACTION OF TRACTION BOUNDARY CONDITIONS

The traction boundary condition requires that $\tau_{r\theta} = 0$ for every value of θ at $r = R$. From Equation (30) it follows that

$$D_1 = 0$$

$$\text{at } r = R, \quad \frac{d}{dr}\left(\frac{1}{r}A_n\right) = 0, \quad \frac{d}{dr}\left(\frac{1}{r}B_n\right) = 0, \quad n = 1, 2, \ldots \tag{33}$$

The constant D_1 must be discarded; but the functions $A_n(r)$ and $B_n(r)$ are as yet unspecified, subject only to the requirements of Equation (33).

It can be shown that if Equation (33) is satisfied, then the resultant force components are still given by Equation (32).

2.5 ORTHOTROPIC STRESS-STRAIN RELATIONS IN POLAR COORDINATES

The finite element is constructed of a linearly elastic, orthotropic material with principal axes of orthotropy in the x, y coordinate directions. If initial stresses and strains and thermal strains are neglected, the stress-strain law in its most simple form is

$$\begin{Bmatrix} \epsilon_x \\ \epsilon_y \\ \gamma_{xy} \end{Bmatrix} = \begin{bmatrix} \frac{1}{E_x} & -\frac{\nu_{xy}}{E_y} & 0 \\ -\frac{\nu_{yx}}{E_x} & \frac{1}{E_y} & 0 \\ 0 & 0 & \frac{1}{G_{xy}} \end{bmatrix} \begin{Bmatrix} \tau_x \\ \tau_y \\ \tau_{xy} \end{Bmatrix} = [C_{xy}] \begin{Bmatrix} \tau_x \\ \tau_y \\ \tau_{xy} \end{Bmatrix} \tag{34}$$

with $$\frac{\nu_{xy}}{E_y} = \frac{\nu_{yx}}{E_x} \quad .$$

Note the order of subscripts in the definitions of the Poisson's ratios.

Because the stresses and strains will be specified in polar coordinates, it is useful to transform the stress-strain relations to polar coordinates. Begin with the transformations of stress and strain, as follows [1, p.67]:

$$\begin{Bmatrix} \epsilon_r \\ \epsilon_\theta \\ \gamma_{r\theta} \end{Bmatrix} = [T] \begin{Bmatrix} \epsilon_x \\ \epsilon_y \\ \gamma_{xy} \end{Bmatrix} \quad , \quad \begin{Bmatrix} \tau_x \\ \tau_y \\ \tau_{xy} \end{Bmatrix} = [T]^T \begin{Bmatrix} \tau_r \\ \tau_\theta \\ \tau_{r\theta} \end{Bmatrix} \tag{35}$$

where $$[T] = \begin{bmatrix} \cos^2\theta & \sin^2\theta & \sin\theta\cos\theta \\ \sin^2\theta & \cos^2\theta & -\sin\theta\cos\theta \\ -2\sin\theta\cos\theta & 2\sin\theta\cos\theta & \cos^2\theta - \sin^2\theta \end{bmatrix} \tag{36}$$

Then $$\begin{Bmatrix} \epsilon_r \\ \epsilon_\theta \\ \gamma_{r\theta} \end{Bmatrix} = [T][C_{xy}][T]^T \begin{Bmatrix} \tau_r \\ \tau_\theta \\ \tau_{r\theta} \end{Bmatrix} = [C_{r\theta}] \begin{Bmatrix} \tau_r \\ \tau_\theta \\ \tau_{r\theta} \end{Bmatrix} \tag{37}$$

The desired material property matrix is $[C_{r\theta}]$, which has the following form:

$$[C_{r\theta}] = C_1 [C^1_{r\theta}] + C_2 [C^2_{r\theta}] + C_3 [C^3_{r\theta}] + C_4 [C^4_{r\theta}] \tag{38}$$

where $$C_1 = \frac{1}{8}\left(\frac{3}{E_x} + \frac{3}{E_y} - 2\frac{\nu_{xy}}{E_y} + \frac{1}{G_{xy}}\right)$$

$$C_2 = \frac{1}{2}\left(\frac{1}{E_x} + \frac{1}{E_y} + 2\frac{\nu_{xy}}{E_y} + \frac{1}{G_{xy}}\right)$$

$$C_3 = \frac{1}{2}\left(\frac{1}{E_x} - \frac{1}{E_y}\right) \qquad (39)$$

$$C_4 = \frac{1}{8}\left(\frac{1}{E_x} + \frac{1}{E_y} + 2\frac{\nu_{xy}}{E_y} - \frac{1}{G_{xy}}\right)$$

and $$\left[C^1_{r\theta}\right] = \begin{bmatrix} 1 & 1 & 0 \\ 1 & 1 & 0 \\ 0 & 0 & 0 \end{bmatrix}, \quad \left[C^2_{r\theta}\right] = \begin{bmatrix} 0 & -\frac{1}{2} & 0 \\ -\frac{1}{2} & 0 & 0 \\ 0 & 0 & 1 \end{bmatrix} \qquad (40)$$

$$\left[C^3_{r\theta}\right] = \begin{bmatrix} \cos 2\theta & 0 & -\sin 2\theta \\ 0 & -\cos 2\theta & -\sin 2\theta \\ -\sin 2\theta & -\sin 2\theta & 0 \end{bmatrix} \qquad (41)$$

$$\left[C^4_{r\theta}\right] = \begin{bmatrix} \cos 4\theta & -\cos 4\theta & -2\sin 4\theta \\ -\cos 4\theta & \cos 4\theta & 2\sin 4\theta \\ -2\sin 4\theta & 2\sin 4\theta & -4\cos 4\theta \end{bmatrix} \qquad (42)$$

If the $\left[C_{r\theta}\right]$ array is written in the form

$$\left[C_{r\theta}\right] = \begin{bmatrix} C_{11} & C_{12} & C_{13} \\ C_{21} & C_{22} & C_{23} \\ C_{31} & C_{32} & C_{33} \end{bmatrix} \qquad (43)$$

then
$$
\begin{aligned}
C_{11} &= C_1 + C_3 \cos 2\theta + C_4 \cos 4\theta \\
C_{22} &= C_1 - C_3 \cos 2\theta + C_4 \cos 4\theta \\
C_{33} &= C_2 - C_4\, 4 \cos 4\theta \\
C_{21} &= C_{12} = C_1 - \tfrac{1}{2} C_2 - C_4 \cos 4\theta \\
C_{31} &= C_{13} = -C_3 \sin 2\theta - C_4\, 2 \sin 4\theta \\
C_{32} &= C_{23} = -C_3 \sin 2\theta + C_4\, 2 \sin 4\theta
\end{aligned}
\tag{44}
$$

For possible use, Equation (39) can be inverted to give

$$
\begin{aligned}
\frac{1}{E_x} &= C_1 + C_3 + C_4 \\
\frac{1}{E_y} &= C_1 - C_3 + C_4 \\
\frac{\nu_{xy}}{E_y} &= -C_1 + \tfrac{1}{2} C_2 + C_4 \\
\frac{1}{G_{xy}} &= C_2 - 4C_4
\end{aligned}
\tag{45}
$$

Finally, note that for isotropic material, $C_3 = C_4 = 0$.

2.6 COMPATIBILITY CONSIDERATIONS

With an exact solution to any plane stress problem in polar coordinates, there is a necessary condition that the strains satisfy the compatibility equation

$$
\frac{\partial^2 \epsilon_r}{\partial \theta^2} - r \frac{\partial \epsilon_r}{\partial r} + r \frac{\partial^2 (r\epsilon_\theta)}{\partial r^2} - \frac{\partial^2 (r\gamma_{r\theta})}{\partial r\, \partial \theta} = 0 \,. \tag{46}
$$

With a complementary virtual work formulation, the strains will be derived from the assumed stresses by means of Equation (37); and there is no admissibility requirement that the strains should satisfy Equation (46). Indeed, the approximate satisfaction of Equation (46) is one of the consequences of the vanishing of the complementary virtual work. However, a better approximate solution should be obtained if the assumed stress state is compatible; so there is motivation to attempt to select the functions $H(r)$, $A_n(r)$, $B_n(r)$ in Equation (28) so that the resulting stresses will be compatible. This was attempted but with no success. Therefore, in what follows, the stress components are not compatible for orthotropic material; and it is left up to the principle of complementary virtual work to achieve the "most compatible" stress state within the assumptions.

The domain of the finite element is doubly connected, and it is known that Equation (46) is not sufficient to guarantee single valued displacements in a multiply-connected domain. Based on experience with isotropic material [1, Sec. 43], it is anticipated that the displacements associated with the constants D_2 and D_3 in Equation (28) will be multi-valued. These constants should not be discarded because they account for the non-zero resultant forces on the hole boundary, as shown in Equation (32). Therefore, additional terms should be added to the D_2 and D_3 coefficients in order to enforce single-valued displacements. This will be demonstrated for the D_2 coefficient, as follows. Assume the stress function

$$\phi(r,\theta) = D_2 r\theta \sin\theta + Ar\ln r \cos\theta$$

Note that the additional term has the proper form to provide periodic stresses, as shown in Equation (28). Then from Equation (27)

$$\tau_r = D_2 \frac{2\cos\theta}{r} + A\frac{\cos\theta}{r}$$

$$\tau_\theta = A\frac{\cos\theta}{r}$$

$$\tau_{r\theta} = A\frac{\sin\theta}{r}$$

with the strains derived from Equations (37), (43), and (44). Polar coordinate strain-displacement relations are [1, p.76]

$$\begin{aligned} \epsilon_r &= \frac{\partial u}{\partial r} \\ \epsilon_\theta &= \frac{u}{r} + \frac{1}{r}\frac{\partial v}{\partial \theta} \\ \gamma_{r\theta} &= \frac{1}{r}\frac{\partial u}{\partial \theta} + \frac{\partial v}{\partial r} - \frac{v}{r} \end{aligned} \tag{47}$$

Following the procedure outlined in [1, Sec. 31], the requirement for existence of displacement functions $u(r,\theta)$ and $v(r,\theta)$ can be written as

$$\begin{aligned} &[f(\theta; C_3, C_4; D_2, A)] \ln r - [A(4C_1 - 2C_3) + D_2(4C_1 - C_2)]\sin\theta \\ &\quad + g(C_1, C_2, C_3, C_4; D_2, A)\sin 3\theta + h(C_1, C_2, C_3, C_4; D_2, A)\sin 5\theta \\ &\quad + \frac{d^2F(\theta)}{d\theta^2} + F(\theta) + r\frac{dG(r)}{dr} - G(r) = 0 \end{aligned} \tag{48}$$

where $F(\theta)$ and $G(r)$ are functions which appear in the equations for displacement components u and v.

Clearly Equation (48) can never be satisfied unless the function $f(\theta; C_3, C_4; D_2, A) = 0$; and it can be shown that this is possible only for an isotropic material with $C_3 = C_4 = 0$. This is simply a manifestation of the fact that the stress state derivable from Equation (28) is not compatible for arbitrary values of the coefficients.

If the $\ln r$ term in Equation (48) is disregarded, then the equation can be satisfied by requiring

$$r\frac{dG(r)}{dr} - G(r) = -K \tag{49}$$

$$\frac{d^2F(\theta)}{d\theta^2} + F(\theta) = K + [A(4C_1 - 2C_3) + D_2(4C_1 - C_2)]\sin\theta - g\sin 3\theta - h\sin 5\theta \qquad (50)$$

Equation (50) will possess a multivalued solution proportional to $\theta\cos\theta$, which would mean multivalued displacement components, unless the coefficient of $\sin\theta$ vanishes. Therefore, it is necessary to require

$$A = -D_2\,\frac{4C_1 - C_2}{4C_1 - 2C_3}$$

Define $$\bar{C} = \frac{4C_1 - C_2}{4C_1 - 2C_3} \qquad (51)$$

Conclude that the stress function $\phi(r,\theta)$ must include the following terms in order to eliminate multivalued displacements.

$$\phi(r,\theta) = D_2\,(r\theta\sin\theta - \bar{C}\,r\ln r\cos\theta) + D_3(r\theta\cos\theta + \bar{C}\,r\ln r\sin\theta) \qquad (52)$$

For isotropic material, $\bar{C} = \frac{1-\nu}{2}$, which agrees with [1, Sec. 43].

2.7 FURTHER SPECIFICATION OF THE STRESS FUNCTION

Equation (28), as modified by Equation (52) and $D_1 = 0$, includes arbitrary functions $H(r)$, $A_n(r)$, $B_n(r)$ which are as-yet unspecified. Even though the resulting stresses cannot be compatible for orthotropic material, it appears reasonable to select these functions so that the resulting stresses would be compatible for isotropic material. Then the solution should be very good for the limiting case of isotropic material because the stresses will satisfy equilibrium and compatibility in the domain and traction boundary conditions on S_T. Furthermore, if the orthotropic material is not too far removed from isotropic, in some vague and unspecified manner, a relatively few stress terms may provide a suitable answer.

The isotropic stress function is shown in [1, p.133] which gives the following expressions for the functions:

$$H(r) = a_0 \ln r + b_0 r^2 \tag{53}$$

$$A_1(r) = b_1 r^3 + a_1' \frac{1}{r}$$

$$B_1(r) = d_1 r^3 + c_1' \frac{1}{r} \tag{54}$$

$$A_n(r) = b_n r^{n+2} + a_n r^n + b_n' r^{-n+2} + a_n' r^{-n}, \quad n = 2, 3, \ldots$$

$$B_n(r) = d_n r^{n+2} + c_n r^n + d_n' r^{-n+2} + c_n' r^{-n}, \quad n = 2, 3, \ldots \tag{55}$$

However, there is a flaw - possibly a fatal flaw - in the use of Equation (55) for A_n and B_n. It will be seen later that in order to obtain a sufficient number of stress coefficients it might be necessary to include terms up through A_{14}, B_{14} or possibly even more. This would mean that the radial dependence would include terms from r^{16} down to r^{-12}. This extreme range of exponents is likely to lead to a very ill-conditioned array [H], which is derived as shown in Equation (14) by integrating over the domain of the finite element. For this reason, Equations(55) are discarded, and the functions $A_n(r)$, $B_n(r)$ are assumed as follows:

$$A_2(r) = a_2 r^2 + b_2' + a_2' \frac{1}{r^2}$$

$$B_2(r) = c_2 r^2 + d_2' + c_2' \frac{1}{r^2} \tag{56}$$

$$A_3(r) = a_3 r^3 + b_3' \frac{1}{r} + a_3' \frac{1}{r^3}$$

$$B_3(r) = c_3 r^3 + d_3' \frac{1}{r} + c_3' \frac{1}{r^3} \tag{57}$$

$$A_n(r) = \sum_{i=0}^{N} C_i^n r^i + \sum_{j=1}^{M} \bar{C}_j^n \frac{1}{r^j}, \qquad n = 4, 5, \ldots$$

$$B_n(r) = \sum_{i=0}^{N} S_i^n r^i + \sum_{j=1}^{M} \bar{S}_j^n \frac{1}{r^j}, \qquad n = 4, 5, \ldots \tag{58}$$

In Equation (56), the r^4 term has been neglected since this term vanishes for the case of an infinite isotropic plate under uniform stress at infinity [1, p. 91]. In Equation (57), the r^5 term is neglected because it does not appear in the case of an infinite isotropic plate with linear variation of stress at infinity [2, p. 470]. Finally, Equation (55) has been discarded completely for $n \geq 4$ and replaced by Equation (58), which expresses $A_n(r)$, $B_n(r)$ as polynomials in r. The functions are written in a form to allow for differing numbers of terms with positive and negative exponents. This flexibility in specifying functions $A_n(r)$ and $B_n(r)$ will permit the selection of a sufficient number of stress coefficients without the extreme range of exponents which naturally appears with fully compatible stresses. Note that the resulting stress state will now be incompatible even for isotropic material.

This numerical difficulty with compatible stresses is obvious in Equation (55) which,of course, is valid only for isotropic material. It is suspected, however, that the same problem will arise if orthotropic compatible stresses are used for the assumed stress state. This suggests that a fully compatible solution for orthotropic material might never be achieved due to appearance of ill-conditioned matrices in the formulation.

2.8 CONSIDERATIONS OF SYMMETRY

If two coordinate axes, say x and y, are established in a plane, there are four possible symmetry conditions which can be established relative to those axes. These conditions can be defined by describing the following four functions which possess the symmetry properties:

$$SS(x,y) = SS(x,-y) = SS(-x, y) = SS(-x, -y)$$

$$SA(x,y) = SA(x,-y) = -SA(-x,y) = -SA(-x,-y)$$

$$AS(x,y) = -AS(x,-y) = AS(-x,y) = -AS(-x,-y)$$

$$AA(x,y) = -AA(x,-y) = -AA(-x,y) = AA(-x,-y)$$

The function SS(x,y) is symmetric about both x and y axes; it will be called a symmetric-symmetric (SS) function. Function SA(x,y) is symmetric about the x-axis and antisymmetric about the y-axis; it is a symmetric-antisymmetric (SA) function. Likewise, function AS(x,y) is an AS function; and AA(x,y) is an AA function.

With the four symmetry conditions established, it can be shown that any function f(x,y) can be written as the sum of four functions, each of which possesses one of the four symmetry conditions. This is demonstrated by first writing the identity

$$f(x,y) = \frac{1}{4}[f(x,y) + f(x,-y) + f(-x,y) + f(-x,-y)]$$

$$+ \frac{1}{4}[f(x,y) + f(x,-y) - f(-x,y) - f(-x,-y)]$$

$$+ \frac{1}{4}[f(x,y) - f(x,-y) + f(-x,y) - f(-x,-y)]$$

$$+ \frac{1}{4}[f(x,y) - f(x,-y) - f(-x,y) + f(-x,-y)]$$

Define $SS(x,y) = \frac{1}{4}[f(x,y) + f(x,-y) + f(-x,y) + f(-x,-y)]$

$$SA(x,y) = \frac{1}{4}[f(x,y) + f(x,-y) - f(-x,y) - f(-x,-y)]$$

$$AS(x,y) = \frac{1}{4}[f(x,y) - f(x,-y) + f(-x,y) - f(-x,-y)]$$

$$AA(x,y) = \frac{1}{4}[f(x,y) - f(x,-y) - f(-x,y) + f(-x,-y)]$$

It can be confirmed that these functions do indeed possess the indicated symmetry properties and, as stated,

$$f(x,y) = SS(x,y) + SA(x,y) + AS(x,y) + AA(x,y)$$

What has been described above for functions of x and y is also applicable to stress and displacement states. That is, any arbitrary stress and displacement state can be represented as the sum of SS, SA, AS, and AA states. These four states are defined in Figure 3. Note that a stress state is symmetric about a line if the stress states at two symmetrically located points are mirror images of each other; the stress state is antisymmetric about a line if the stress states at two symmetrically located points are negative mirror images of each other. Similar definitions apply to displacements. These physical definitions of symmetry and antisymmetry for stresses and displacements mean that individual stress and displacement components might actually have different characters when signs are established according to usual conventions. For example, in the SS state of Figure 3, the stress τ_r is an SS function while stress $\tau_{r\theta}$ is an AA function, displacement u_y is an AS function, and displacement u_x is an SA function.

2.9 FINAL FORM FOR THE STRESS FUNCTION AND STRESS COMPONENTS

The radial coordinate, r, is first normalized or nondimensionalized in terms of the radius of the circular hole, R, giving

$$\rho = \frac{r}{R} \quad .$$

Then, if the stress function is written as $\phi(\rho, \theta)$, the stresses will be given by

$$R^2\tau_r = \frac{1}{\rho}\frac{\partial\phi}{\partial\rho} + \frac{1}{\rho^2}\frac{\partial^2\phi}{\partial\theta^2}$$

$$R^2\tau_\theta = \frac{\partial^2\phi}{\partial\rho^2} \qquad (59)$$

$$R^2\tau_{r\theta} = -\frac{\partial}{\partial\rho}\left(\frac{1}{\rho}\frac{\partial\phi}{\partial\theta}\right)$$

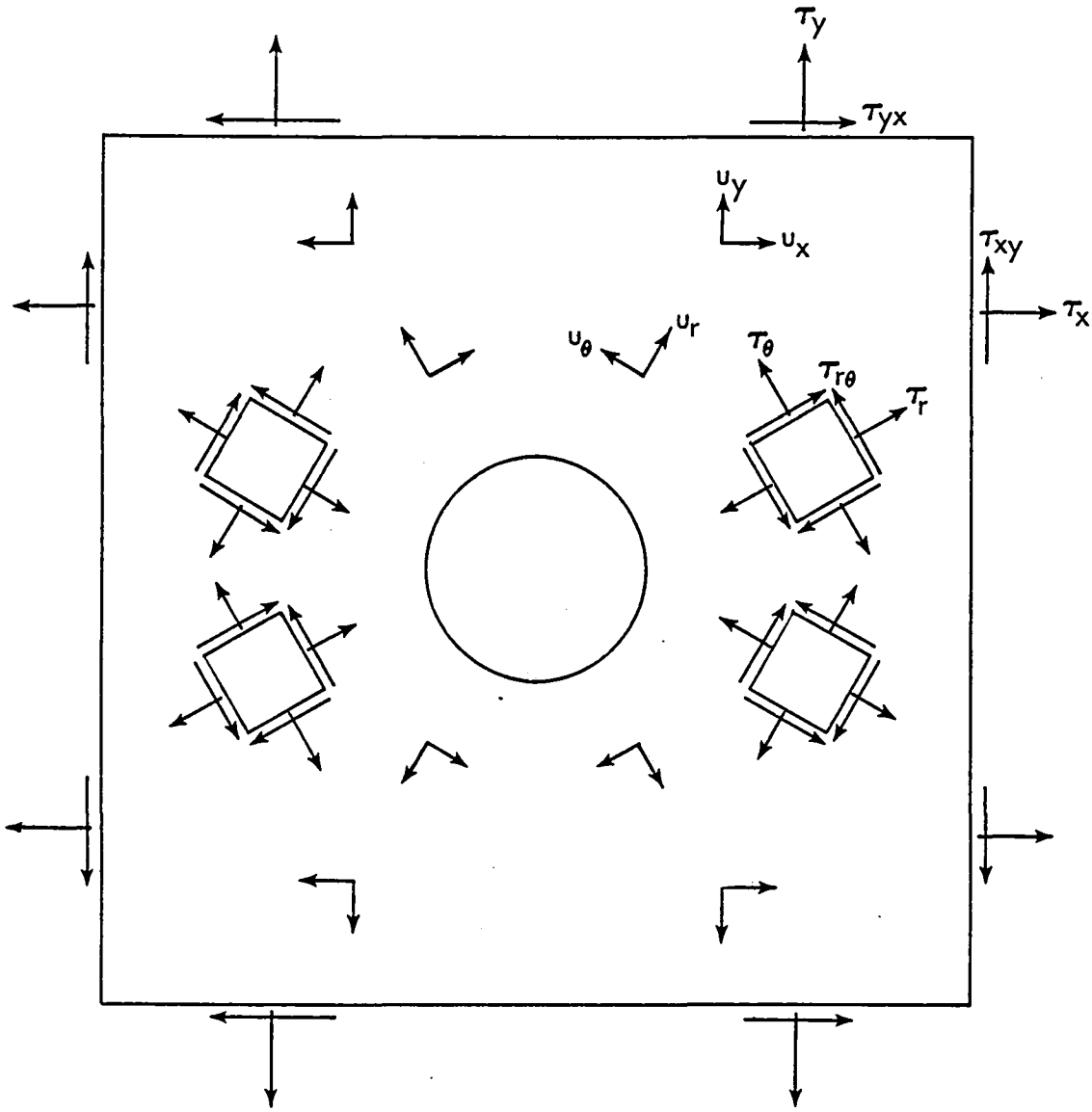

Figure 3a. Symmetric-Symmetric State

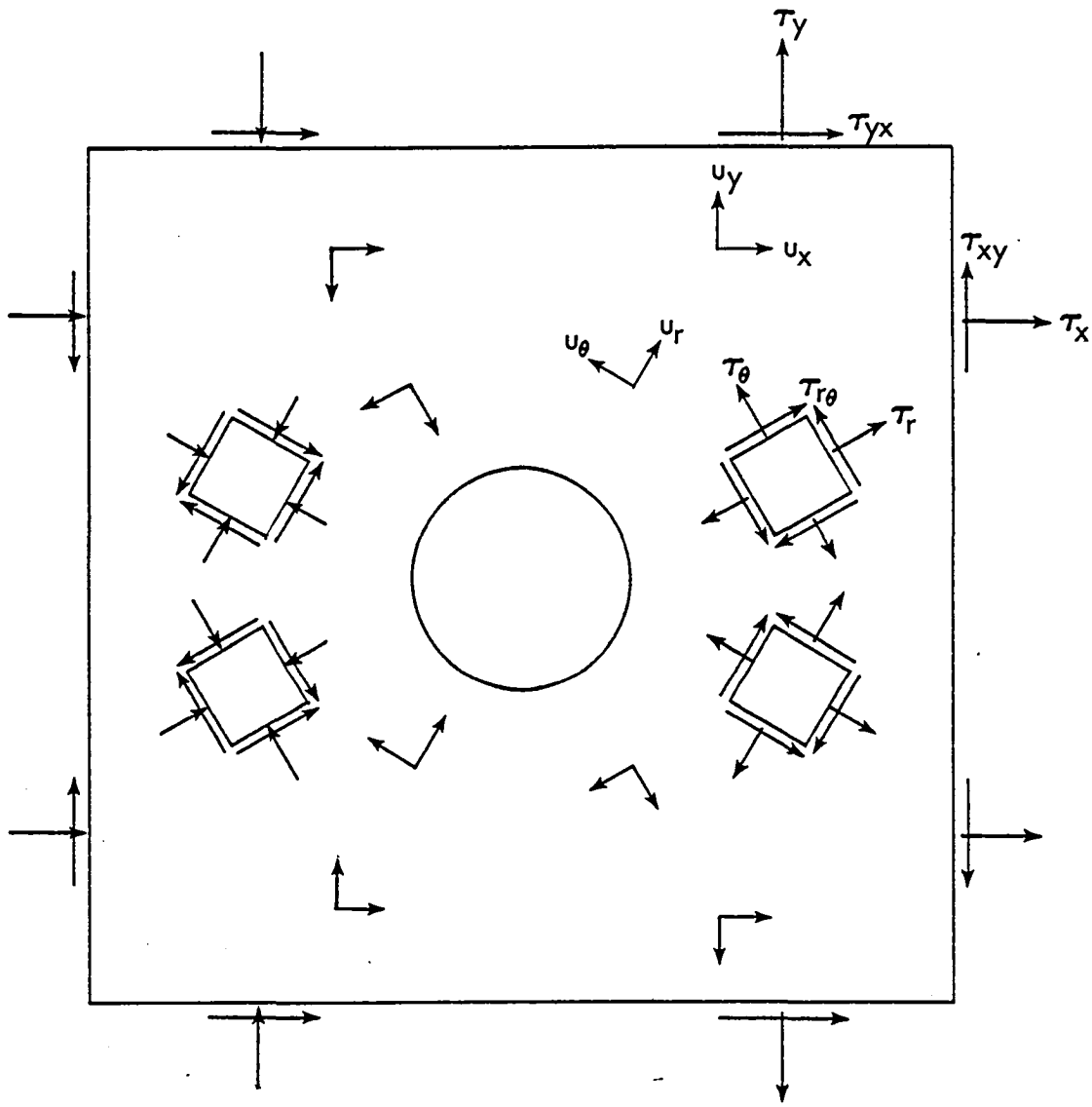

Figure 3b. Symmetric - Antisymmetric State

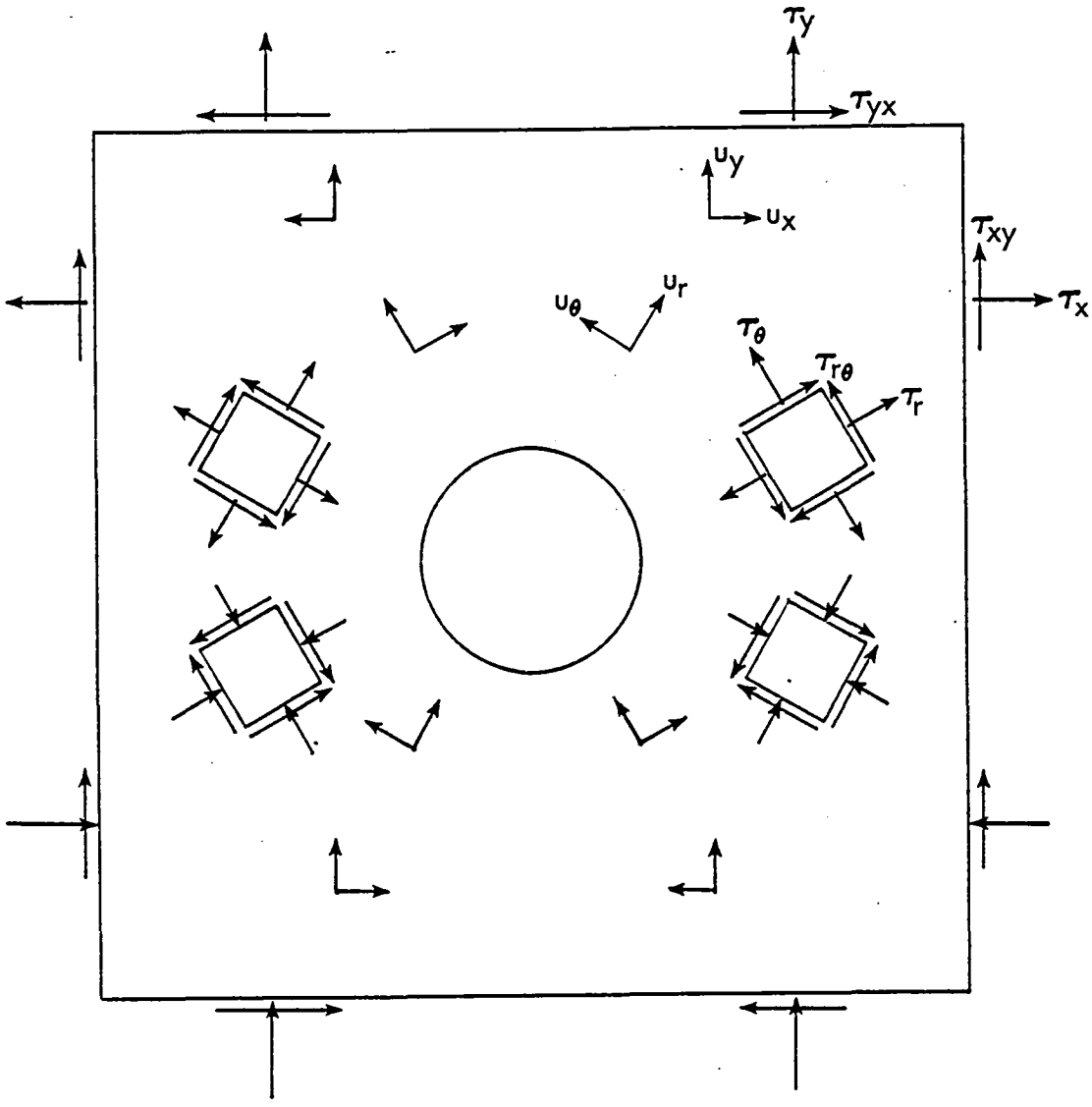

Figure 3c. Antisymmetric-Symmetric State

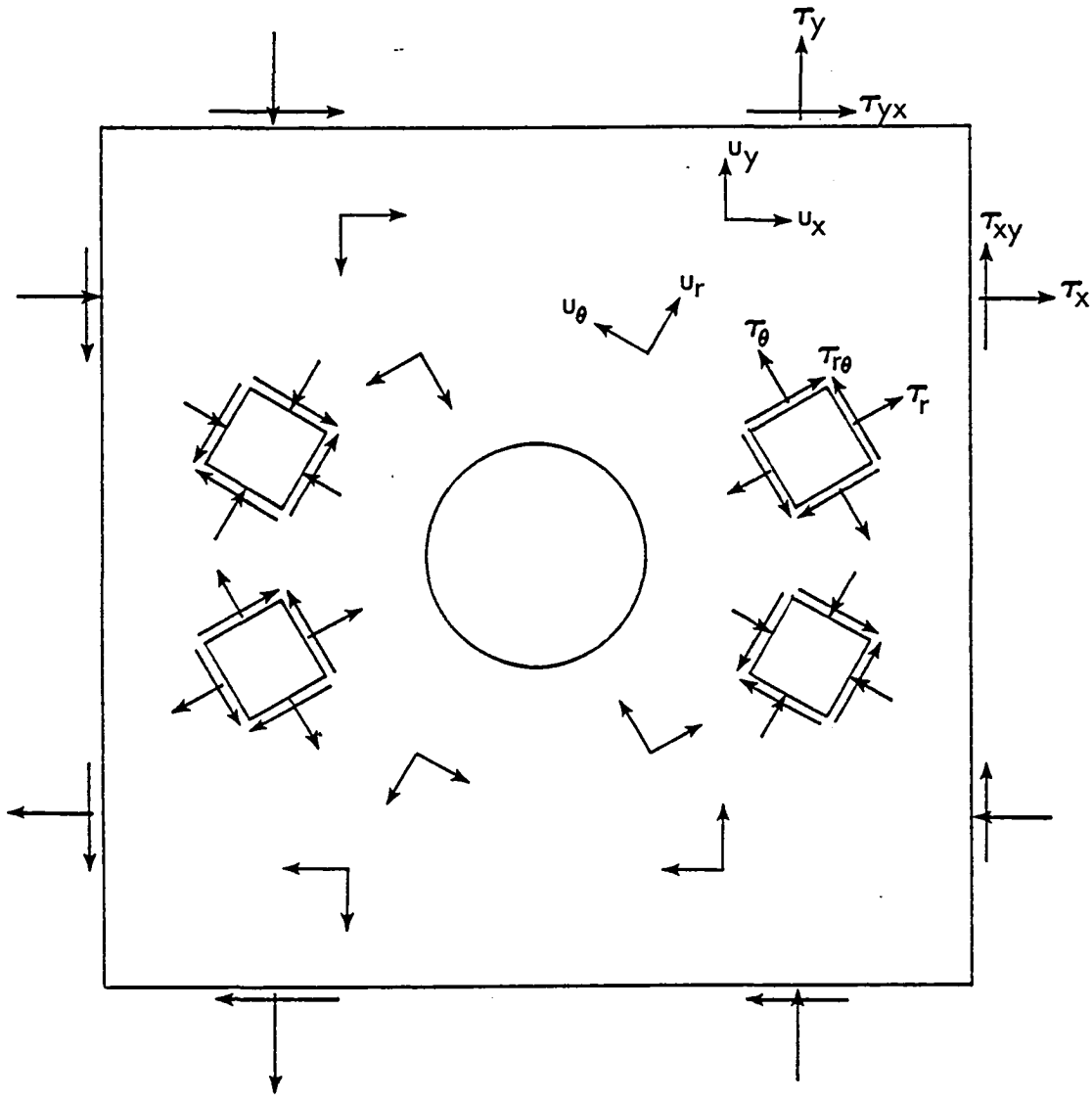

Figure 3d. Antisymmetric-Antisymmetric State

and the equilibrium equations are

$$\frac{\partial}{\partial\rho}(R^2\tau_r) + \frac{1}{\rho}\frac{\partial}{\partial\theta}(R^2\tau_{r\theta}) + \frac{1}{\rho}(R^2\tau_r - R^2\tau_\theta) = 0$$

$$\frac{1}{\rho}\frac{\partial}{\partial\theta}(R^2\tau_\theta) + \frac{\partial}{\partial\rho}(R^2\tau_{r\theta}) + \frac{2}{\rho}(R^2\tau_{r\theta}) = 0 \qquad (60)$$

The stress component $\tau_{r\theta}$ is first calculated from the stress function given by Equations (28), (52), (53), (54), (55) with $D_1 = 0$. The arbitrary constants are then related as necessary to satisfy the traction boundary requirement that $\tau_{r\theta} = 0$ at $\rho = 1$. The final stress function is then divided into its four components according to the four possible symmetry conditions of the stress state, with the final result shown in Equations (62) and (63). The three stress components are derived from Equation (59) and recorded in Equations (64), (66), and (68). It can be confirmed that these stresses do indeed satisfy the equilibrium equations, Equations (60), and provide $\tau_{r\theta}$ at $\rho = 1$.

In Equations (62), (64), (66), and (68), the SS, SA, AS, AA symmetry conditions are numbered 1, 2, 3, 4 respectively. The coefficient $B_{i,j}$ denotes the i^{th} coefficient for the j^{th} symmetry condition. The quantities N1, N2, N3, N4 denote the upper limits on the harmonic expansion for each symmetry condition. Then for each harmonic above the third, the quantities I1, I2, I3, I4 and J1, J2, J3, J4 denote the upper limits on the summations of terms with radial coordinate dependence. These quantities could be functions of harmonic number; but in what follows, they are assumed constant.

For harmonics beyond the third, there is obviously a great deal of arbitrariness in the number of terms included in the assumed stress state. However, it is possible to number the coefficients in such a way as to allow for the arbitrariness.

Define $\quad K1n = 4 + (\frac{n-4}{2})(I1 + J1)$, $\quad K3n = 4 + (\frac{n-5}{2})(I3 + J3)$

$$K2n = 4 + (\frac{n-5}{2})(I2 + J2) \text{ , } \quad K4n = 2 + (\frac{n-4}{2})(I4 + J4) \qquad (61)$$

With the definitions of Equation (61), it can be confirmed that the coefficient subscripts shown in Equation (62) will be properly sequenced for arbitrary values of N, I, J.

$$\phi(\rho,\theta) = B_{11}(\ln\rho) + B_{21}\left(\frac{1}{2}\rho^2\right)$$

$$+ \left[B_{31}\,\frac{1}{2}(1+\rho^2) + B_{41}\,\frac{1}{6}(\rho^{-2}+3\rho^2)\right]\cos 2\theta \qquad \text{SS}$$

$$+ \sum_{n=4,6}^{N1}\left[\sum_{i=1}^{I1} B_{i+K1n,1}\,F(\rho;i) + \sum_{j=1}^{J1} B_{j+K1n+I1,1}\,G(\rho;j)\right]\cos n\theta$$

$$+ B_{12}\left[\rho\theta\sin\theta - \bar{C}\left(\rho\ln\rho - \frac{1}{2}\rho^3\right)\cos\theta\right] + B_{22}\,\frac{1}{2}(\rho^{-1}+\rho^3)\cos\theta$$

$$+ \left[B_{32}\,\frac{1}{2}(\rho^{-1}+\rho^3) + B_{42}\,\frac{1}{12}(\rho^{-3}+2\rho^3)\right]\cos 3\theta \qquad \text{SA}$$

$$+ \sum_{n=5,7}^{N2}\left[\sum_{i=1}^{I2} B_{i+K2n,2}\,F(\rho;i) + \sum_{j=1}^{J2} B_{j+K2n+I2,2}\,G(\rho;j)\right]\cos n\theta$$

$$+ B_{13}\left[\rho\theta\cos\theta + \bar{C}\left(\rho\ln\rho - \frac{1}{2}\rho^3\right)\sin\theta\right] + B_{23}\,\frac{1}{2}(\rho^{-1}+\rho^3)\sin\theta$$

$$+ \left[B_{33}\,\frac{1}{2}(\rho^{-1}+\rho^3) + B_{43}\,\frac{1}{12}(\rho^{-3}+2\rho^3)\right]\sin 3\theta \qquad \text{AS}$$

$$+ \sum_{n=5,7}^{N3}\left[\sum_{i=1}^{I3} B_{i+K3n,3}\,F(\rho;i) + \sum_{j=1}^{J3} B_{j+K3n+I3,3}\,G(\rho;j)\right]\sin n\theta$$

$$+ \left[B_{14}\,\frac{1}{2}(1+\rho^2) + \frac{1}{6}B_{24}(\rho^{-2}+3\rho^2)\right]\sin 2\theta$$

$$+ \sum_{n=4,6}^{N4}\left[\sum_{i=1}^{I4} B_{i+K4n,4}\,F(\rho;i) + \sum_{j=1}^{J4} B_{j+K4n+I4,4}\,G(\rho;j)\right]\sin n\theta \qquad \text{AA} \qquad (62)$$

where

$$F(\rho;i) = \rho^{i} + i - 1$$

$$G(\rho;j) = \rho^{-j} - j + 1 \qquad (63)$$

$$R^2\tau_r(\rho,\theta) = B_{11}(\rho^{-2}) + B_{21}(1)$$

$$-\left[B_{31}(1+2\rho^{-2}) + B_{41}(1+\rho^{-4})\right]\cos 2\theta \qquad \text{SS}$$

$$+\sum_{n=4,6}^{N1}\left[\sum_{i=1}^{I1} B_{i+K1n,1}\,F_r(\rho;i,n) + \sum_{j=1}^{J1} B_{j+K1n+I1,1}\,G_r(\rho;j,n)\right]\cos n\,\theta$$

$$+\left\{B_{12}\left[2\rho^{-1} + \bar{C}\,(\rho-\rho^{-1})\right] + B_{22}(\rho-\rho^{-3})\right\}\cos\theta$$

$$-\left[B_{32}(3\rho+5\rho^{-3}) + B_{42}(\rho+\rho^{-5})\right]\cos 3\theta \qquad \text{SA}$$

$$+\sum_{n=5,7}^{N2}\left[\sum_{i=1}^{I2} B_{i+K2n,2}\,F_r(\rho;i,n) + \sum_{j=1}^{J2} B_{j+K2n+I2,2}\,G_r(\rho;j,n)\right]\cos n\,\theta$$

$$+\left\{B_{13}\left[-2\rho^{-1} + \bar{C}\,(\rho^{-1}-\rho)\right] + B_{23}(\rho-\rho^{-3})\right\}\sin\theta$$

$$-\left[B_{33}(3\rho+5\rho^{-3}) + B_{43}(\rho+\rho^{-5})\right]\sin 3\theta \qquad \text{AS}$$

$$+\sum_{n=5,7}^{N3}\left[\sum_{i=1}^{I3} B_{i+K3n,3}\,F_r(\rho;i,n) + \sum_{j=1}^{J3} B_{j+K3n+I3,3}\,G_r(\rho;j,n)\right]\sin n\,\theta$$

$$-\left[B_{14}(1+2\rho^{-2}) + B_{24}(1+\rho^{-4})\right]\sin 2\theta$$

$$\text{AA}$$

$$+\sum_{n=4,6}^{N4}\left[\sum_{i=1}^{I4} B_{i+K4n,4}\,F_r(\rho;i,n) + \sum_{j=1}^{J4} B_{j+K4n+I4,4}\,G_r(\rho;j,n)\right]\sin n\,\theta \qquad (64)$$

where
$$F_r(\rho;\,i,\,n) = (i-n^2)\rho^{i-2} - n^2(i-1)\rho^{-2} \qquad (65)$$

$$G_r(\rho;j,n) = -(j+n^2)\,\rho^{-(j+2)} + n^2(j+1)\,\rho^{-2}$$

$$R^2 \tau_\theta(\rho,\theta) = B_{11}(-\rho^{-2}) + B_{21}(1)$$

$$+\left[B_{31}(1) + B_{41}(1+\rho^{-4})\right]\cos 2\theta \qquad \text{SS}$$

$$+\sum_{n=4,6}^{N1}\left[\sum_{i=1}^{I1} B_{i+K1n,1}\, F_\theta(\rho;i) + \sum_{j=1}^{J1} B_{j+K1n+I1,1}\, G_\theta(\rho;j)\right]\cos n\theta$$

$$+\left\{B_{12}\left[\bar{C}(3\rho-\rho^{-1})\right] + B_{22}(3\rho+\rho^{-3})\right\}\cos\theta$$

$$+\left[B_{32}(3\rho+\rho^{-3}) + B_{42}(\rho+\rho^{-5})\right]\cos 3\theta \qquad \text{SA}$$

$$+\sum_{n=5,7}^{N2}\left[\sum_{i=1}^{I2} B_{i+K2n,2}\, F_\theta(\rho;i) + \sum_{j=1}^{J2} B_{j+K2n+I2,2}\, G_\theta(\rho;j)\right]\cos n\theta$$

$$+\left\{B_{13}\left[-\bar{C}(3\rho-\rho^{-1})\right] + B_{23}(3\rho+\rho^{-3})\right\}\sin\theta$$

$$+\left[B_{33}(3\rho+\rho^{-3}) + B_{43}(\rho+\rho^{-5})\right]\sin 3\theta \qquad \text{AS}$$

$$+\sum_{n=5,7}^{N3}\left[\sum_{i=1}^{I3} B_{i+K3n,3}\, F_\theta(\rho;i) + \sum_{j=1}^{J3} B_{j+K3n+I3,3}\, G_\theta(\rho;j)\right]\sin n\theta$$

$$+\left[B_{14}(1) + B_{24}(1+\rho^{-4})\right]\sin 2\theta$$

$$\text{AA}$$

$$+\sum_{n=4,6}^{N4}\left[\sum_{i=1}^{I4} B_{i+K4n,4}\, F_\theta(\rho;i) + \sum_{j=1}^{J4} B_{j+K4n+I4,4}\, G_\theta(\rho;j)\right]\sin n\theta \qquad (66)$$

where $F_\theta(\rho;\, i) = i(i-1)\rho^{i-2}$

$$G_\theta(\rho;\, j) = j(j+1)\rho^{-(j+2)} \qquad (67)$$

$$R^2 \tau_{r\theta}(\rho,\theta) = \left[B_{31}(1-\rho^{-2}) + B_{41}(1-\rho^{-4})\right]\sin 2\theta$$

$$+ \sum_{n=4,6}^{N1}\left[\sum_{i=1}^{I1} B_{i+K1n,1}\, F_{r\theta}(\rho;i,n) + \sum_{j=1}^{J1} B_{j+K1n+I1,1}\, G_{r\theta}(\rho;j,n)\right]\sin n\theta \qquad \text{SS}$$

$$+\left\{B_{12}\left[\bar{C}(\rho-\rho^{-1})\right] + B_{22}(\rho-\rho^{-3})\right\}\sin\theta$$

$$+\left[B_{32}(3\rho-3\rho^{-3}) + B_{42}(\rho-\rho^{-5})\right]\sin 3\theta \qquad \text{SA}$$

$$+ \sum_{n=5,7}^{N2}\left[\sum_{i=1}^{I2} B_{i+K2n,2}\, F_{r\theta}(\rho;i,n) + \sum_{j=1}^{J2} B_{j+K2n+I2,2}\, G_{r\theta}(\rho;j,n)\right]\sin n\theta$$

$$+\left\{B_{13}\left[\bar{C}(\rho-\rho^{-1})\right] - B_{23}(\rho-\rho^{-3})\right\}\cos\theta$$

$$-\left[B_{33}(3\rho-3\rho^{-3}) + B_{43}(\rho-\rho^{-5})\right]\cos 3\theta \qquad \text{AS}$$

$$- \sum_{n=5,7}^{N3}\left[\sum_{i=1}^{I3} B_{i+K3n,3}\, F_{r\theta}(\rho;i,n) + \sum_{j=1}^{J3} B_{j+K3n+I3,3}\, G_{r\theta}(\rho;j,n)\right]\cos n\theta$$

$$-\left[B_{14}(1-\rho^{-2}) + B_{24}(1-\rho^{-4})\right]\cos 2\theta$$

$$- \sum_{n=4,6}^{N4}\left[\sum_{i=1}^{I4} B_{i+K4n,4}\, F_{r\theta}(\rho;i,n) + \sum_{j=1}^{J4} B_{j+K4n+I4,4}\, G_{r\theta}(\rho;j,n)\right]\cos n\theta \qquad \text{AA}$$

(68)

where

$$F_{r\theta}(\rho;i,n) = n(i-1)(\rho^{i-2} - \rho^{-2})$$

$$G_{r\theta}(\rho;j,n) = n(j+1)\left[\rho^{-2} - \rho^{-(j+2)}\right] \qquad (69)$$

SECTION 3

SPECIFIED BOUNDARY DISPLACEMENTS

3.1 EXTERIOR BOUNDARY

As mentioned earlier, the exterior boundary is completely S_u type, with displacements specified so as to maintain continuity with the adjacent elements. In the work which follows, it is assumed that each adjacent element contains only two nodes on the boundary common with the hole element, with linear displacement between nodes; see Figure 4a. Therefore, the displacement on the exterior boundary of the hole element will be specified as linear between nodes. If a nondimensional coordinate ξ is established such that $\xi = 0$ at node i and $\xi = 1$ at node j, then both displacement components between i and j will have the form

$$v(\xi) = v_i(1 - \xi) + v_j(\xi) \tag{70}$$

where v_i denotes the value of displacement v at node i. These specified displacements obviously satisfy the rigid body mode requirement of Equation (21) because the most general rigid body motion of an initially straight segment between nodes will result in linear displacements.

If the adjacent elements have a more complicated boundary displacement, this complementary virtual work formulation can very easily be modified. For example, suppose the adjacent elements contained three nodes per boundary common with the hole element and suppose the displacement is quadratic along that boundary; see Figure 4b. Then the displacement components on the hole external boundary between nodes i,j,k will have the form

$$v(\xi) = v_i \frac{1}{2}(\xi^2 - \xi) + v_j(1 - \xi^2) + v_k \frac{1}{2}(\xi^2 + \xi) \ . \tag{71}$$

If this portion of the boundary receives a rigid body displacement, then it will follow that

$$v_j = \frac{1}{2}(v_i + v_k) \tag{72}$$

Then if Equation (72) is substituted into Equation (71), the displacement at every point between nodes i and k is given by

$$v(\xi) = v_i \frac{1}{2}(1 - \xi) + v_k \frac{1}{2}(1 + \xi)$$

This linear displacement function shows that Equation (71) contains rigid body motions and does satisfy Equation (21).

3.2 INTERIOR BOUNDARY

Although the circular hole boundary is S_τ with respect to shear stress, it is S_u with respect to radial displacement. Therefore, it is necessary to specify the radial displacement, u_r, on the boundary. The generalized displacements will be the values of displacement at discrete points (the nodes) with displacements between nodes given by specified functions of position on the boundary.

Consider a segment of the boundary between two nodes; see Figure 5.

Let θ_i = initial angle for the segment

θ_f = final angle for the segment

Begin with the assumption

$$u_r(\theta) = u_i g_i(\theta) + u_f g_f(\theta) \tag{73}$$

subject to the requirements that

$$\begin{aligned} g_i(\theta_i) &= 1 \ , & g_i(\theta_f) &= 0 \\ g_f(\theta_i) &= 0 \ , & g_f(\theta_f) &= 1 \end{aligned} \tag{74}$$

which guarantee that Equation (73) does furnish the proper nodal displacements.

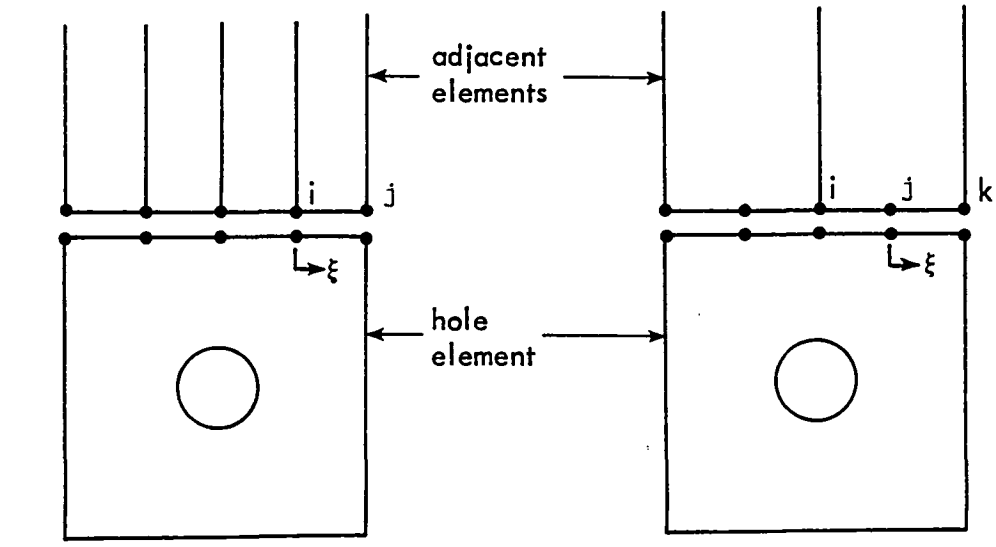

a) Linear Edge Displacements

b) Quadratic Edge Displacements

Figure 4. Displacement Continuity Between Adjacent Elements

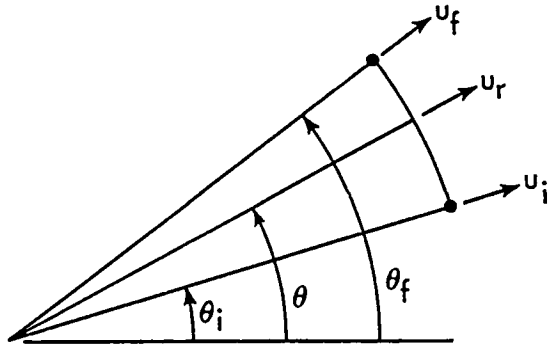

Figure 5. Segment of Hole Boundary Between Two Nodes

Now consider a rigid body motion of the hole boundary, with components $\bar{u}$, $\bar{v}$ in the x, y directions. The radial component of this rigid body motion will be

$$\bar{u}_r(\theta) = \bar{u} \cos\theta + \bar{v} \sin\theta \tag{75}$$

which means that the nodal values of rigid body displacement are

$$\begin{aligned} \bar{u}_i &= \bar{u} \cos\theta_i + \bar{v} \sin\theta_i \\ \bar{u}_f &= \bar{u} \cos\theta_f + \bar{v} \sin\theta_f \end{aligned} \tag{76}$$

If these nodal values are substituted into Equation (73) the displacement between nodes is given by

$$u_r(\theta) = (\bar{u} \cos\theta_i + \bar{v} \sin\theta_i)\, g_i(\theta) + (\bar{u} \cos\theta_f + \bar{v} \sin\theta_f)\, g_f(\theta)$$

or

$$u_r(\theta) = \bar{u}\left[g_i(\theta) \cos\theta_i + g_f(\theta) \cos\theta_f\right] + \bar{v}\left[g_i(\theta) \sin\theta_i + g_f(\theta) \sin\theta_f\right] \tag{77}$$

If Equation (73) is to contain rigid body modes, it is necessary that Equation (77) have the same form as Equation (75) which represents rigid body motion between nodes. This leads finally to the requirement that

$$\begin{bmatrix} \cos\theta_i & \cos\theta_f \\ \sin\theta_i & \sin\theta_f \end{bmatrix} \begin{Bmatrix} g_i(\theta) \\ g_f(\theta) \end{Bmatrix} = \begin{Bmatrix} \cos\theta \\ \sin\theta \end{Bmatrix}$$

which gives the following unique expressions for $g_i(\theta)$ and $g_f(\theta)$:

$$g_i(\theta) = \frac{\sin(\theta_f - \theta)}{\sin(\theta_f - \theta_i)} \quad , \qquad g_f(\theta) = \frac{\sin(\theta - \theta_i)}{\sin(\theta_f - \theta_i)} \tag{78}$$

It can be seen that Equations(78) satisfy Equations (74). Therefore, the final form of the specified radial displacement between nodes is as follows:

$$u_r(\theta) = u_i \frac{\sin(\theta_f - \theta)}{\sin(\theta_f - \theta_i)} + u_f \frac{\sin(\theta - \theta_i)}{\sin(\theta_f - \theta_i)} \tag{79}$$

This assumption provides proper nodal values and does contain rigid body motions, which guarantees that Equation (21) is satisfied on the hole boundary.

If the boundary nodes are given the same radial displacement, it would be desirable for the displacement u_r to be uniform between nodes. In order to see if Equation (79) contains uniform displacement, set $u_i = u_f = u$ and get

$$u_r(\theta) = u \frac{1}{\sin(\theta_f - \theta_i)} \left[\sin(\theta_f - \theta) + \sin(\theta - \theta_i)\right] \tag{80}$$

Unfortunately, Equation (80) does not reduce to uniform displacement, which means that Equation (79) does not contain uniform displacement. However, if $(\theta_f - \theta_i) \ll 1$, it can be shown that Equation (80) gives the approximate result

$$u_r(\theta) = u$$

Therefore, Equation (79) will give essentially uniform displacement as the arc length between nodes becomes sufficiently small.

The following displacement function does include uniform displacement for any arc length:

$$u_r(\theta) = \frac{u_i}{2\sin(\theta_f - \theta_i)} \left[\sin(\theta_f - \theta) - \sin(\theta - \theta_i) + \sin(\theta_f - \theta_i)\right]$$

$$+ \frac{u_f}{2\sin(\theta_f - \theta_i)} \left[\sin(\theta - \theta_i) - \sin(\theta_f - \theta) + \sin(\theta_f - \theta_i)\right] \tag{81}$$

However, Equation (81) does not include rigid body motions.

In conclusion, it is impossible to devise a displacement function which contains both rigid body motion and uniform displacement. It is much more useful to include rigid body motion, so Equation (79) will be used in the following work.

SECTION 4

DEVELOPMENT OF THE ELEMENT STIFFNESS MATRIX

4.1 STRESS STATE DUE TO IMPOSED BOUNDARY DISPLACEMENTS

Begin with the expression for complementary virtual work, as given in Equation (7) and repeated below:

$$CVW = t\int_A \lfloor \delta\tau \rfloor \{\epsilon\}\, dA - t\int_{S_u} \lfloor \delta T \rfloor \{\bar{u}\}\, ds$$

In polar coordinates (Figure 1), the differential area element can be expressed as follows in terms of the nondimensional $\rho \equiv \frac{r}{R}$

$$dA = r dr d\theta = R^2 \rho\, d\rho\, d\theta \tag{82}$$

and the differential boundary length can be written as

$$ds = R f(\theta) d\theta \tag{83}$$

where the function $f(\theta)$ depends upon location on the boundary.

The real strains, $\{R^2\epsilon\}$, are expressed in terms of real stresses, $\{R^2\tau\}$, through the stress-strain relations in polar coordinates, as given in Equations (43),(44), and (39):

$$\{R^2\epsilon\} = [C_{r\theta}]\, \{R^2\tau\}$$

Then the CVW can be written as

$$CVW = \frac{t}{R^2}\int_A \lfloor R^2\delta\tau \rfloor [C_{r\theta}]\, \{R^2\tau\}\, \rho\, dp\, d\theta - \frac{t}{R}\int_S \lfloor R^2\delta T \rfloor \{\bar{u}\} f(\theta) d\theta \tag{84}$$

Assume $$\{R^2\delta\tau\} = \sum_{j=1}^{NSC} [\Lambda^j(\rho, \theta)]\, \{a^j\} \tag{85}$$

$$\{R^2 \delta T\} = \sum_{j=1}^{NSC} [T^j(\theta)] \{a^j\} \tag{86}$$

$$\{R^2 \tau\} = \sum_{j=1}^{NSC} [\Lambda^j(\rho, \theta)] \{B^j\} \tag{87}$$

$$\{\bar{u}\} = \sum_{j=1}^{NSC} [\zeta^j(\theta)] \{\bar{q}^j\} \tag{88}$$

These assumptions are consistent with what was shown earlier in Equations (8), (10), (11), and (12), with expanded notation to recognize that each stress, surface traction, and displacement vector can be written as the sum of four symmetry condition vectors. In Equations (85) through (88), the superscript j denotes symmetry condition number; and NSC denotes the number of symmetry conditions to be considered in a particular problem. In general, NSC will be equal to four; however, if the problem is known to contain only certain symmetry conditions, then NSC can take on the proper and limited set of values.

If Equations (85) through (88) are substituted into Equation (84), the result is

$$CVW = \sum_{j=1}^{NSC} \sum_{k=1}^{NSC} \lfloor a^j \rfloor \left\{ \begin{array}{l} \left[\frac{t}{R^2} \int_A [\Lambda^j]^T [C_{r\theta}] [\Lambda^k] \rho d\rho d\theta \right] \{B^k\} \\ - \left[\frac{t}{R} \int_{S_u} [T^j]^T [\zeta^k] f(\theta) d\theta \right] \{\bar{q}^k\} \end{array} \right\} \tag{89}$$

Now, the domain and boundary are symmetric about both the x and y axes. Therefore, a boundary integration of the product of symmetric (antisymmetric) tractions and antisymmetric (symmetric) displacements will vanish. Likewise, a domain integration of the product of symmetric (antisymmetric) stresses and antisymmetric (symmetric) strains will vanish. Also, note that because the x, y axes are material axes for homogeneous and orthotropic material, it follows that symmetric (antisymmetric)

stresses will result in symmetric (antisymmetric) strains. Therefore, because of the symmetry properties of domain, boundary, and integrands, it follows that

$$\int_A [\Lambda^j]^T [C_{r\theta}] [\Lambda^k] \rho \, d\rho \, d\theta = 0, \quad \text{if } j \neq k$$

$$\int_{S_u} [\Gamma^j]^T [\zeta^k] f(\theta) \, d\theta = 0, \quad \text{if } j \neq k \tag{90}$$

$$\int_A [\Lambda^j]^T [C_{r\theta}] [\Lambda^j] \rho \, d\rho \, d\theta = 4 \int_{\text{Quadrant}} [\Lambda^j]^T [C_{r\theta}] [\Lambda^j] \rho \, d\rho \, d\theta$$

$$\int_{S_u} [\Gamma^j]^T [\zeta^j] f(\theta) \, d\theta = 4 \int_{\text{Quadrant}} [\Gamma^j]^T [\zeta^j] f(\theta) \, d\theta \tag{91}$$

Define

$$[H^j] = \int_{\text{Quadrant}} [\Lambda^j]^T [C_{r\theta}] [\Lambda^j] \rho \, d\rho \, d\theta \tag{92}$$

$$[G^j] = \int_{\text{Quadrant}} [\Gamma^j]^T [\zeta^j] f(\theta) \, d\theta \tag{93}$$

After substituting Equations (90) through (93) into Equation (89), the CVW can be written as

$$\text{CVW} = 4 \frac{t}{R} \sum_{j=1}^{NSC} \lfloor a^j \rfloor \left\{ \frac{1}{R} [H^j] \{B^j\} - [G^j] \{\bar{q}^j\} \right\}$$

If CVW = 0 for every $\lfloor a^j \rfloor$, conclude that

$$\frac{1}{R} [H^j] \{B^j\} - [G^j] \{\bar{q}^j\} = \{0\}, \quad j = 1, 2, 3, 4$$

or

$$[B^j] = R\,[H^j]^{-1}\,[G^j]\,\{\bar{q}^j\}\ , \quad j = 1, 2, 3, 4$$

Define $$[BQ^j] = [H^j]^{-1}\,[G^j]\ , \qquad j = 1, 2, 3, 4 \tag{94}$$

Therefore, $$[B^j] = R\,[BQ^j]\,\{\bar{q}^j\}\ , \qquad j = 1, 2, 3, 4 \tag{95}$$

The final expression for the stress state is found by substituting Equation (95) into Equation (87) and solving for $\{\tau\}$ to give

$$\left\{\tau\,(\rho,\theta)\right\} = \frac{1}{R} \sum_{j=1}^{NSC} [\Lambda^j(\rho,\theta)]\,[BQ^j]\,\{\bar{q}^j\} \tag{96}$$

Equation (96) will give the stress state at any point in the domain due to imposed boundary nodal displacements. Note that the nodal displacements are expressed in terms of the four symmetry condition components.

4.2 DEVELOPMENT OF STIFFNESS MATRIX

In the anticipated applications of the hole finite element, the total or overall structural problem will be solved through a displacement formulation which can be most generally based on the principle of virtual work. Therefore, the hole element solution of Equations (94), (95), and (96), based on complementary virtual work, must now be placed into a form which is compatible with the formulation for the remainder of the structure. This is done by developing a stiffness matrix for the hole element which can then be handled in a routine fashion in the displacement based finite element programs.

Begin with the expression for the internal virtual work done by an equilibrium real stress field moving through compatible virtual strains:

$$\delta W_i = -t \int_A \lfloor \delta\epsilon \rfloor\,\{\tau\}\,dA \tag{97}$$

For use in a displacement formulation, the real stresses $\{\bar{\tau}\}$ must be expressed in terms of real nodal displacements; and the virtual strains $\{\delta\epsilon\}$ must be expressed in terms of virtual nodal displacements. But this relationship between nodal displacements and stresses is precisely what is given, to the best approximation possible, by Equations (94), (95), and (96). Therefore, Equation (97) can be rewritten in terms of displacements by first introducing virtual strain-virtual stress relations in the form of Equation (34) and then substituting the stress-displacement relations of Equation (96):

$$\delta W_i = -\frac{t}{R^2}\int_A \left\lfloor R^2\,\delta\bar{\tau}\right\rfloor [C_{r\theta}]\,\{R^2\,\bar{\tau}\}\,\rho\,d\rho\,d\theta$$

$$\delta W_i = -\frac{t}{R^2}\sum_{j=1}^{NSC}\sum_{k=1}^{NSC} R^2\left\lfloor \delta q^j\right\rfloor [BQ^j]^T\left[\int_A [\Lambda^j]^T [C_{r\theta}]\,[\Lambda^k]\,dA\right][BQ^k]\,\{\bar{q}^k\} \qquad (98)$$

After accounting for the symmetry properties of domain and integrand, and after introducing Equation (92), it follows that

$$\delta W_i = -\sum_{j=1}^{NSC}\left\lfloor \delta q^j\right\rfloor\left[4t\,[BQ^j]^T [H^j][BQ^j]\right]\{\bar{q}^j\} \qquad (99)$$

Define $$[KQ^j] = t\,[BQ^j]^T\,[H^j][BQ^j] \qquad (100)$$

Finally, $$\delta W_i = -\sum_{j=1}^{NSC}\left\lfloor \delta q^j\right\rfloor\left[4\,[KQ^j]\right]\{\bar{q}^j\} \qquad (101)$$

After comparing Equation (101) with the result which would have been obtained through a virtual work development of δW_i, it is clear that the array $4[KQ^j]$ is the stiffness matrix associated with displacements in the j^{th} symmetry condition.

More precisely, Equation (100) defines the complementary virtual work approximation to one-fourth of the stiffness matrix associated with boundary displacements in the j^{th} symmetry condition.

4.3 THREE TYPES OF HOLE ELEMENTS

The hole finite element will generally be employed as shown in Figure 6; that is, the total square domain will be included in the finite element model of the structure. However, if the problem has known symmetries in structure and loading, then it is possible to achieve significant economies in both formulation and solution by working with only a portion of the structure.

For systems which are known to possess only one of the four symmetry conditions, the simplifications begin with Equations (85) through (88) in which the summations over all symmetry conditions are eliminated; all quantities are expressed immediately in terms of only the one known symmetry state. Further simplification is achieved in the finite element model of the structure, as shown in Figure 7 for a typical case which is SS in both structure and loading. It is necessary to consider only one quadrant of the structure, which means that it is necessary to consider only one quadrant of the hole finite element when developing the stiffness matrix.

Systems with symmetry or antisymmetry about only one axis can be considered to be the sum of the appropriate two symmetry conditions, which again simplifies Equations (85) through (88). Figure 8 shows a case with symmetry about the y-axis, which is therefore a combination of SS and AS. The model can be simplified to only one half of the structure, which means that only one-half of the hole finite element is necessary.

Evidently there are three different types of hole elements which could be incorporated in a finite element model - the complete or total element in Figure 6, the half element in Figure 8, and the quarter element in Figure 7. With appropriate modifications to the symmetry condition summation, Equation (96) gives the stresses for each type of element; no adjustments are necessary. However, the stiffness matrix expressions in Equations (100) and (101) must be modified for the quarter and half elements.

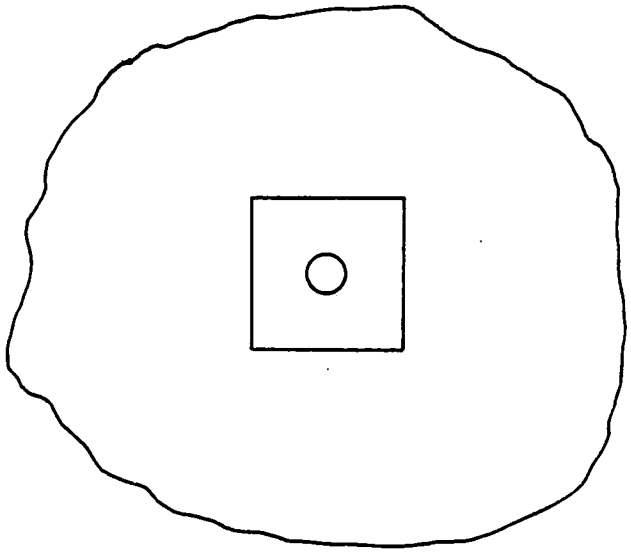

Figure 6. General Problem Requiring the Total Hole Element

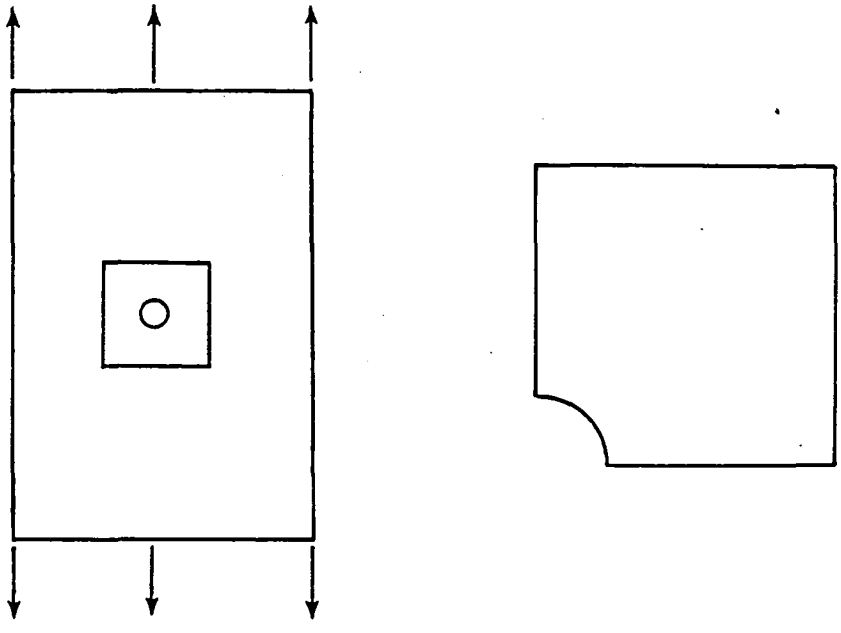

Figure 7. Symmetric-Symmetric Problem, Permitting Use of the Quadrant Hole Element

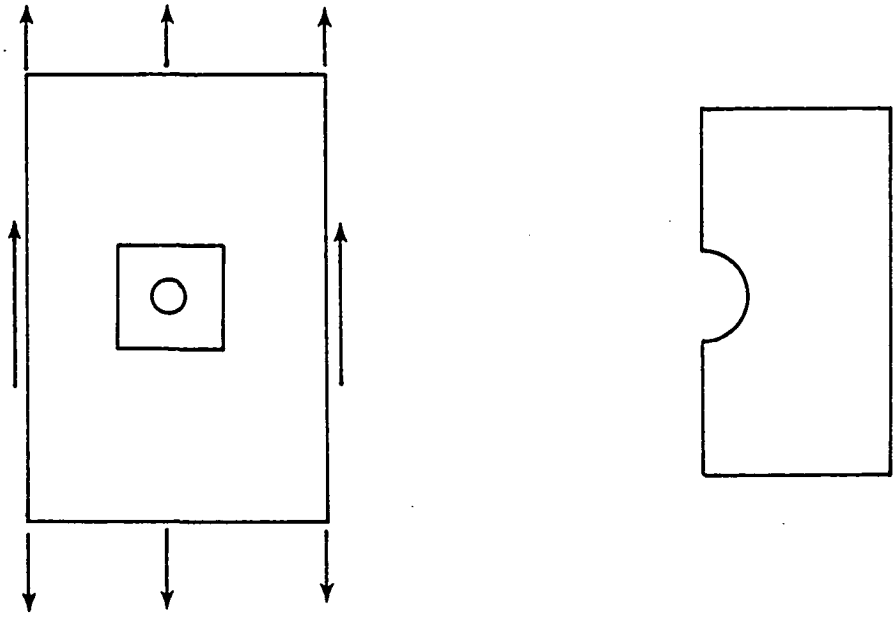

Figure 8. Problem with Symmetry About One Axis, Permitting Use of the Half Hole Element

In Equation (98) it was assumed that the domain integration was taken over the complete hole element. Then

$$\int_A (\quad) dA = 4 \int_{\text{Quadrant}} (\quad) dA$$

which accounts for the multiplicative factor of 4 in Equation (99). Obviously, if the structural problem is to be solved with the half element in Figure 8, then

$$\int_A (\quad) dA = 2 \int_{\text{Quadrant}} (\quad) dA \quad ;$$

and with a quarter element, the physical domain is equal to the quadrant used for integration.

It is now possible to give a physical interpretation to $[KQ^j]$ in Equation (100). Clearly, $[KQ^j]$ is the quadrant element stiffness matrix associated with displacements in the j^{th} symmetry condition.

These results concerning stiffness matrices can be summarized in terms of $[KQ^j]$ of Equation (100), as follows:

for a quadrant element with j^{th} symmetry condition,

$$[KQ^j] = [KQ^j] \tag{102}$$

$$\delta W_i = - \left\lfloor \delta q^j \right\rfloor [KQ^j] \{\bar{q}^j\} \tag{103}$$

for a half element with superposition of two appropriate symmetry conditions,

$$[KH^j] = 2[KQ^j], \text{ for two values of } j \tag{104}$$

$$\delta W_i = -\sum \left\lfloor \delta q^j \right\rfloor [KH^j] \{\bar{q}^j\} \tag{105}$$

for a total element, requiring all symmetry conditions

$$[KT^j] = 4[KQ^j] \ , \quad j = 1, 2, 3, 4 \tag{106}$$

$$\delta W_i = - \sum_{j=1}^{4} \left[\delta q^j\right] [KT^j] \{\bar{q}^j\} \quad . \tag{107}$$

For possible future use, Equations (103), (105), and (107) can be written as

$$\delta W_i = -\sum \left[\delta q^j\right] \left[M[KQ^j]\right] \{\bar{q}^j\} \tag{108}$$

where the summation is over appropriate values and M = 1, 2, or 4 depending upon element type.

4.4 TRANSFORMATION OF DISPLACEMENTS

If the hole finite element is to be combined with other elements and a problem solved with a conventional displacement based program, then it is necessary that the nodal displacements for adjacent elements must be identical at nodes where continuity is required. This nodal continuity is most easily achieved if the nodal displacements for the adjacent elements are expressed in the same coodinate system and have the same physical meaning. In the following discussion, it is assumed that adjacent element displacements are in the same coordinate system (either x, y system or radial) so that it is only necessary to consider the physical meaning of the measures of displacement. The two possible meanings are described as either the symmetry condition displacements or the general state displacements.

Now, for problems with a single symmetry condition which are to be solved with the quadrant element, there is an identify transformation between symmetry condition displacements and the general state displacements. That is, if the system is, say, SS in character, then the general displacements will have zero contribution from SA, AS, and AA; and the general displacement will be identical to the symmetry condition

displacement. In this case, the quadrant element stiffness matrix is given by Equation (100); no further modification is necessary, and the hole element quadrant stiffness can be immediately merged with adjacent element stiffness matrices. Then the problem can be solved with standard displacement based finite element programs.

However, for the half element and total element, the displacements in Equations (105) and (107) are symmetry condition displacements; and these are not the same as general state displacements which represent the superposition of two or four symmetry condition displacements. Therefore, the symmetry condition displacements will be transformed to general displacements before attempting to merge stiffness matrices. The details of the transformations depend upon the number of boundary nodes, but the basic features will be presented for a simple case of each type of element.

First consider the total element shown in Figure 9. Note that the nodal numbers begin at the first quadrant corner node and proceed counterclockwise around the element until all nodes on the outer boundary have been numbered. The next node number is assigned to the circular boundary node at $\theta = 0°$, and numbering continues counterclockwise. Because the external boundary is entirely S_u, there are two displacement degrees of freedom at each exterior boundary node. However, there is only the one radial degree of freedom at each interior node. On the exterior boundary, positive displacements are in the positive coordinate directions. On the interior boundary, positive displacements are outward. These sign conventions and conventions for nodal and displacement numbering are followed for all arrangements of nodes.

Figures 10a, 11a, 12a, and 13a show the nodal displacement patterns associated with SS, SA, AS, and AA displacement fields, respectively. Note that the independent nodal displacements are selected to be in the first quadrant, with all other nodal displacements expressed in terms of the independent values. Also note that the quadrant nodal displacements are numbered beginning at $\theta = 0°$ on the external boundary and returning to $\theta = 0°$ on the inner hole boundary. This convention is followed for all arrangements of nodes.

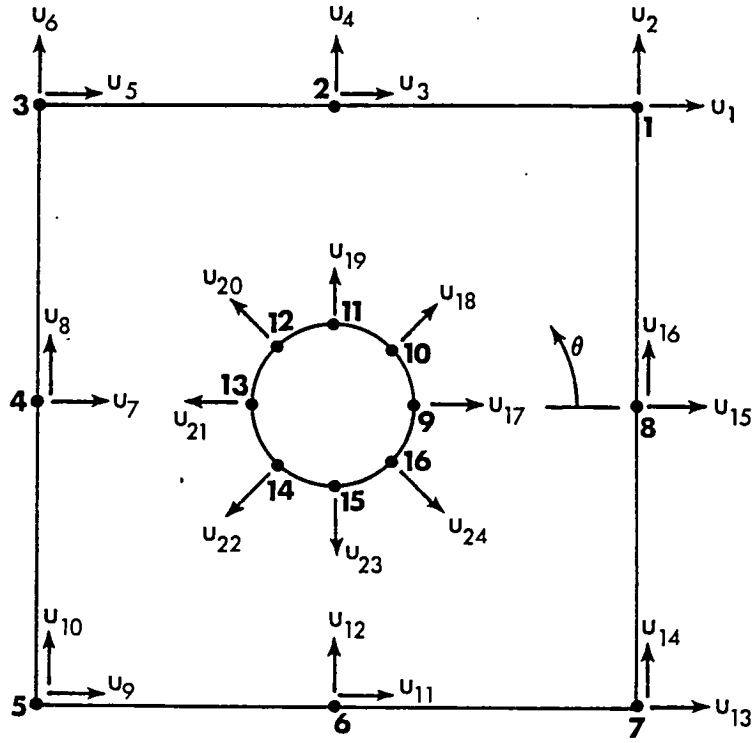

Figure 9. Node and Displacement Numbering for Total Element

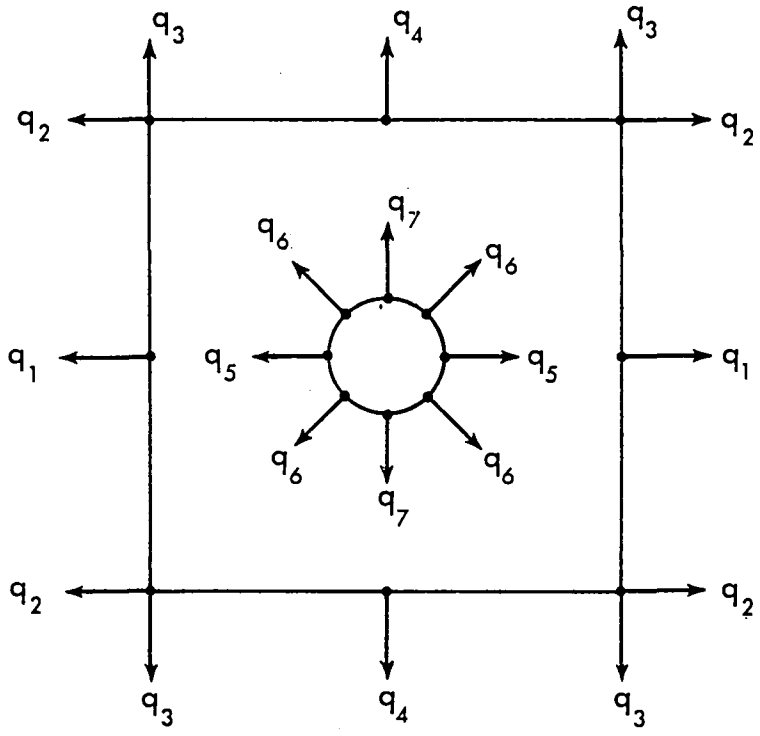

a) SS Displacement Field for Total Element

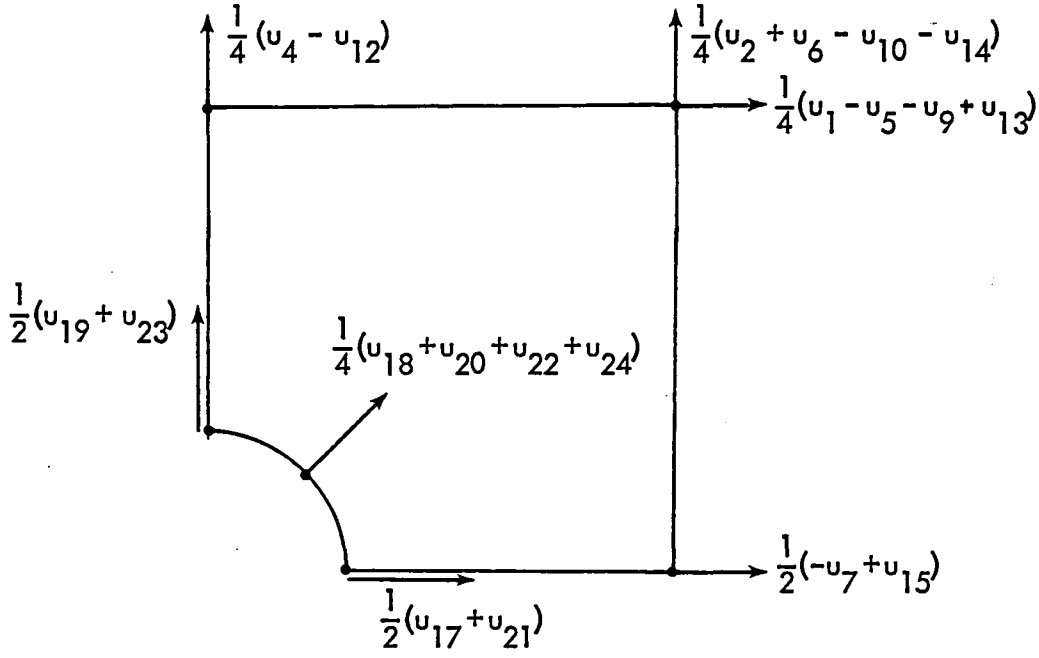

b) SS Decomposition of General Displacement Field

Figure 10. Symmetric-Symmetric Displacements for Total Element

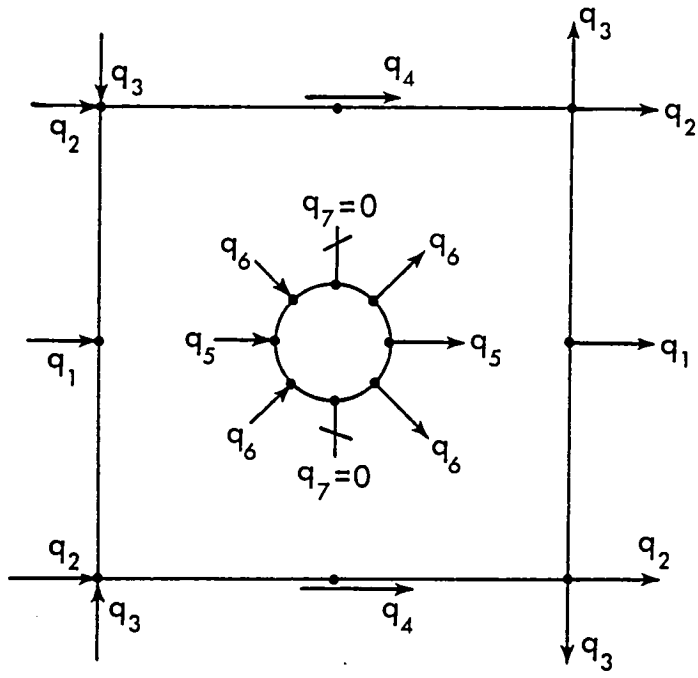

a) SA Displacement Field for Total Element

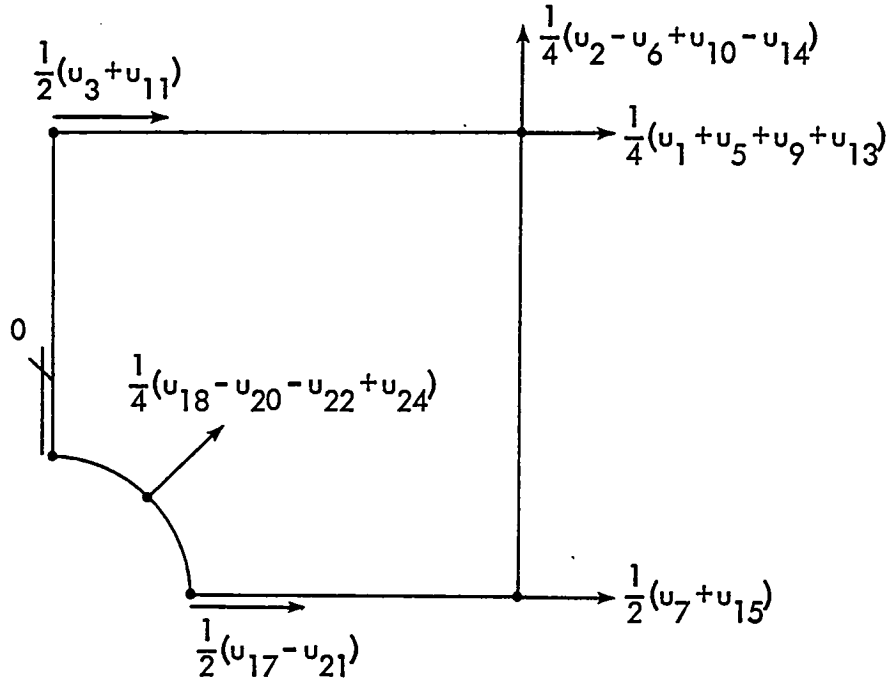

b) SA Decomposition of General Displacement Field

Figure 11. Symmetric-Antisymmetric Displacements for Total Element

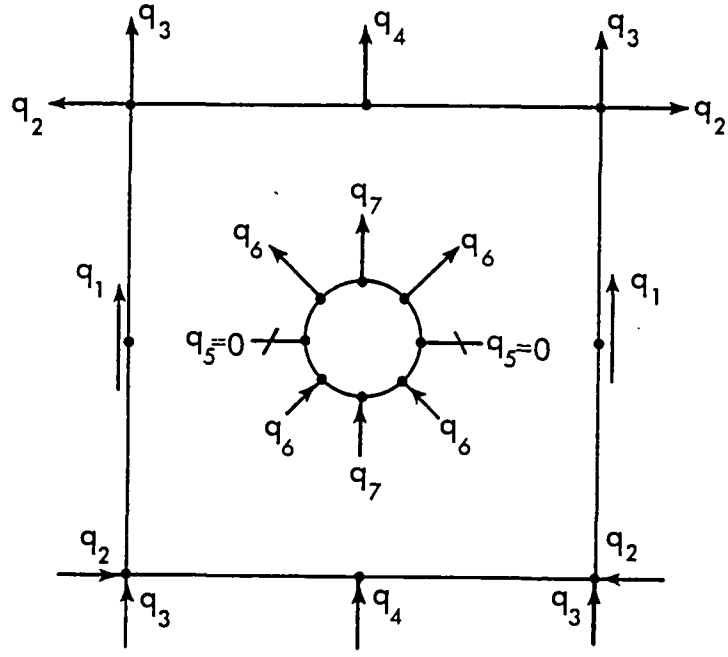

a) AS Displacement Field for Total Element

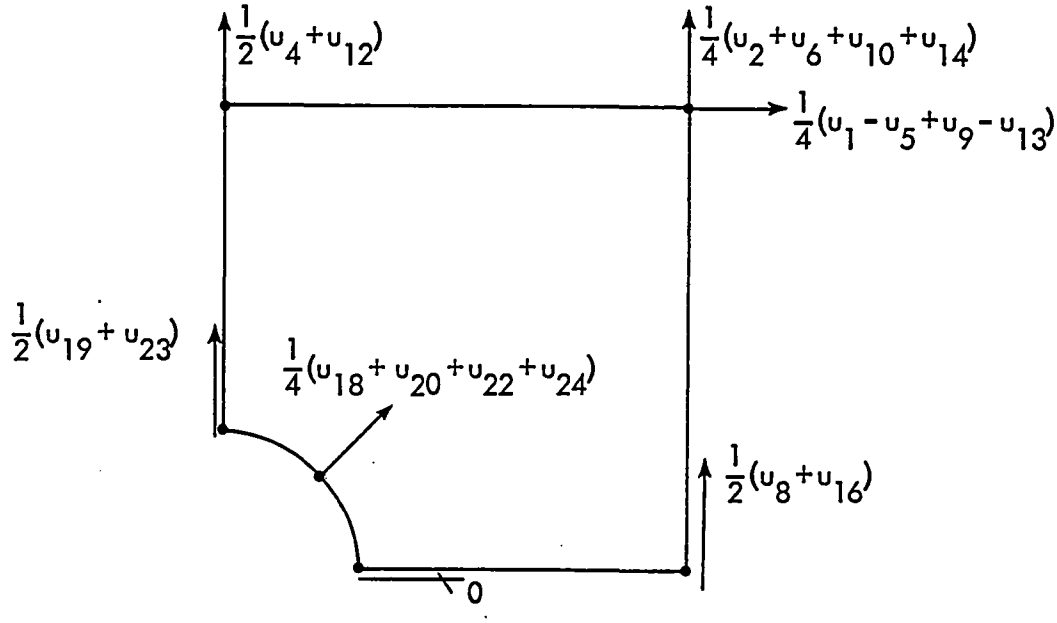

b) AS Decomposition of General Displacement Field

Figure 12. Antisymmetric-Symmetric Displacements for Total Element

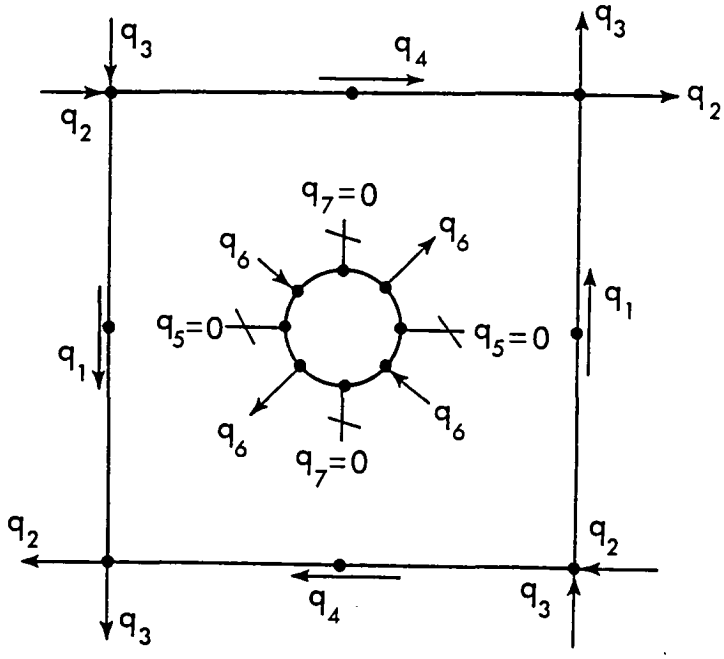

a) AA Displacement Field for Total Element

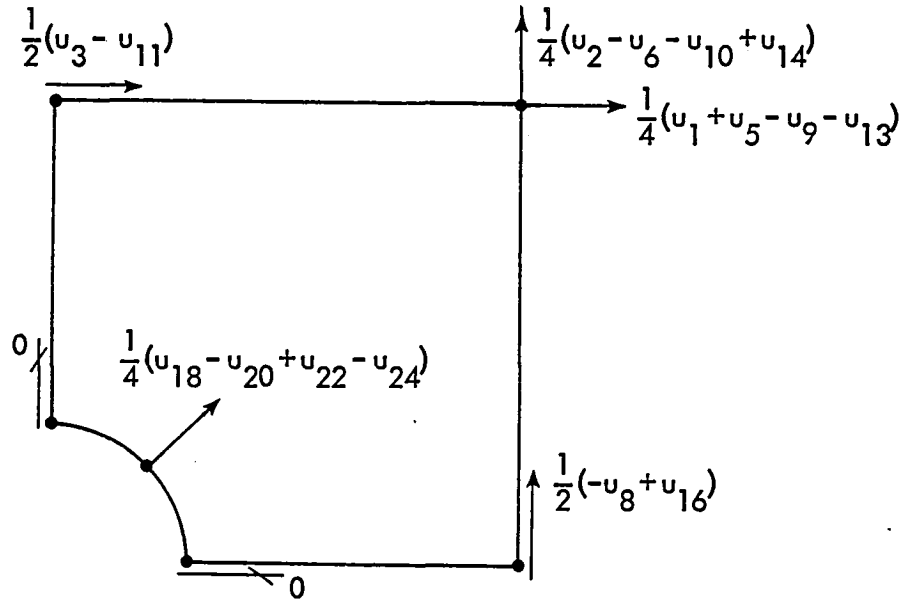

b) AA Decomposition of General Displacement Field

Figure 13. Antisymmetric-Antisymmetric Displacements for Total Element

Figures 10b, 11b, 12b, and 13b give the relationships between the independent nodal displacements and the general nodal displacements of Figure 9. As a check on these relationships, it can be confirmed that the summation of Figures 10b, 11b, 12b, and 13b, extended to the other three quadrants, will indeed give Figure 9. For example, consider the x-direction displacement of the first quadrant corner node. Then

$$(q_2)_{SS} + (q_2)_{SA} + (q_2)_{AS} + (q_2)_{AA} = \frac{1}{4}(u_1 - u_5 - u_9 + u_{13}) +$$

$$\frac{1}{4}(u_1 + u_5 + u_9 + u_{13}) + \frac{1}{4}(u_1 - u_5 + u_9 - u_{13}) + \frac{1}{4}(u_1 + u_5 - u_9 - u_{13}) = u_1$$

as required. As one final example, consider the y-direction displacement of the exterior node at $\theta = 180°$. Then

$$(q_1)_{AS} - (q_1)_{AA} = \frac{1}{2}(u_8 + u_{16}) - \frac{1}{2}(-u_8 + u_{16}) = u_8$$

as required.

A half-element with symmetry about the y axis is shown in Figure 14. Node numbering begins at the lower left exterior corner, proceeds around the outer boundary, and returns to the inner boundary at $\phi = 0°$. There are two degrees of freedom at each exterior node except the nodes on the symmetry axis, which have only one displacement. Positive displacements are as shown in Figure 14 and described for the total element.

The general state is a superposition of SS and AS due to assumption of symmetry about the y-axis; see Figures 15 and 16. Again, the independent displacements are selected to be in the first quadrant, with the same numbering scheme described earlier. As an example of the superposition, consider the radial displacement of the inner node at $\phi = 45°$.

$$(q_6)_{SS} - (q_6)_{AS} = \frac{1}{2}(u_{10} + u_{12}) - \frac{1}{2}(-u_{10} + u_{12}) = u_{10}$$

as required.

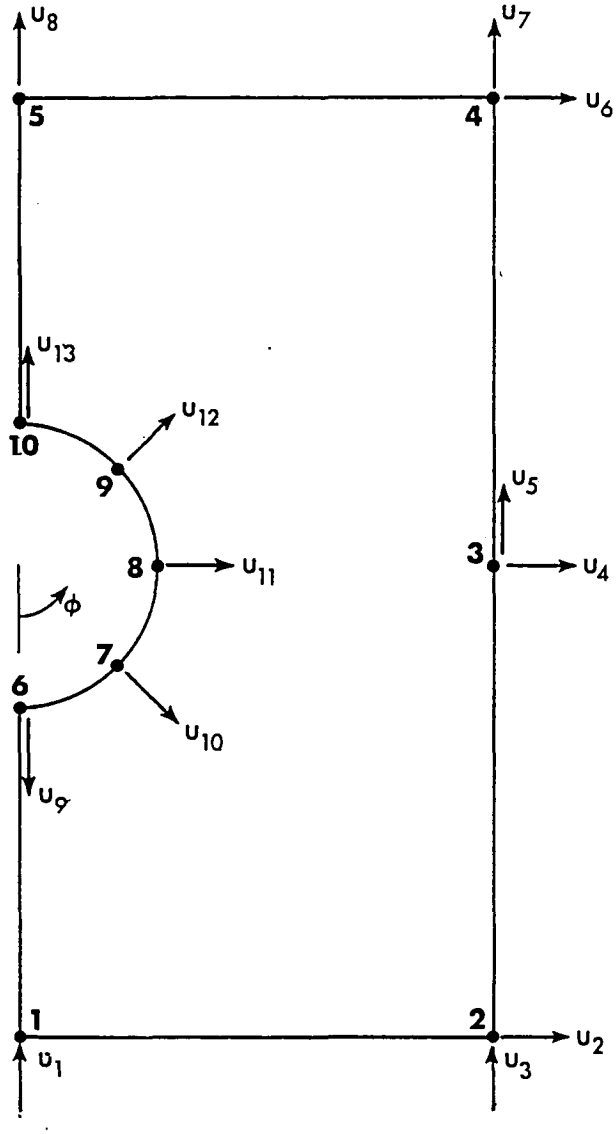

Figure 14. Node and Displacement Numbering for Half Element

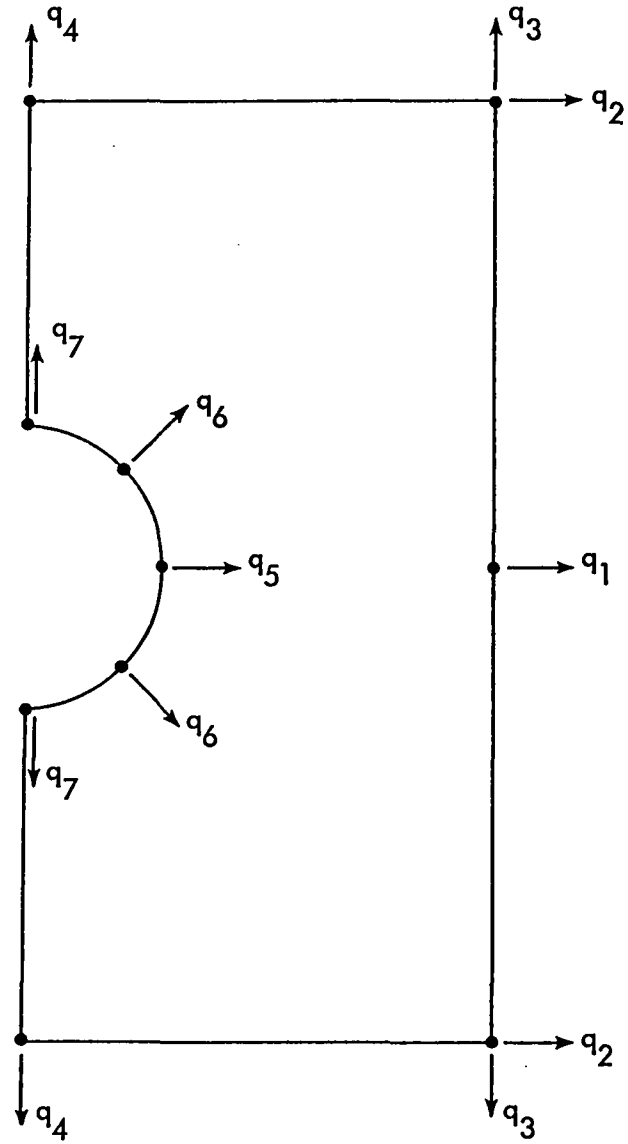

a) SS Displacements for Half Element

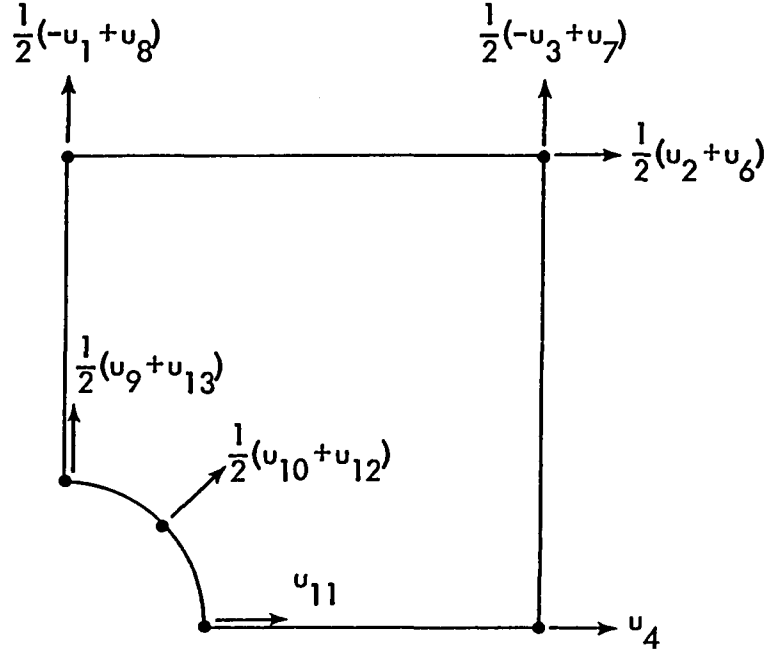

b) SS Decomposition of General Displacements

Figure 15. Symmetric-Symmetric Displacements for Half Element

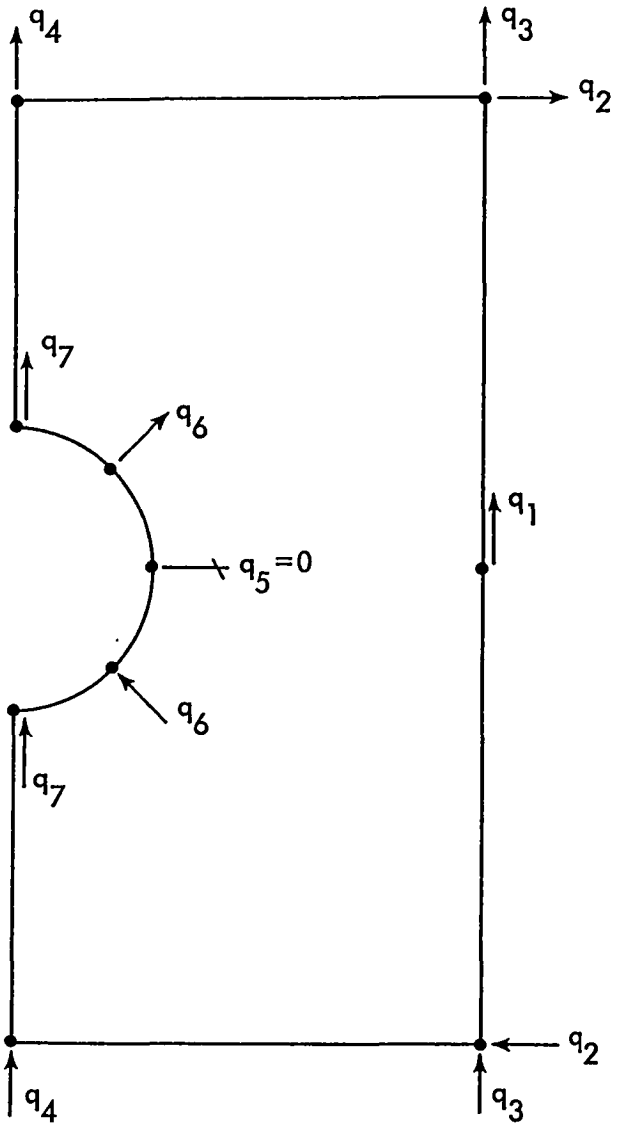

a) AS Displacements for Half Element

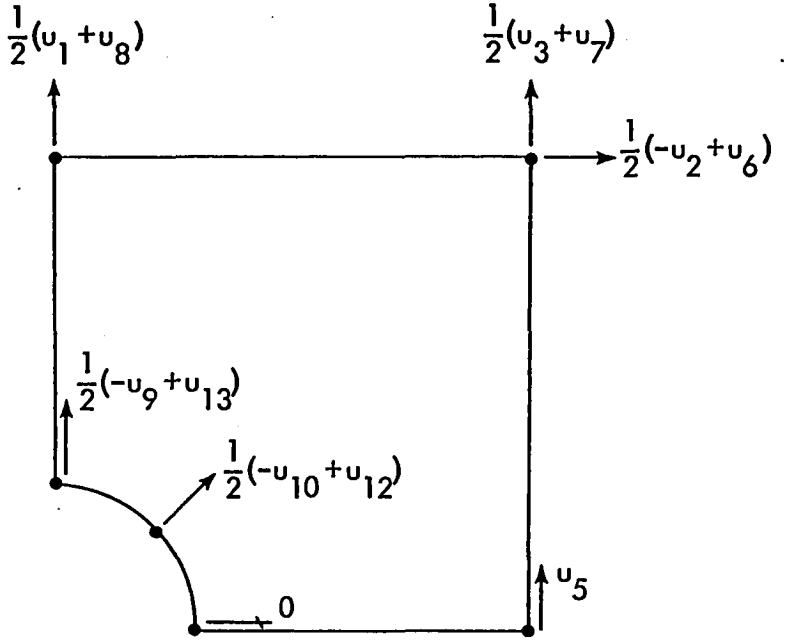

b) AS Decomposition of General Displacements

Figure 16. Antisymmetric-Symmetric Displacements for Half Element

It is now clear that for each symmetry condition, the general state nodal displacement, $\{u\}$, and the symmetry condition nodal displacements, $\{q^j\}$, are related by

$$\{q^j\} = [A^j]\{u\} \tag{109}$$

where the transformation array $[A^j]$ depends upon the type of hole element (total or half) and the details of the nodal arrangement. Recall that for a quadrant element, $[A^j] \equiv [I]$, the identify matrix.

4.5 TRANSFORMATION OF STIFFNESS MATRIX AND STRESS MATRIX

The necessary transformation of the stiffness matrix is established by substituting Equation (109) into Equation (108) in order to express the internal work in general state displacements.

$$\delta W_i = -\sum \lfloor \delta u \rfloor [A^j]^T \left[M[KQ^j] \right] [A^j]\{\bar{u}\}$$

Define $$[K^j] = [A^j]^T [KQ^j][A^j] \tag{110}$$

Then $$\delta W_i = -\lfloor \delta u \rfloor \left[M \sum [K^j] \right] \{\bar{u}\}$$

Define $$[K] = M \sum [K^j] \tag{111}$$

and it is clear that Equation (111) supplies the proper hole element stiffness matrix associated with general state displacements and this stiffness matrix is suitable for standard treatment by displacement based programs.

Equation (96) gives the stress state in terms of symmetry condition displacements, $\{\bar{q}^j\}$. This equation can also be transformed to general state displacements as follows:

$$\{\tau\} = \frac{1}{R} \sum [\Lambda^j][BQ^j][A^j]\{\bar{u}\} \tag{112}$$

A more efficient evaluation of the stiffness matrix is possible by substituting Equations (94) and (100) into Equation (110):

$$[K^j] = t[A^j]^T [G^j]^T [H^j]^{-T} [H^j][H^j]^{-1} [G^j][A^j]$$

Define $$[\bar{G}^j] = [G^j][A^j] \tag{113}$$

Then, $$[K^j] = t[\bar{G}^j]^T [H^j]^{-1} [\bar{G}^j] \tag{114}$$

where it is recognized that array $[H^j]$, as defined by Equation (92), is symmetric.

Equation (112) can also be reformulated as follows:

$$\{\tau\} = \frac{1}{R} \sum [\Lambda^j][H^j]^{-1} [G^j][A^j]\{\bar{u}\}$$

Define $$[S^j] = [H^j]^{-1} [G^j][A^j] = [H^j]^{-1} [\bar{G}^j] \tag{115}$$

Then, $$\{\tau(\rho, \theta)\} = \frac{1}{R} \sum [\Lambda^j(\rho, \theta)][S^j]\{\bar{u}\} \tag{116}$$

4.6 COMMENTS ON PROCEDURE

The essential feature of the development presented in this section is the realization that symmetry conditions exist for stress, tractions, and displacements and then exploiting this feature to the fullest. This permitted the derivation of stiffness and stress matrices for the total hole element with the work integrations limited to just one quadrant of the element. This is a significant savings of computational effort compared to those formulations which integrate over the total element.

When solving problems with the quadrant or half elements shown in Figures 7 and 8, the internal stresses are guaranteed to be continuous across the symmetry boundaries. This is true because the solution is in reality based on a total element which has correct symmetry conditions imposed; and the stresses are defined continuously in

the total domain. This can be contrasted with an alternative approach which begins with a true quarter element with no reference to the total domain. If the complementary virtual work procedure is used to develop the quarter element stiffness matrix, and if four of these quadrants are then combined properly to model a total element, there will be traction discontinuities across those boundaries which are interior to the total element; and these discontinuities could cause troubles when attempting to evaluate stresses in the interior of the total element.

However, it should be noted that the imposition of additional specified displacements along interior lines will tend to stiffen the total finite element when compared to an element with no specified interior displacements. The implications of this with regard to the use of true quarter or octant elements should be explored numerically.

SECTION 5

DESCRIPTION OF THE COMPUTER CODE

5.1 INTRODUCTION

Computer code has been prepared to perform all calculations leading to the stiffness matrix of Equations(114) and (111) and the stress equations of Equation (116). This chapter describes certain features of the code without going into details of the programming.

5.2 ELEMENT GEOMETRY

The number of nodes on both the exterior and interior boundaries of the hole element can be specified by the program user. Because all integrations are performed in the first quadrant only, there are the geometric constraints that exterior nodes must be placed at the four corners and at the four side midpoints, and interior nodes must be placed at $\theta = 0°$, $90°$, $180°$, and $270°$; see Figure 17.

The boundaries of the quadrant are divided into sides 1, 2, and 3, as shown in Figure 17. It is assumed that the nodes are equally spaced along each side, so that the nodal information is input by specifying the number of segments in each side of the quadrant; this is done through an array $\lfloor NSEG \rfloor$. For example, in Figure 17, $\lfloor NSEG \rfloor = \lfloor 2 \quad 1 \quad 3 \rfloor$.

It is assumed that the hole is centered in the square. The ratio of square dimension, 2L, to hole diameter, 2R, can be varied as desired by the user; however, it is recommended that $\frac{L}{R} \cong 2$, with $\frac{L}{R} = 4$, if possible.

5.3 NUMBER OF STRESS COEFFICIENTS

In Section 1.6 it is shown that there is a relationship between the number of degrees of freedom and the number of stress coefficients. What was shown there for a general state of deformation must also be true for each of the separate symmetry condition states.

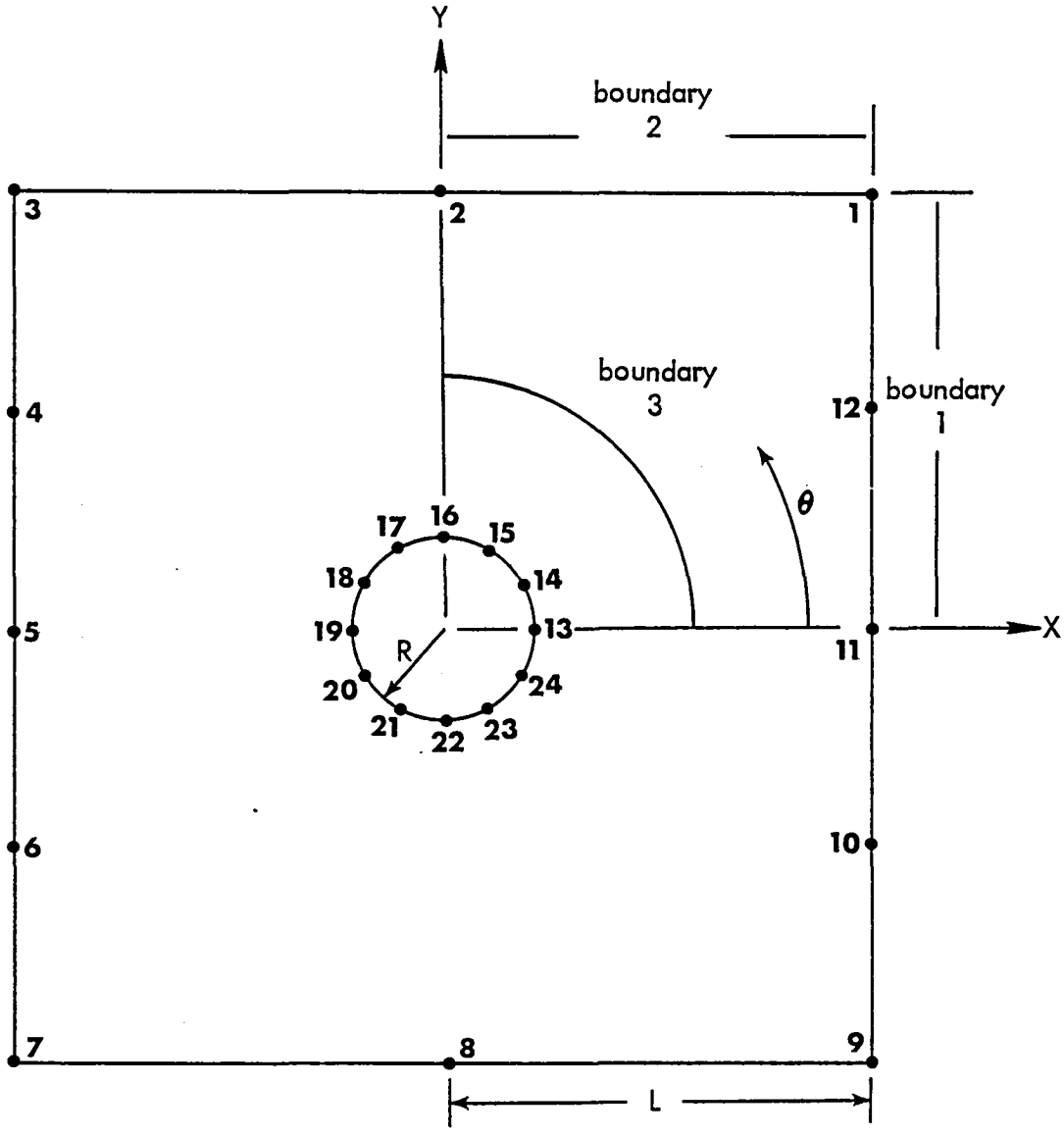

Figure 17. Hole Element Geometry

First, note that the rigid body motions consist of one SA state (displacement in the x-direction), one AS state (displacement in the y-direction), and one AA state (rotation about the center of the element). There is no rigid body SS state. These observations establish the values of $\bar{R}$ to be used when checking the requirement that rank $[G] = (F-\bar{R})$.

In the notation of Equation (23), let $\lfloor \bar{q}_{RB} \rfloor$ denote all of the nodal displacements on the exterior boundaries; clearly, $\lfloor \bar{q}_{RB} \rfloor \equiv \lfloor 0 \rfloor$ will suppress all true rigid body motions for all symmetry conditions. Then $\lfloor \bar{q}_1 \rfloor$ will denote the displacements on the hole boundary. Let NSEG3 denote the number of segments on the hole boundary (side 3). Then as is shown in Figures 10 through 13, the number of elements in $\lfloor \bar{q}_1 \rfloor$ (the number of degrees of freedom on side 3), denoted by (F-S) in Equation (23), is a function of symmetry condition, as follows:

$$\begin{aligned} &\text{for SS} && : (F-S) = NSEG3 + 1 \\ &\text{for SA and AS} && : (F-S) = NSEG3 \\ &\text{For AA} && : (F-S) = NSEG3-1 \end{aligned} \tag{117}$$

In Equations (24) and (25), the array $[G_1]$ is the boundary work array associated with work done by radial stresses moving through radial displacements on the hole boundary; there will be an array $[G_1^i]$ for each symmetry condition. Because rank $[G_1^i]$ must equal to $(F-S)_i$ for each symmetry condition, it follows that each $[G_1^i]$ must have at least $(F-S)_i$ independent rows. This means there must be at least $(F-S)_i$ independent states of radial stress on the hole boundary.

Now, consider Equation (64), which shows the assumed form for $R^2\tau_r$. Clearly, at $\rho = 1$, the stress states associated with B_{11} and B_{21} are not independent; this is also true for B_{31} and B_{41} and for many other sets of coefficients. In general, the radial stress states which have the same harmonic function of θ are dependent when evaluated along any circle. Therefore, since there must be at least $(F-S)_i$ independent radial stresses on the hole boundary, it follows that there must be a minimum of $(F-S)_i$ harmonics in the stress state for each symmetry condition.

For symmetry conditions SS, SA, and AS, the first two harmonics supply four coefficients; for condition AA, the first harmonic supplies two coefficients. These first harmonics are never enough because the number of coefficients is not adequate for the number of degrees of freedom. Therefore, additional harmonics, supplied by the summations in Equation (64), are always necessary. Let AH denote the minimum number of additional harmonics required; this is a function of symmetry condition, as follows:

$$\begin{aligned} &\text{for SS, SA, AS: } AH = (F-S) - 2 \\ &\text{for AA : } AH = (F-S) - 1 \end{aligned} \tag{118}$$

Substitution of Equation (117) into Equation (118) gives

$$\begin{aligned} &\text{for SS : } AH = NSEG3-1 \\ &\text{for SA,AS,AA : } AH = NSEG3-2 \end{aligned} \tag{119}$$

For specified NSEG3, Equation (119) gives the minimum number of additional harmonics necessary to provide proper rank to the arrays $[G_1^i]$. Fewer harmonics will introduce spurious rigid body modes involving hole boundary displacements with zero displacement on the external boundaries.

Suppose there are more than (F-S) independent rows in the $[G_1]$ array. This is perfectly all right as far as rigid body considerations are concerned. The rank of array $[G_1]$ will equal (F-S), and Equation (25) will be satisfied only by the trivial solution $\{\bar{q}_1\} = \{0\}$. However, excess independent rows mean excess harmonics in the expression for radial stress; and this leads to reduced accuracy in satisfaction of any radial traction boundary conditions which might exist on the hole boundary.

This can be explained with reference to Section 1.7, entitled "Treatment of Boundary Conditions." Although the hole boundary has been treated as S_u boundary with specified nodal radial displacements, actual traction boundary conditions can be approximately satisfied by proper selection of the hole nodal displacements. This means there are (F-S) displacements available to provide proper values for

radial stress at the hole boundary. If there are more than (F-S) independent stress states at the boundary, then there are not enough displacements to permit best satisfaction of the traction conditions. If there are exactly (F-S) independent stress states, then in some unspecified and probably non-unique manner it is possible to achieve excellent satisfaction of traction boundary conditions. This observation, while vague in the details, has been numerically confirmed. In open hole test problems described in a following section, the radial stresses on the hole boundary were decreased by three orders of magnitude (10^{-2} down to 10^{-5} or better) by removing excess harmonics from the assumed stress state.

In summary, if the number of additional harmonics is selected to satisfy Equation (119), then spurious rigid body modes on the hole boundary will be eliminated and traction boundary conditions will be as well satisfied as is possible. With the number of additional harmonics known, the total number of stress coefficients depends upon the summation limits I and J in Equation (62). It is only necessary to ensure that rank $[G] = (F-\bar{R})$ for each symmetry condition; this generally requires NSEG3 ≥ 3.

5.4 AREA INTEGRATION

The internal complementary work leads to the area integral shown in Equation (92) and repeated below:

$$[H^j] = \int_{Quad} [\Lambda^j(\rho,\theta)]^T [C_{r\theta}(\theta)][\Lambda^j(\rho,\theta)]\rho \, d\rho d\theta$$

From the structure of Equations (64), (66), and (68), it can be shown that the arrays $[\Lambda^j(\rho,\theta)]$ can be written as

$$[\Lambda^j(\rho,\theta)] = \sum_{m=1}^{IJ1} \rho^{m-(J+3)} [{}_m\Lambda^j(\theta)] \qquad (120)$$

where IJ1 = I+J+1

I, J = summation limits shown in Equation (62).

In words, the arrays $[\Lambda^j(\rho,\theta)]$ are decomposed into the summation of products of individual powers of ρ multiplied by functions of θ.

Substitute Equation (120) into Equation (92) to get

$$[H^j] = \sum_{m=1}^{[J]1} \sum_{n=1}^{[J]1} \int_{Quad} \rho^{m+n-2(J+3)} [{}_m\Lambda^j(\theta)]^T [C_{r\theta}(\theta)][{}_n\Lambda^j(\theta)]\rho \, d\rho \, d\theta \quad (121)$$

Let P denote the typical integral in Equation (121). Then, it is clear that P has the form

$$P = \int_{Quad} f(\rho)\, g(\theta)\, d\rho\, d\theta \quad (122)$$

where $$f(\rho) = \rho^{m+n-2J-5} \quad (123)$$

The integration limits are established with reference to Figure 18. The quadrant is divided into two octants identified by the exterior boundary side number. In each octant, the upper limit on ρ is given by

$$\rho_{max} = \frac{L/R}{\cos\phi} \quad (124)$$

where L/R = ratio of quadrant dimension to hole radius.

Define $$F(\phi) = \int_{\rho=1}^{\rho_{max}} f(\rho)\, d\rho \quad (125)$$

After substituting Equation (123) into Equation (125) the result is

$$F(\phi) = \begin{cases} \dfrac{1}{m+n-2J-4}\left[\left(\dfrac{L/R}{\cos\phi}\right)^{m+n-2J-4} - 1\right], & (m+n-2J-4) \neq 0 \\ \ln \dfrac{L/R}{\cos\phi}, & (m+n-2J-4) = 0 \end{cases} \quad (126)$$

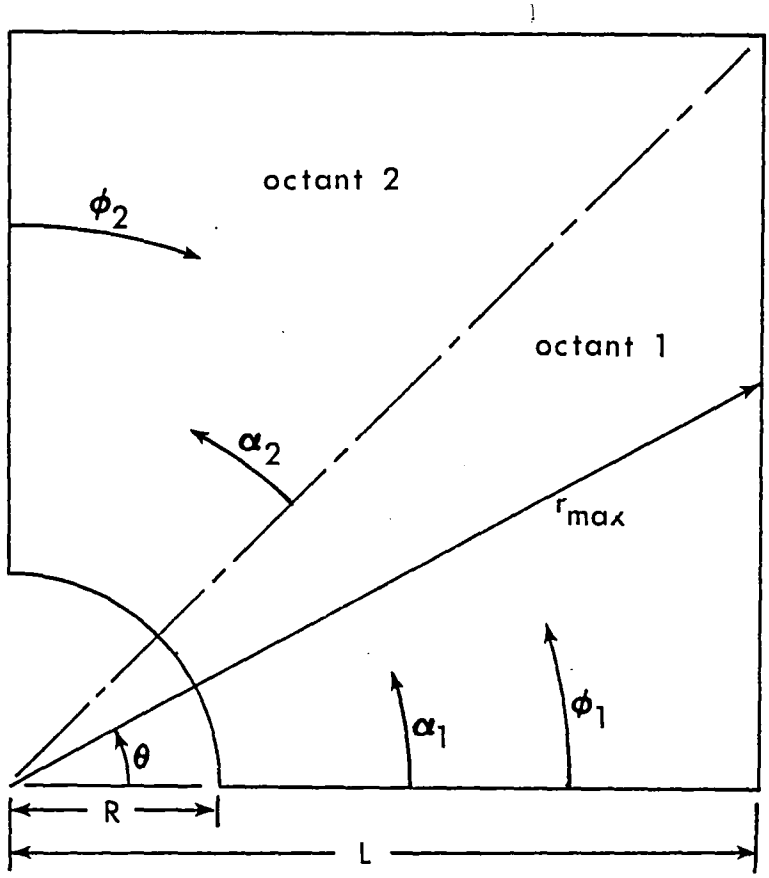

Figure 18. Notation Used for Volume and Boundary Integration in the Quadrant

Now the quadrant integration can be written as the following sum of two octant integrations:

$$P = \int_{\alpha_1=0}^{\alpha_1 = \frac{\pi}{4}} F(\phi_1) g(\alpha_1)\, d\alpha_1 + \int_{\alpha_2=0}^{\alpha_2 = \frac{\pi}{4}} F(\phi_2) g(\tfrac{\pi}{4} + \alpha_2)\, d\alpha_2 \qquad (127)$$

where $\phi_1 = \alpha_1$, in octant 1

$\phi_2 = \frac{\pi}{4} - \alpha_2$, in octant 2

Alternatively the integral is given by

$$P = \int_{\phi=0}^{\phi=\frac{\pi}{4}} F(\phi)\ [g(\phi) + g(\tfrac{\pi}{2} - \phi)]\, d\phi \qquad (128)$$

The area integrals in their original forms are too complicated for exact evaluation, so numerical integration is necessary. However, it is possible to first reduce the area integrals to line integrals through performing the radial integration in the closed form of Equation (126). Although numerical techniques are still necessary to evaluate the line integrals in Equation (127), the results should be more accurate than what would be achieved with comparable effort on the original area integrals.

5.5 BOUNDARY INTEGRATION

The external complementary work is calculated from the product of tractions and displacements on all three sides of the quadrant. The result is given in Equation (93), repeated below.

$$[G^j] = \int_{Quad} [T^j]^T [\zeta^j]\, f(\theta)\, d\theta$$

The function $f(\theta)$, used to define the differential boundary length as shown in Equation (83), is determined as follows, with reference to Figure 18.

Along side 1, the arc length s_1 is given by $s_1 = L \tan \theta$. From this, it follows that $ds_1 = R \frac{L}{R} \sec^2 \theta \, d\theta$; and by comparison with Equation (83), $f(\theta) = (L/R) \sec^2 \theta$. If ρ_{max} is introduced from Equation (124), the result can be written as follows:

$$f(\theta) = \frac{\rho_{max}^2}{L/R} \tag{129}$$

Along side 2, $s_2 = L[1 - \tan(\frac{\pi}{2} - \theta)]$. Therefore, $ds_2 = R \frac{L}{R} \sec^2 (\frac{\pi}{2} - \theta) \, d\theta$. Since $\rho_{max} = \frac{L/R}{\cos(\frac{\pi}{2} - \theta)}$, it follows once again that $f(\theta)$ is given by Equation (129).

Along side 3, $s_3 = R\theta$ and $ds_3 = R d\theta$.
Therefore, $f(\theta) = 1$.

The tractions on sides 1 and 2 are in the x and y directions while the stresses are assumed in polar coordinates. Therefore, at each point on the exterior boundary, the stresses are first evaluated and then transformed to cartesian components by well-known equations such as given in [1, p. 67].

On side 3, the radial traction is immediately given by the negative of the radial stress component.

The integrals in Equation (93) are finally evaluated numerically as discussed in the next section.

5.6 NUMERICAL INTEGRATION

In the numerical evaluation of the area integrals, each octant, described by $0° \leq \phi \leq 45°$, is divided into a user specified number of integration intervals. That is, each octant is divided into a specified number of equal increments of the angle variable. Then the integral in Equation (127) is evaluated in each interval by Gaussian quadrature with a user specified number of Gauss points.

For the boundary integration, each side is first divided into segments by the nodes. Then each segment is further subdivided into integration intervals, with the number of intervals possibly different for each side. Finally, the integral is evaluated in each interval by Gaussian quadrature.

As mentioned above, the number of Gaussian quadrature points per interval is user specified. However, the existing computer code limits the choices to 3, 5, 7, or 9 points. This choice can, of course, be expanded if desired.

SECTION 6
SAMPLE PROBLEMS

6.1 INTRODUCTION

NASTRAN was chosen as the host program for this element because it is such a widely used, well-known program with a large element library and many capabilities. The hole element implemented into NASTRAN is a variable-noded total element and is defined via ADUM7, CDUM7, and PDUM7 input cards. The format of these cards are given in Appendix A and the default geometry of the element is shown in Figure 19. The user may specify the number of nodes on each of the three boundaries shown in the figure. The nodes on the exterior of the element have two cartesian degrees of freedom whereas the nodes on the hole wall have only a single radial degree of freedom. Tangential degrees of freedom at the hole wall do not appear in the element formulation because the stiffness matrix was derived through a complementary virtual work formulation based on assumed stresses which satisfy the tangential traction-free conditions on the hole boundary (see Section 2.1). The ratio of element diameter to hole diameter is determined from grid point locations and is thus a user choice; however, a ratio of four is recommended. The material properties may be isotropic or orthotropic and are defined by MAT1 and MAT2 cards. Characteristics which are not defined for this element include mass properties, thermal loading, material non-linearity, and differential stiffness.

The example problems which follow were solved using the NASTRAN program at Lockheed-Georgia Company with the orthotropic hole element implemented. They are intended to demonstrate the performance of the element in a variety of applications.

6.2 ISOTROPIC PLATE WITH UNIAXIAL TENSION

The orthotropic hole element can be used in isotropic applications by simply specifying isotropic elastic coefficients. This is demonstrated by presenting the solution for an infinite isotropic plate with unit uniaxial tension at infinity (see Figure 20). The finite element model is shown in Figure 21. The plate width is 20 times the hole diameter, which represents an essentially infinite plate. Poisson's ratio is set at 0.3205.

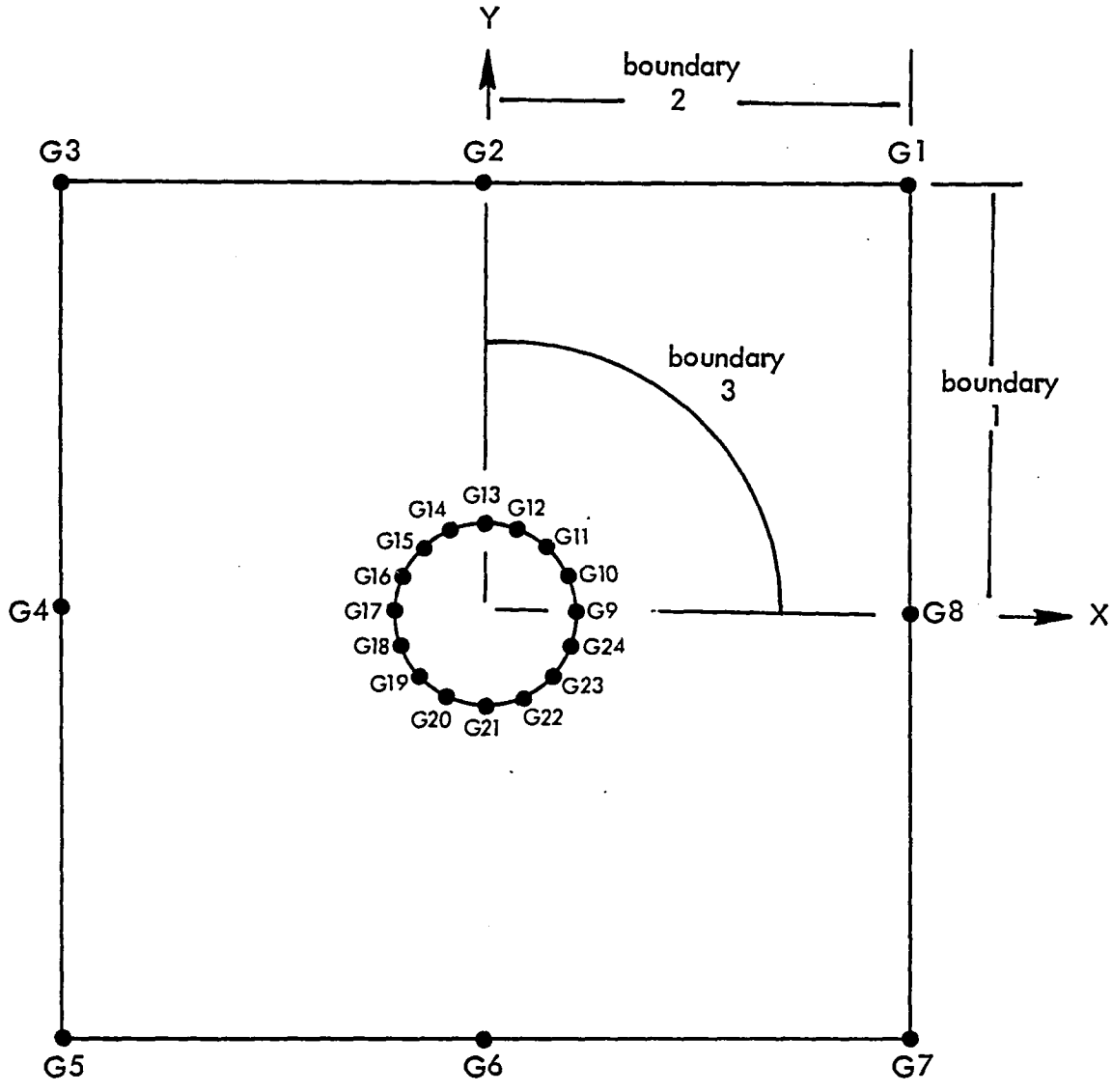

Figure 19 . Default Geometry of Hole Element

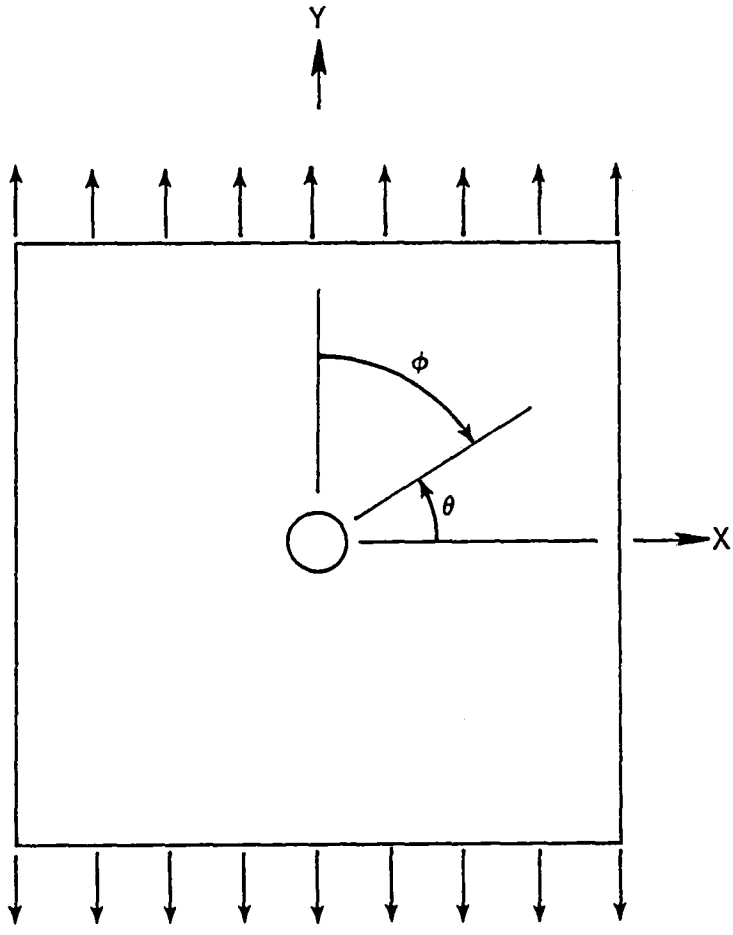

Figure 20. Unit Tensile Traction in the Y-Direction

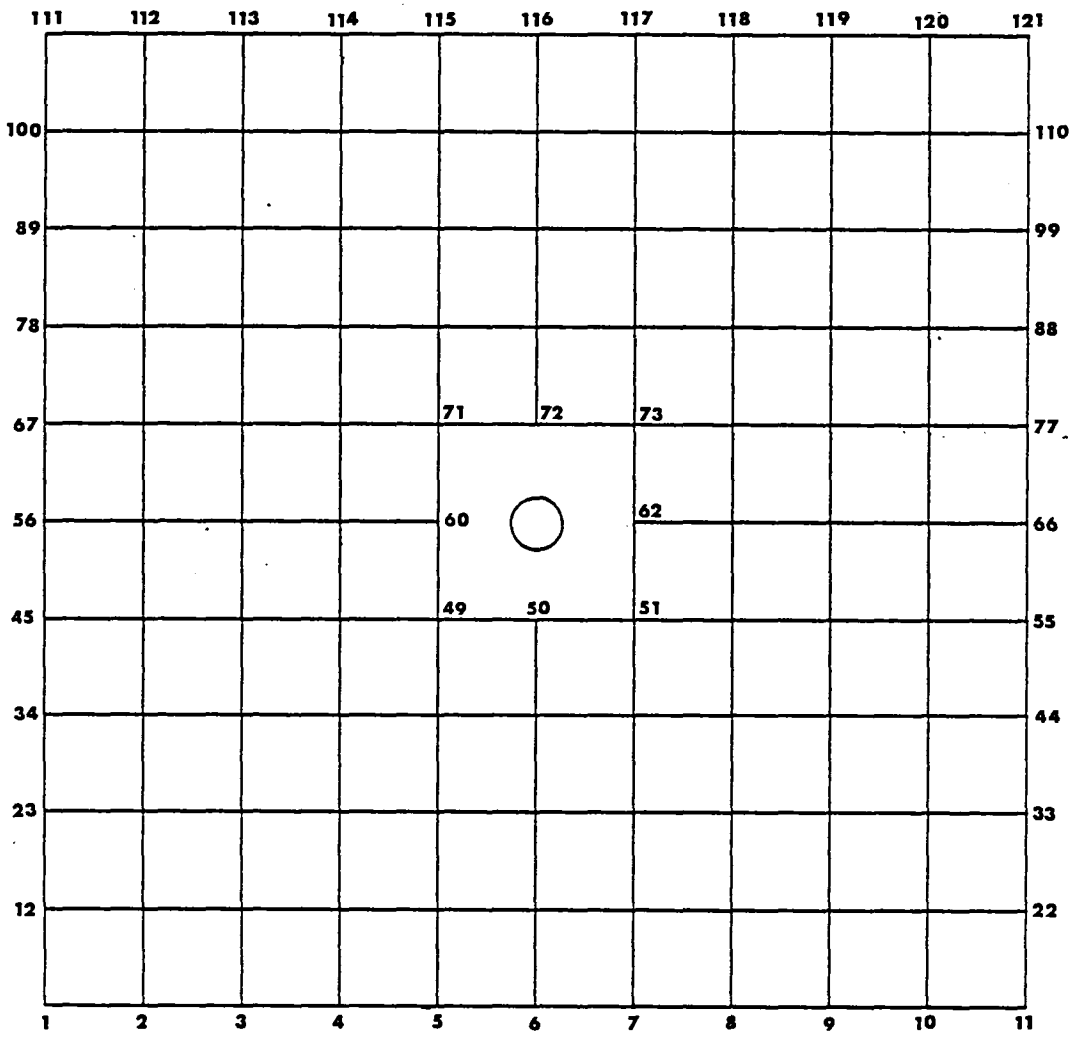

Figure 21. Finite Element Model

Table I presents results for the three stress components at four values of radius and four values of θ. The hole element stiffness and stress matrices were based on array $\lfloor NSEG \rfloor = \lfloor 1 \quad 1 \quad 3 \rfloor$ with radial variation given by powers of ρ from ρ^{-5} to ρ^{+1}.

The hole boundary is given by $r=1$. Note the excellent satisfaction of the zero radial stress boundary condition; the results were typically 10^{-6} times the magnitude of external loading. The circumferential stress results are also very good, with an error of only 0.2% on the maximum tension stress concentration factor and 1.5% on the maximum compression stress. The zero shear stress condition is of course perfectly satisfied since it was included in the original stress assumptions.

The stresses away from the hole boundary are also very well represented by the hole element results.

6.3 ISOTROPIC PLATE WITH HALF COSINE LOADED HOLE

A load transfer problem for which a comparison solution is available [3] is that of an infinite isotropic plate with Poisson's ratio equal to 0.25, loaded with uniform traction on one end and a cosine variation of radial tractions on the hole boundary (see Figure 22). The total load on the end is equal to 2P, and the radial tractions on the loaded hole boundary are given by

$$T_r = \frac{4P}{\pi} \cos\phi, \qquad -\frac{\pi}{2} \leqq \phi \leqq +\frac{\pi}{2}$$

The finite element model is shown in Figure 21; and Table II presents results in the region around the hole, based on $\lfloor NSEG \rfloor = \lfloor 1 \quad 1 \quad 4 \rfloor$ and radial terms from ρ^{-5} to ρ^{+1}. The value of P is set equal to 1.0.

The stresses at the hole boundary are very well represented by the finite element results. The radial stresses follow the cosine curve over the loaded region and are of the order of 10^{-2} on the unloaded portion of the boundary. The variation of circumferential stress is reasonably accurate, with an error of 3% on the maximum stress concentration.

In the region around the hole, the results from the hole element solution continue to give a good description of the stress state.

TABLE I

STRESSES FOR AN ISOTROPIC PLATE SUBJECTED TO UNIAXIAL TENSION

	θ deg	τ_r^*	τ_r^{**}	τ_θ^*	τ_θ^{**}	$\tau_{r\theta}^*$	$\tau_{r\theta}^{**}$
r = 1	0	0	0	3.006	3.000	0	0
	30	0	0	2.005	2.000	0	0
	60	0	0	-0.006	0	0	0
	90	0	0	-1.015	-1.000	0	0
r = 2	0	0.279	0.281	1.221	1.219	0	0
	30	0.327	0.328	0.923	0.922	0.572	0.568
	60	0.422	0.422	0.325	0.328	0.571	0.568
	90	0.467	0.469	0.028	0.031	0	0
r = 3	0	0.145	0.148	1.076	1.074	0	0
	30	0.295	0.296	0.815	0.815	0.516	0.513
	60	0.594	0.593	0.296	0.296	0.516	0.513
	90	0.739	0.741	0.031	0.037	0	0
r = 4	0	0.083	0.088	1.036	1.037	0	0
	30	0.278	0.278	0.784	0.784	0.482	0.482
	60	0.659	0.659	0.284	0.278	0.488	0.482
	90	0.851	0.850	0.010	0.025	0	0

* Finite Element Results
** Reference 1

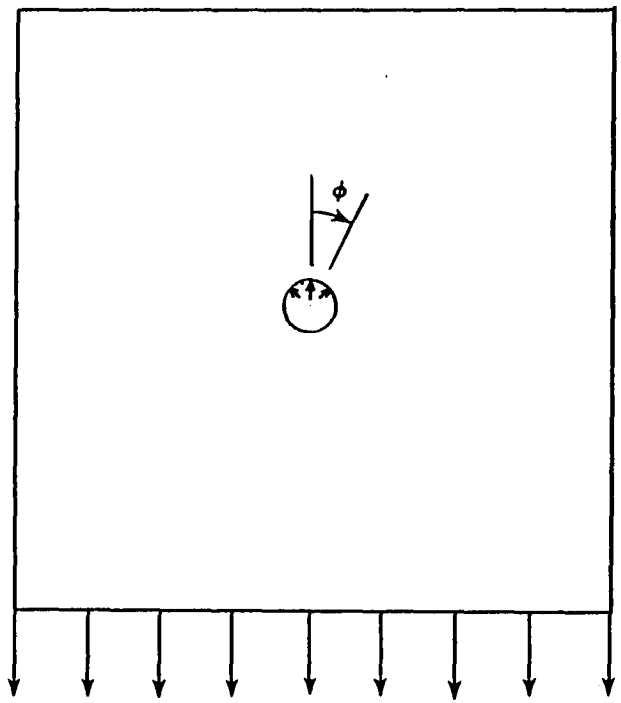

a) External Loading

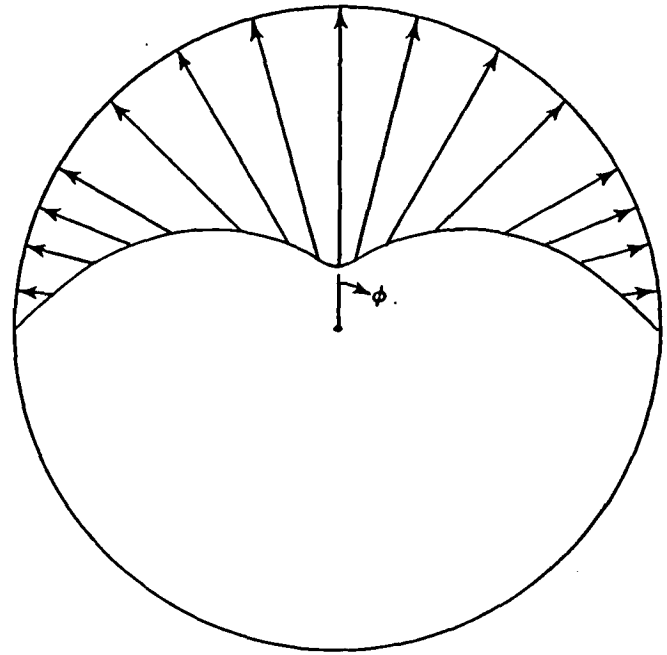

b) Half Cosine Distribution of Traction on the Hole Boundary

Figure 22. Load Transfer Problem

TABLE II

STRESSES FOR AN ISOTROPIC PLATE WITH LOAD TRANSFER

	ϕ deg	τ_r^*	τ_r^{**}	τ_θ^*	τ_θ^{**}	$\tau_{r\theta}^*$	$\tau_{r\theta}^{**}$
r = 1	0	-1.271	-1.273	0.372	0.412	0	0
	30	-1.099	-1.103	0.467	0.470	0	0
	60	-0.649	-0.637	0.659	0.612	0	0
	90	-0.041	0	0.834	0.810	0	0
	120	-0.012	0	0.415	0.373	0	0
	150	0.003	0	0.056	0.053	0	0
	180	0.003	0	-0.094	-0.065	0	0
r = 1.2	0	-0.995	-0.977	0.314	0.348	0	0
	30	-0.844	-0.829	0.358	0.381	0.035	0.021
	60	-0.445	-0.429	0.460	0.443	0.046	0.029
	90	0.038	0.034	0.477	0.415	-0.032	-0.031
	120	0.055	0.078	0.289	0.274	-0.097	-0.081
	150	0.023	0.038	0.070	0.088	-0.064	-0.051
	180	0.006	0.024	-0.015	-0.011	0	0
r = 1.5	0	-0.726	-0.726	0.232	0.241	0	0
	30	-0.604	-0.609	0.256	0.253	0.042	0.026
	60	-0.288	-0.293	0.295	0.266	0.046	0.028
	90	0.045	0.037	0.266	0.231	-0.047	-0.045
	120	0.094	0.086	0.179	0.152	-0.119	-0.105
	150	0.055	0.049	0.062	0.055	-0.083	-0.070
	180	0.035	0.033	0.010	0.012	0	0

* Finite Element Results

** Reference 3

In the finite element model of the structure, the tractions are applied as concentrated nodal forces. On the hole boundary, these nodal forces are the work equivalent loads based on the cosine variation of the radial traction between nodes and the assumed radial displacement of Equation (79). The results are as follows.

Let Δ = angular increment subtended by arc length between two nodes on the hole boundary

F_r = radial nodal force at node located by angle ϕ.

Then, at $\phi = 0°$, $F_r = \frac{4P}{\pi}\Delta$

at $\phi = \pm\bar{\phi}$, $F_r = \frac{4P}{\pi}\Delta\cos\bar{\phi}$

at $\phi = \pm 90°$, $F_r = \frac{2P}{\pi}\left(1 - \frac{\Delta}{\tan\Delta}\right)$

These results can be partially checked as follows. Consider a hole boundary with N segments per quadrant. Then the summation of nodal force components in the y direction is

$$\sum F_y = \frac{4P}{\pi}\Delta + 2\left(\frac{4P}{\pi}\Delta\cos^2\Delta\right) + 2\left(\frac{4P}{\pi}\Delta\cos^2 2\Delta\right) + \ldots + 2\left[\frac{4P}{\pi}\Delta\cos^2(N-1)\Delta\right]$$

$$\sum F_y = \frac{4P}{\pi}\Delta\left[1 + 2(\cos^2\Delta + \cos^2 2\Delta + \ldots + \cos^2(N-1)\Delta\right]$$

Since $\Delta = \frac{\pi}{2N}$, it follows that

$$\sum F_y = \frac{2P}{N}\left[1 + 2\sum_{i=1}^{N-1}\cos^2 i\,\frac{\pi}{2N}\right]$$

It can be shown that

$$\sum_{i=1}^{N-1} \cos^2 i\,\frac{\pi}{2N} = \frac{N-1}{2}, \quad N \geq 2$$

Therefore, $\sum F_y = \frac{2P}{N}\left[1 + 2\left(\frac{N-1}{2}\right)\right] = 2P$

as required for equilibrium.

6.4 ±45° LAMINATED PLATE

The example problems with isotropic material serve to confirm the basic theoretical approach and to partially validate the computer solution. There remains only to demonstrate satisfactory performance in the intended applications with orthotropic materials. The first material selected has material properties as follows:

$$E_x = E_y = E, \quad G_{xy} = 1.697528E, \quad \nu_{yx} = \nu_{xy} = 0.735$$

Note that even though $E_x = E_y$, this material is rather "far" from isotropic, with some unspecified measure, due to the large value of Poisson's ratio and the fact that E,G, and ν do not satisfy the isotropic relationship. These properties describe the ±45° graphite/epoxy laminate considered in [4].

The first loading is unit tensile tractions in the y-direction, applied as shown in Figure 20 with the finite element model given in Figure 21. The traction boundary conditions at the hole boundary are satisfied, with radial stress of the order 10^{-6} times the external loading. Figure 23 shows the variation of circumferential stress around the hole boundary for $\lfloor NSEG \rfloor = \lfloor 1 \quad 1 \quad 3 \rfloor$ and two different sets of powers of ρ. Also shown is the exact solution for an infinite plate, given by

$$\tau_\theta = \frac{3.05786\cos^2\theta - 1}{2.8809072(\cos^4\theta - \cos^2\theta) + 1}$$

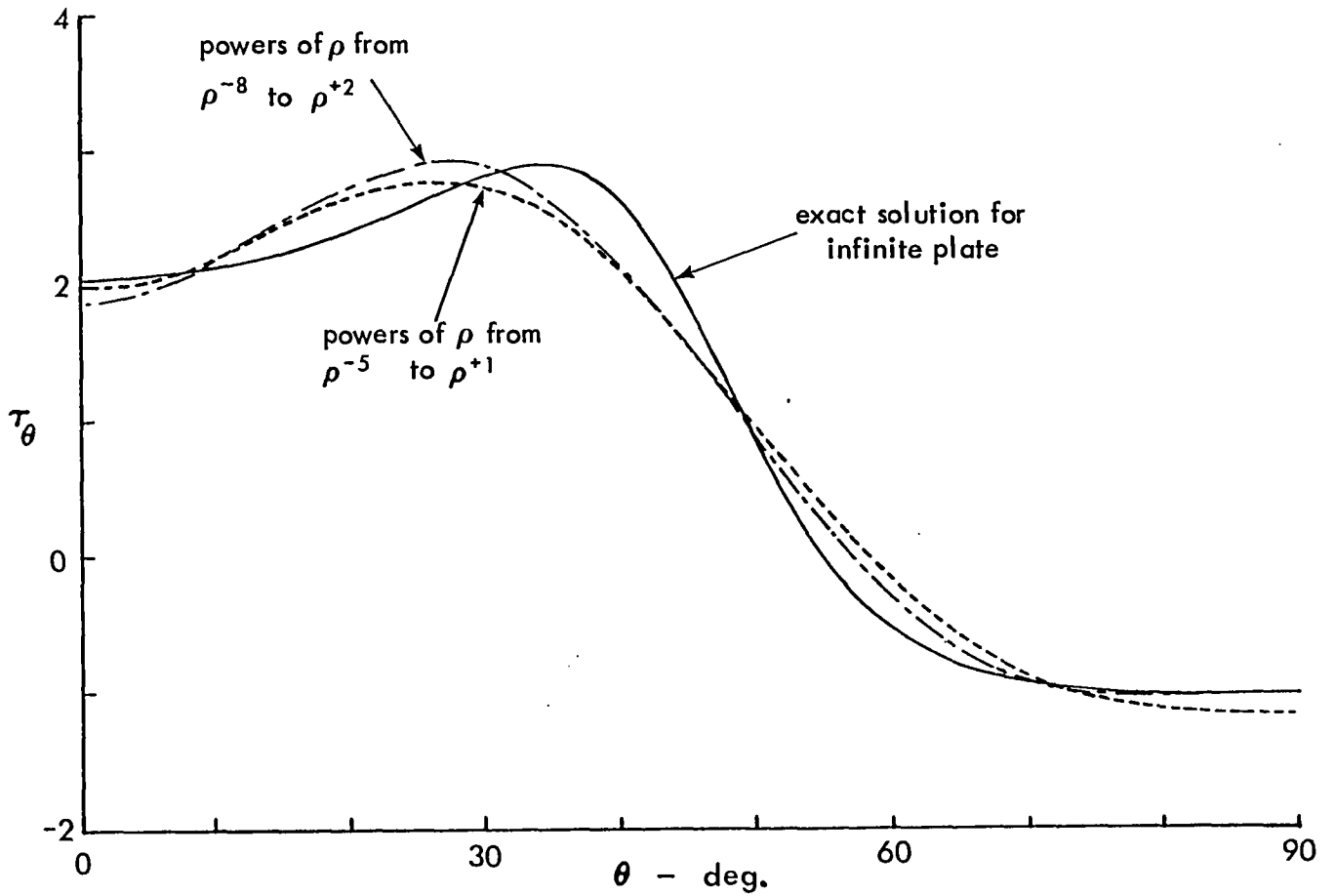

Figure 23. Circumferential Stress at the Open Hole Boundary for a ±45° Laminate with Unit Uniaxial Tensile Traction

which can be deduced from [5, p.175]. The orthotropic hole element results contain the essential feature that the maximum stress concentration does not occur at the familiar location of $\theta = 0°$. The worst solution shown has an error in maximum stress of only 3.8%, and the best error is only 0.7%.

The hole loaded with half-cosine distributed tractions has also been solved; see Figure 22. The resulting radial stresses on the boundary are essentially identical to the results achieved in the case of isotropic material, as should be. The maximum circumferential stress on the hole boundary is $\tau_\theta = 0.79$ at $\phi = 125°$, which can be compared with the hole element results for isotropic material of $\tau_\theta = 0.84$ at $\phi = 85°$. Again, it is seen that the location of maximum stress has shifted around the circle from the familiar location.

6.5 PLYWOOD

The next material selected has properties as follows (see Section 2.5 for notation):

$$E_y = E, \qquad E_x = 2E, \qquad G_{xy} = 0.11667E, \qquad \nu_{xy} = 0.036$$

These properties describe a plywood material for which [5] contains many results for an infinite plate. Note that the plywood properties are quite different from the ±45° lamination properties, both in magnitudes and relationships. This provides further checks on the ability of the hole element to handle different types of orthotropic material.

The types of loading considered are unit tensile tractions in the y-direction (Figure 20), unit compressive tractions in the x-direction with constraint in the y-direction (Figure 24a), and uniform unit internal pressure on the hole boundary (Figure 24b). For all cases, the finite element model is shown in Figure 21; and $\lfloor NSEG \rfloor = \lfloor 1 \quad 1 \quad 6 \rfloor$, with powers of ρ from ρ^{-5} to ρ^{+1}.

For the uniaxial tension, there is the usual excellent satisfaction of traction boundary condition, with τ_r of the order 10^{-6}. Circumferential stresses around the hole boundary are shown in Figure 25. Also shown are the exact results for an infinite plate, given by

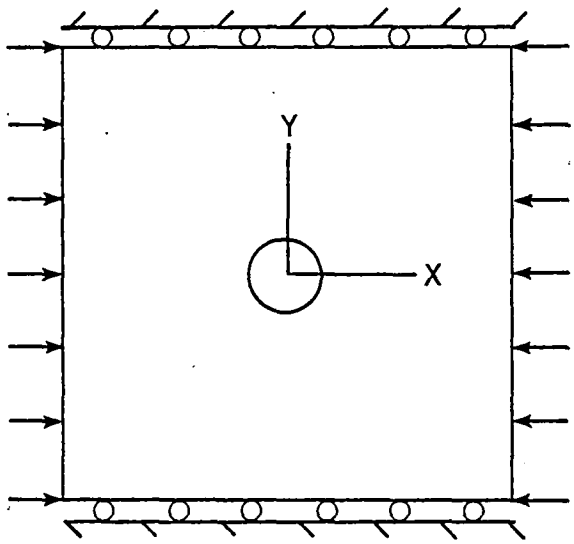

a) Constrained Compression

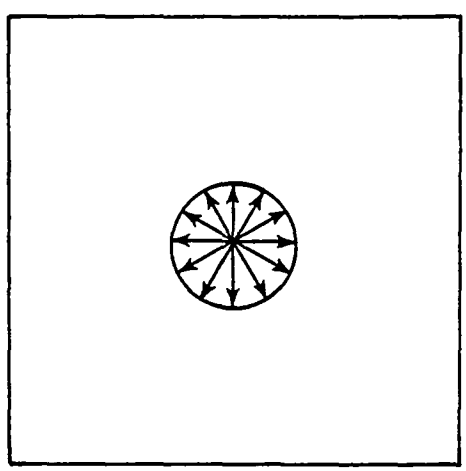

b) Internal Pressure

Figure 24. External Loadings

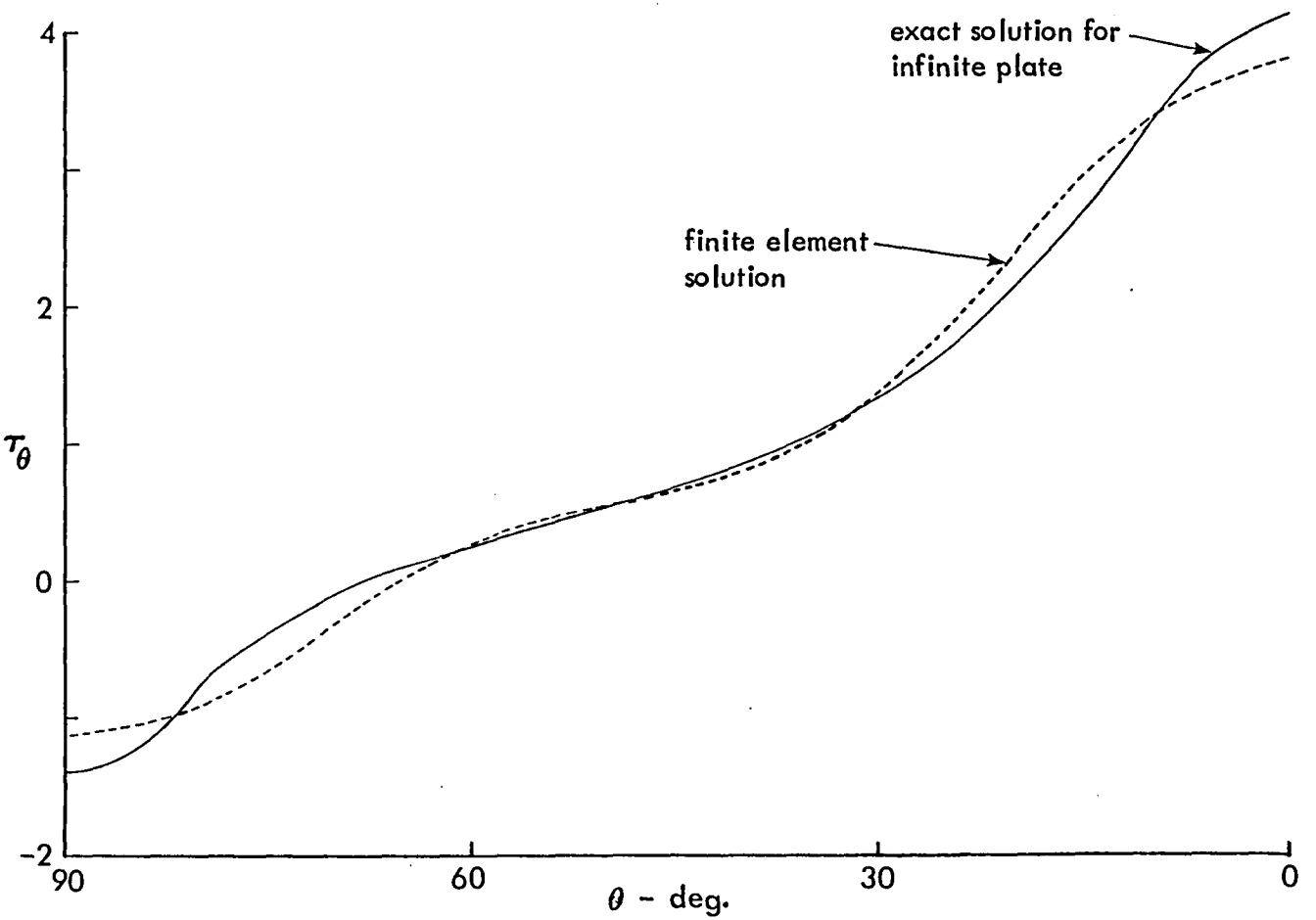

Figure 25. Circumferential Stress at the Open Hole Boundary for Plywood with Unit Uniaxial Tensile Traction

$$\tau_\theta = \frac{4.8557 \cos^2\theta - 0.7071}{-6.9994 \cos^4\theta + 7.4994 \cos^2\theta + 0.5} ,$$

which can be deduced from [5, p.175]. The general features of the variation of stress are demonstrated by the hole element results. There is an 8% error in maximum stress.

The constrained compression results satisfy the hole boundary conditions, with τ_r of the order 10^{-5}. Circumferential stresses around the boundary are shown in Figure 26. The exact results for infinite plate are given by

$$\tau_\theta = \frac{1.1155 - 6.5174 \sin^2\theta}{-13.9989 \sin^4\theta + 12.9989 \sin^2\theta + 2} ,$$

deduced from [5, p.179]. There is an 18% error in maximum stress.

The internal pressure results provided boundary radial stresses of the magnitude -1.00002, which is again excellent satisfaction of boundary conditions. Circumferential stresses around the boundary are shown in Figure 27, compared to infinite plate exact results given by [5, p.173]

$$\tau_\theta = \frac{4.8829 - 15.8432 \sin^2\theta + 13.9989 \sin^4\theta}{2 + 12.9989 \sin^2\theta - 13.9989 \sin^4\theta}$$

The general shape of the distribution is indicated, but there is a 21% error in the maximum stress. Also, there is a small region where the stress becomes compression, which is not to be expected for the internal pressure loading and is not shown by the exact solution.

6.6 MULTIPLE HOLES

Figure 28 shows a finite element model of a plate containing five holes. For economy in modeling, it is desirable to develop the hole element stiffness matrix only once and

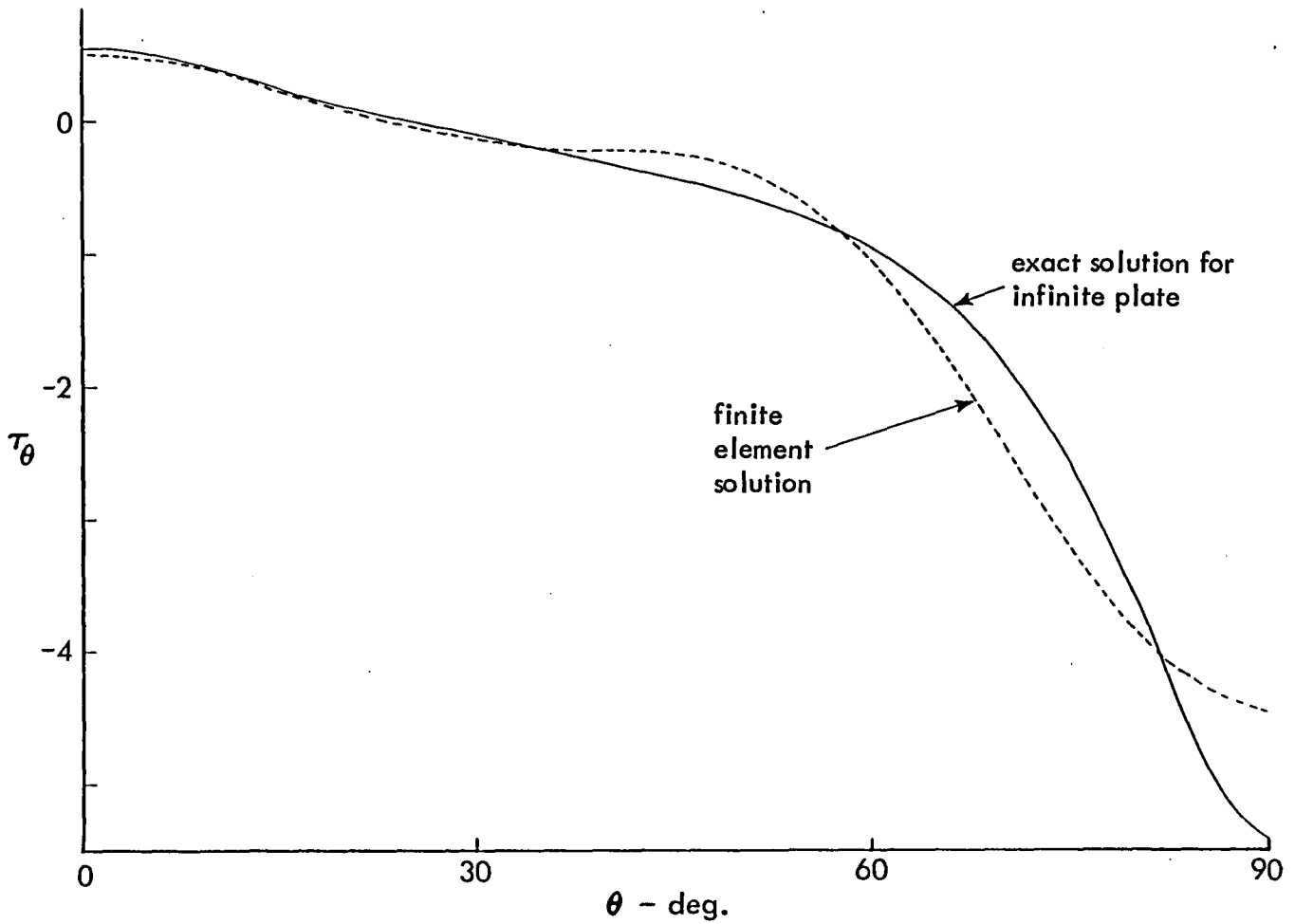

Figure 26. Circumferential Stress at the Open Hole Boundary for Plywood with Unit Constrained Compression

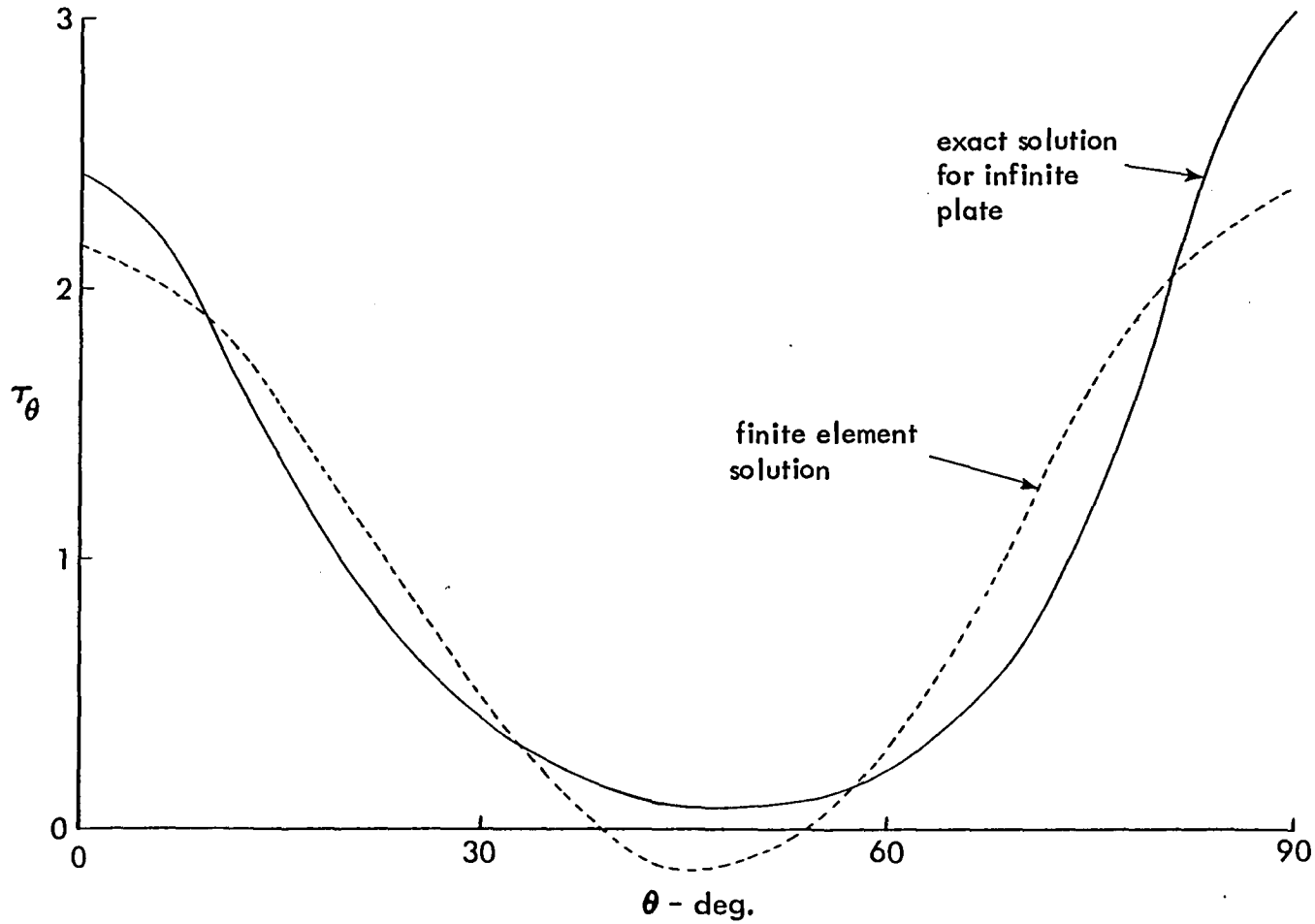

Figure 27. Circumferential Stress at the Hole Boundary for Plywood with Unit Internal Pressure on the Boundary

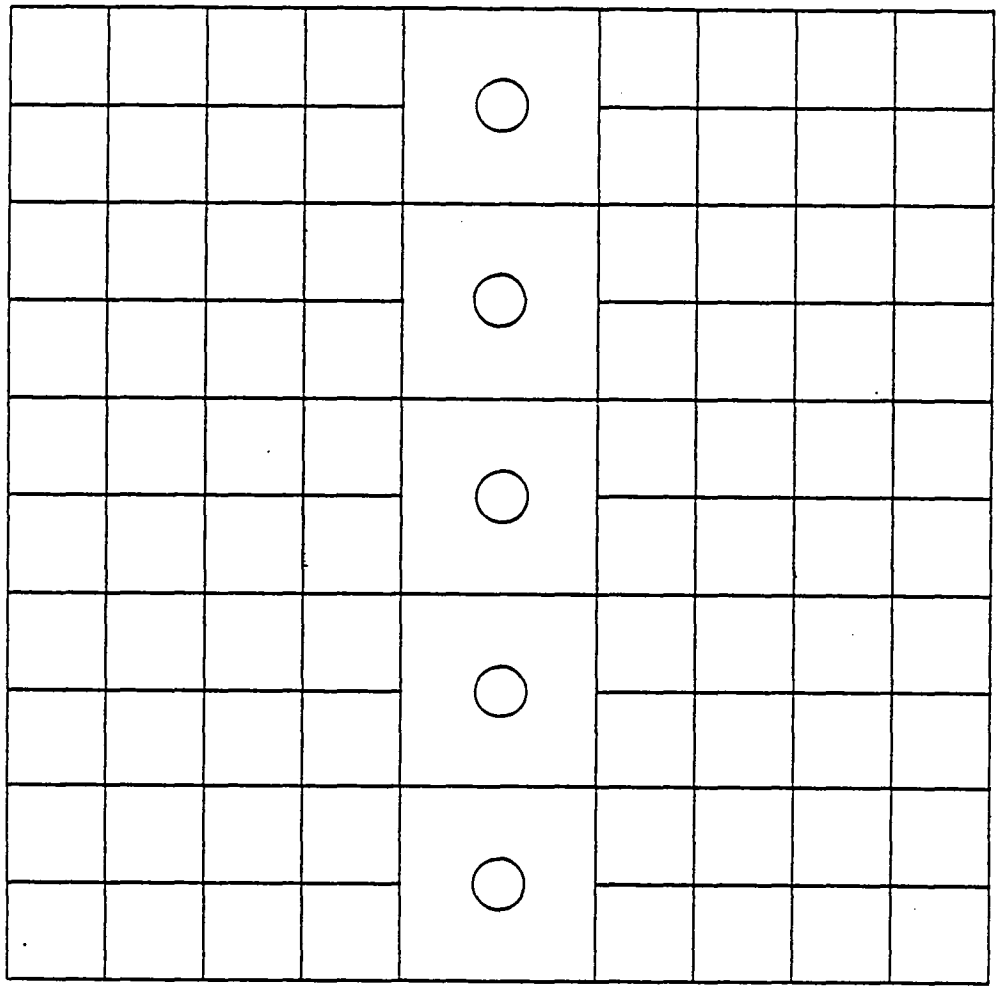

Figure 28. Finite Element Model for a Plate with Multiple Holes

then transform this matrix as necessary to represent all the hole elements. This is possible in NASTRAN by using the congruency feature, and this feature has been checked by determining the solution to Figure 28 with tension applied parallel to the row of holes. The material is isotropic with Poisson's ratio of 0.3205.

The maximum stress concentration factor is given in [6, p.94] for an intermediate hole in an infinite row of holes. In order to simulate the infinite row, the displacements at each loaded end of the model were constrained to be uniform across the width of the plate. The finite element result for stress concentration is 2.78, based on $\lfloor NSEG \rfloor = \lfloor 1 \quad 1 \quad 3 \rfloor$ and powers of ρ from ρ^{-5} to ρ^{+1}. Reference 6 gives 2.65; there is a 5% difference in results.

6.7 EFFECT OF VARYING THE HOLE SIZE

All the preceding examples used a hole element with the ratio of square dimension to hole diameter equal to four, which is the recommended value. However, the computer code does allow the user to vary this ratio, and this feature of the code was tested.

A problem for which theoretical results are available is that of an infinite strip under unit uniaxial tensile traction with a hole diameter equal to half the plate width. The finite element model consists of a hole element which spans the strip width plus sufficient linear strain quadrilaterals added symmetrically to achieve a model with length to width ratio of five. The hole element stiffness matrix is based on $\lfloor NSEG \rfloor = \lfloor 2 \quad 2 \quad 4 \rfloor$, with powers of ρ from ρ^{-5} to ρ^{+1}. The material is isotropic, with Poisson's ratio of 0.25.

The maximum stress occurs on the hole boundary at $\theta = 0°$. Reference 5, page 84, gives a stress concentration factor of 4.32. The finite element result is 3.95, for an 8% difference; this is an excellent result for such a relatively crude model.

SECTION 7

IMPLEMENTING THE HOLE ELEMENT INTO NASTRAN

The orthotropic hole element has been implemented into NASTRAN through the dummy element capability. This capability permits the user to enter his own element subroutines for the purpose of generating the stiffness matrix contributions and for the computation and output of stresses [7, section 6.8.5].

The hole element has been implemented as a DUM7 element. The procedure used to implement the element is as follows.

- Create a subroutine KDUM7 which computes and outputs to functional module EMG the element stiffness matrix. Subroutine KDUM7 calls 15 new auxiliary subroutines in performing its task. Table III gives the function of each of these subroutines. Subroutine EMGPRO was updated to increase the allowable number of words in the element summary table. LINK8 was remapped and the overlay structure was modified.

- Create two subroutines SDUM71 and SDUM72 to compute and output to functional module SDR2 the element stresses. Subroutine SDUM72 calls one new auxiliary subroutine, STRS1S, which evaluates the elements of the assumed stress state. Subroutine SDR2E was changed to call SDUM72 once for each line of stress output. This was required because this element produces many lines of stress output for each element in the model. LINK13 was remapped.

- Subroutine GPTABD was modified to increase the number of words SDR2 passes from phase 1 element stress recovery routines to phase 2 routines. The following subroutines were changed to increase the allowable number of data items on the CDUM7 bulk data card:

TABLE III

NEW SUBROUTINES WRITTEN FOR NASTRAN

NAME	FUNCTION
ORTHOL	Computes the orthotropic hole element stiffness matrix
SETRUN	Sets up dimension blocks and controls the execution
STRES1	Gives stresses for shear free hole boundary
BNDWRK	Performs exterior boundary integration around a quadrant
BNDTRC	Evaluates tractions on outer boundary
RDSTRS	Evaluates radial stress on inner hole boundary
VOLINT	Evaluates the volume integrals in a quadrant
INTGND	Forms the volume integrand
ELAS	Evaluates elastic property matrices
VOLST1	Evaluates stress terms in the volume for shear free hole
INVS	Inverts symmetric square array
AMTRX1	Evaluates nodal transformation matrices for total element
EQUIL	Checks total element equilibrium
HLCOND	Modifies arrays to account for open holes
SQCHK	Evaluates stresses in quadrant of open hole element

IFX4BD	IFPDCO	IFS2P	IFS5P
IFX7BD	IFP3B	IFS3P	IFXDBD
IFP	IFS1P	IFS4P	IFX5BD

LINK1 was remapped.

- The following subroutines were modified to account for the increased size of the element connectivity table, ECT:

GP1	TA1A	TA1ETD
GP2	TA1B	TA1H

LINK2 was remapped.

Listings of all new and modified subroutines are supplied under separate cover.

APPENDIX A

NASTRAN INPUT CARDS FOR THE ORTHOTROPIC HOLE ELEMENT

BULK DATA DECK

Input Data Card ADUM7 Hole Element

Description: Defines attributes for the N-node hole element

Format and Example:

ADUM7	NG	NC	NP	ND					
ADUM7	24	29	11	3					

Field: Contents

NG Number of grid points connected by CDUM7 element (Integer ≦ 64)

NC Number of additional entries on the CDUM7 connection card. All entries which follow the grid point identification numbers are additional. (Integer ≧ 0)

NP Number of additional entries on the PDUM7 property card. All entries which follow the MID entry are additional. (Integer ≧ 1)

ND Number of displacement components at each grid point used in generation of differential stiffness matrix (Always input 3)

Remarks: 1. The value of NC given in the example above is not typical but is consistent with the CDUM7 and PDUM7 examples. Typically, if additional entries are present on the CDUM7 card, they will consist of only the NSEG array (i.e. NC=3).

Input Data Card CDUM7 Hole Element Connection

Description: Defines an N-node hole element of the structural model

Format and Example:

CDUM7	EID	PID	G1	G2	G3	G4	-etc-	GN	abc
CDUM7	101	10	12	15	96	97		11	ABC

+bc	NSEG1	NSEG2	NSEG3	NINT1	NINT2	NINT3	NIPB	NIO	def
+BC	1	1	4	2	2	2	5	2	DEF

+ef	NIPV	LP1	LP2	LP3	LP4	LN1	LN2	LN3	ghi
+EF	5	3	3	3	3	3	3	3	GHI

+hi	LN4	ITOTRT	IQDTRT	ICOND	IACHK	IELMNT	IBNDRT	IVOLRT	jkl
+HI	3	0	0	0	0	0	0	0	JKL

+KI	IHINVS	ISC1	ISC2	ISC3	NLC				
+KL	0	1	4	1	4				

Field	Contents
EID	Element identification number (Integer > 0)
PID	Identification number of a PDUM7 property card (Integer > 0)
G1....GN	Grid point identification numbers of connection points (Integer > 0, G1 ≠ G2....≠ GN)

Input Data Card CDUM7 Hole Element Connection (Continued)

Field	Contents
NSEGi	Number of segments on boundary i (see Figure A-1, Integers, Defaults are NSEG1 = 1, NSEG2 = 1, NSEG3 = 4)
NINTi	Number of integration intervals per segment for boundary i (Integer, Defaults = 2)
NIPB	Number of Gaussian integration points per interval for boundary integration (Integer, Default = 5)
NIO	Number of integration intervals per volume octant (Integer, Default = 2)
NIPV	Number of Gaussian integration points for volume integral (Integer, Default = 5)
LPi	Number of stress terms with powers of $r > -2$. Input for each symmetry condition where i = 1 is symmetric-symmetric, i = 2 is symmetric-antisymmetric, i = 3 is antisymmetric-symmetric, and i = 4 is antisymmetric-antisymmetric. (Integer ≥ 3, Defaults = 3)
LNi	Number of stress terms with powers of $r < -2$. Input rules are the same as for LPi. (Integer ≥ 3, Defaults = 3)
ITOTRT	If greater than zero, causes a print of the elemental stiffness and stress matrices. (Integer, Default = 0)
IQDTRT	If greater than zero, causes a print of intermediate stiffness and stress matrices for a quadrant of the element (Integer, Default = 0)
ICOND	If greater than zero, causes a static condensation of the element stiffness and stress matrices through elimination of the degrees of freedom on a traction free hole wall (Integer, Default = 0)
IACHK	If greater than zero, causes a print of the transformation matrix which relates total and quadrant displacements (Integer, Default = 0)
IELMNT	When equal to 0, produces total element stiffness and stress matrices. If -1, quadrant element matrices are generated, and if +1, half element matrices are generated. (The only option currently available is 0)
IBNDRT	If greater than zero, prints the boundary work matrix (Integer, Default = 0)

Input Data Card CDUM7 Hole Element Connection (Concluded)

Field	Contents
IVOLRT	If greater than zero, prints the volume work matrix (Integer, Default = 0)
IHINVS	If greater than zero, prints the identity matrix resulting from the check of the inversion of the volume work matrix (Integer, Default = 0)
ISC1, ISC2, ISC3 NLC	If IELMNT is +1 or -1, symmetry conditions must be defined. In the program code, symmetry conditions are set with DO loops such as DO XX I = ISC1, ISC2, ISC3 See the description of LPi for definition of symmetry conditions. The user should chose ISC1, ISC2, ISC3 to implement the conditions he wishes. NLC is the number of times the DO loop is executed. This is for dimension purposes. (Integer, Defaults: ISC1 = 1, ISC2 = 4, ISC3 = 1, NLC = 4)

Remarks:

1. Element identification numbers must be unique with respect to all other element identification numbers.
2. The element must be planar with a square outer boundary and a circular inner boundary. The nodes on the outer boundary, as well as the inner boundary, must be equally spaced.
3. Nodes on the hole wall have only radial degrees of freedom, therefore tangential restraints are required. This is necessary because in a general finite element model there are six degrees of freedom associated with each node and the stiffness matrix will be singular if restraints are not applied to those degrees of freedom not included in the element formulation. The tangential restraints are imposed only to eliminate the singularity in the stiffness matrix. The actual tangential displacements are not zero, and circumferential strain is developed at the hole boundary.
4. For reference purposes, the values given for all additional entries on the example input card are default values. If default values are acceptable for all additional entries, they may be omitted from the input. If a variable is given a non-default value, all preceding variables must be defined; all subsequent variables may be omitted.

Input Data Card PDUM7 Hole Element Property

Description: Defines the properties of a N-node hole element. Referenced by the CDUM7 card.

Format and Example:

PDUM7	PID	MID	T	DTH	THMX	NR	R1	R2	abc
PDUM7	10	2	.1	10.	359.	4	1.	1.5	ABC

+bc	R3	-etc-	RN	PRT1	PRT2	PRT3			
+BC	2.0		3.5	0	0	0			

Field:	Contents
PID	Property identification number (Integer > 0)
MID	Material identification number (Integer > 0)
T	Thickness (Real)
DTH,THMX, NR,Ri	Defines stress output locations. Stresses will be computed and printed for the NR radii defined by R1,R2,...,RN and at angles beginning at 0° and incremented by DTH, up to a maximum angle of THMX (See Figure A-2). DTH, THMX, and Ri are real, NR is integer ≦20. Defaults: DTH = 10°, THMX = 359.999, NR = 4, Ri equally spaced from hole wall to element boundary. Note: Ri are normalized to a unit radius.
PRT1	If greater than zero, causes a print of the total element stress matrices (Integer)
PRT2	If greater than zero, causes a print of displacements in the element local coordinate system (Integer)
PRT3	If greater than zero, causes a print of the stress coefficients associated with elemental nodal displacements (Integer)

Remarks:

1. All PDUM7 cards must have unique identification numbers.

2. Stress output for this element (see Figure A-3) may be interpreted as follows:

   Field S1 - The radius, r, at which stresses are computed.

   Field S2 - The angle, θ, at which the stresses in fields S3, S4, and S5 are computed.

   Field S3 - τ_r

   Field S4 - τ_θ

   Field S5 - $\tau_{r\theta}$

   Field S6 - The angle, θ, at which the stresses in fields S7, S8, and S9 are computed

   Field S7 - τ_r

   Field S8 - τ_θ

   Field S9 - $\tau_{r\theta}$

   Note that each line of output has stress values for two values of θ.

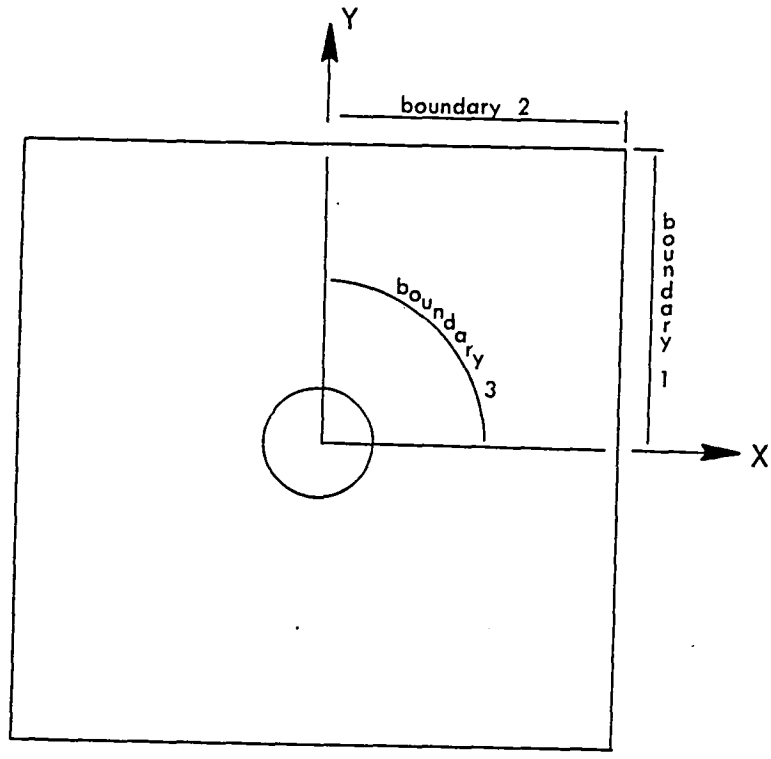

Figure A-1. Boundaries of Hole Element

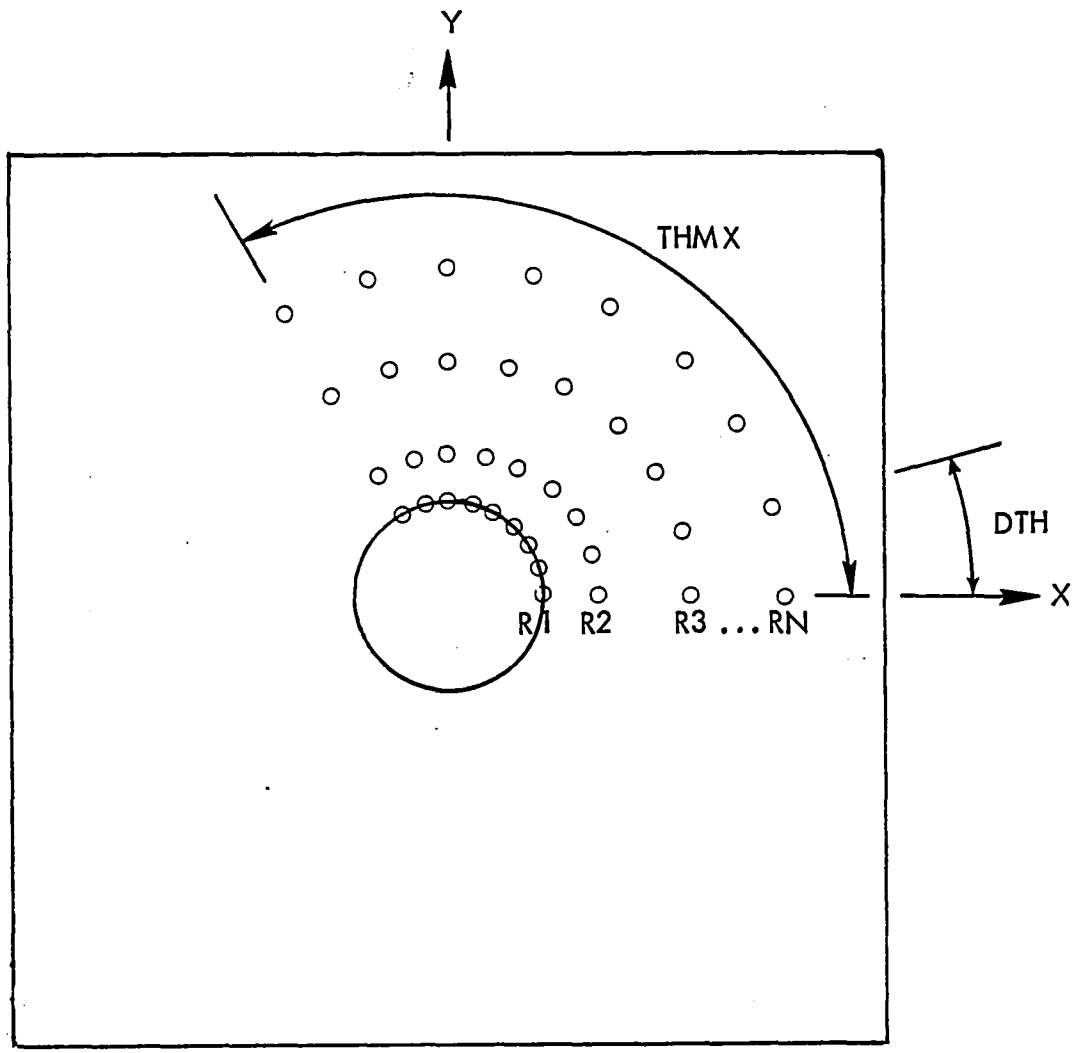

Figure A-2. Definition of Stress Output Locations

STRESSES IN USER ELEMENTS (CDUM7)

EL-ID	S1	S2	S3	S4	S5	S6	S7	S8	S9
101	1.00000+00	.0	-1.00002+00	2.16965+00	.0	1.00000+01	-1.00002+00	1.87722+00	.0
101	1.00000+00	2.00000+01	-1.00002+00	1.20470+00	.0	3.00000+01	-1.00002+00	4.92311-01	.0
101	1.00000+00	4.00000+01	-1.00002+00	-2.07667-02	.0	5.00000+01	-1.00002+00	-1.15771-01	.0
101	1.00000+00	6.00000+01	-1.00001+00	3.14727-01	.0	7.00000+01	-1.00003+00	1.14210+00	.0
101	1.00000+00	8.00000+01	-1.00002+00	2.00699+00	.0	9.00000+01	-1.00001+00	2.38925+00	.0
101	1.00000+00	1.00000+02	-1.00002+00	2.00699+00	.0	1.10000+02	-1.00002+00	1.14210+00	.0
101	1.00000+00	1.20000+02	-1.00002+00	3.14727-01	.0	1.30000+02	-1.00002+00	-1.15771-01	.0
101	1.00000+00	1.40000+02	-1.00002+00	-2.07666-02	.0	1.50000+02	-1.00002+00	4.92311-01	.0
101	1.00000+00	1.60000+02	-1.00003+00	1.20470+00	.0	1.70000+02	-1.00002+00	1.87722+00	.0
101	1.00000+00	1.80000+02	-1.00001+00	2.16965+00	.0	1.90000+02	-1.00002+00	1.87722+00	.0
101	1.00000+00	2.00000+02	-1.00003+00	1.20470+00	.0	2.10000+02	-1.00001+00	4.92311-01	.0
101	1.00000+00	2.20000+02	-1.00001+00	-2.07664-02	.0	2.30000+02	-1.00002+00	-1.15771-01	.0
101	1.00000+00	2.40000+02	-1.00002+00	3.14726-01	.0	2.50000+02	-1.00002+00	1.14209+00	.0
101	1.00000+00	2.60000+02	-1.00002+00	2.00699+00	.0	2.70000+02	-1.00001+00	2.38925+00	.0
101	1.00000+00	2.80000+02	-1.00002+00	2.00699+00	.0	2.90000+02	-1.00002+00	1.14210+00	.0
101	1.00000+00	3.00000+02	-1.00002+00	3.14727-01	.0	3.10000+02	-1.00002+00	-1.15771-01	.0
101	1.00000+00	3.20000+02	-1.00002+00	-2.07668-02	.0	3.30000+02	-1.00002+00	4.92311-01	.0
101	1.00000+00	3.40000+02	-1.00002+00	1.20470+00	.0	3.50000+02	-1.00002+00	1.87722+00	.0
101	2.00000+00	.0	-5.58641-01	2.25113-01	-1.03193-07	1.00000+01	-5.08474-01	2.19175-01	8.92768-02
101	2.00000+00	2.00000+01	-3.22810-01	2.28357-01	7.53823-02	3.00000+01	-5.55220-02	2.77907-01	2.12145-02
101	2.00000+00	4.00000+01	1.04826-01	3.29556-01	-2.18516-02	5.00000+01	7.00230-02	3.28963-01	-2.30723-02
101	2.00000+00	6.00000+01	-1.08895-01	2.81705-01	-2.80853-02	7.00000+01	-3.31603-01	2.39523-01	-5.01258-02
101	2.00000+00	8.00000+01	-4.84922-01	2.29345-01	-4.52527-02	9.00000+01	-5.31094-01	2.31504-01	2.15142-08
101	2.00000+00	1.00000+02	-4.84923-01	2.29345-01	4.52528-02	1.10000+02	-3.31602-01	2.39523-01	5.01258-02
101	2.00000+00	1.20000+02	-1.08896-01	2.81705-01	2.80853-02	1.30000+02	7.00227-02	3.28963-01	2.30721-02

Figure A-3. Sample NASTRAN Stress Output for the CDUM7 Element

APPENDIX B
INTERPRETATION OF OUTPUT

Figure B-1 gives an example of the output which permits the user to confirm that the hole element input was correct. Number of segments per side shows the entries in array $\lfloor NSEG \rfloor$, and number of intervals per segment shows the entries in array $\lfloor NINT \rfloor$. Number of terms with powers of $R > -2$ ($R < -2$) gives the values of I1, I2, I3, and I4 (J1, J2, J3, and J4) in Equation (63). For each symmetry condition, number of stress coefficients gives the correct number based on the minimum number of harmonics necessary to eliminate spurious rigid body motions; these numbers are determined by the program based on input of NSEG3 and values of I and J in Equation (63).

The material properties are described first by the values of E_x, E_y, ν_{xy}, and G_{xy}. The number of elastic constants, NEC, displays the number of independent constants; NEC=2 denotes an isotropic material. Constants C1, C2, C3, and C4 are the coefficients defined by Equation (39); and CBAR denotes the $\bar{C}$ defined in Equation (51).

The element geometry is described by the value of the hole radius, the L/R value (see Figure 17), and the plate thickness.

The quantities ISC1, ISC2, and ISC3 are used by the program to determine the symmetry conditions involved in the derivation of the hole element stiffness matrix; NLC denotes the number of load conditions used. In the present form of the program, which incorporates only the total element, ISC1, ISC2, ISC3, and NLC must have their default values of 1, 4, 1, and 4 respectively.

NBMAX is simply the largest element in the array of stress coefficients. MXLPN1 denotes the largest number of powers of ρ for all symmetry conditions; this is the maximum IJ1 in Equation (120). The values NBMAX and MXLPN1 are used for DIMENSION purposes in the program.

The displacement degrees of freedom are denoted as follows:

```
                                                SIDE  1      SIDE  2      SIDE  3
NUMBER OF SEGMENTS PER SIDE                       1              1              3
NUMBER OF INTERVALS PER SEGMENT                   2              2              2

                                                                SYMMETRY CONDITION
                                                SS             SA             AS             AA
NUMBER OF TERMS WITH POWERS OF R > -2             3              3              3              3
NUMBER OF TERMS WITH POWERS OF R < -2             3              3              3              3
NUMBER OF STRESS COEFFICIENTS                    16             10             10              8


ELASTIC CONSTANTS          EX =  .322498+07   EY =  .322498+07   NUXY =  .73500+00   GXY =  .547788+07   NEC = 4
                           C1 =  .19829-06    C2 =  .62893-06    C3 =  .00000        C4 =  .11159-06   CBAR =  .2070679E+00

ELEMENT GEOMETRY           HOLE RADIUS =  .10000+01      SQUARE SIDE LENGTH/HOLE DIAMETER =  4.0000      THICKNESS =  .10000+01

   ISC1 =  1     ISC2 =  4     ISC3 =  1     NUMBER OF LOAD CASES =  4        NBMAX = 16        NXLPN1 =  7

      NODOF =  8      NGHTOF =  4      NGFTOF =  4       NTTOF = 28


             JMAX = 14950

                                                BOUNDARY MATRIX FOR  5 INTEGRATION POINTS PER INTERVAL     NDOF =  8

      NUMBER OF INTERVALS PER OCTANT =  2      NUMBER OF INTEGRATION POINTS PER INTERVAL = 5
```

Figure B-1. Program Output Concerning the Hole Element

EQUILIBRIUM CHECK FOR FINAL STIFFNESS MATRIX

		X-EQUILIBRIUM	Y-EQUILIBRIUM	MOMENT EQUILIBRIUM
COLUMN	1	-.3314-008	-.7033-008	-.8021-007
COLUMN	2	-.7033-008	-.3314-008	.8021-007
COLUMN	3	.1760-008	.0000	.8109-007
COLUMN	4	.0000	-.3621-008	-.1998-017
COLUMN	5	-.3314-008	.7033-008	-.8021-007
COLUMN	6	.7033-008	-.3314-008	-.8021-007
COLUMN	7	-.3421-008	.4996-018	.4661-018
COLUMN	8	-.4218-018	.1760-008	.8109-007
COLUMN	9	-.3314-008	-.7033-008	.8021-007
COLUMN	10	-.7033-008	-.3314-008	-.8021-007
COLUMN	11	.1760-008	.4218-018	-.8109-007
COLUMN	12	.0000	-.3621-008	.4661-018
COLUMN	13	-.3314-008	.7033-008	.8021-007
COLUMN	14	.7033-008	-.3314-008	.8021-007
COLUMN	15	-.3621-008	-.3331-018	-.4661-018
COLUMN	16	.4218-018	.1760-008	-.8109-007
COLUMN	17	.6201-008	.0000	.0000
COLUMN	18	.2051-008	.2170-008	.9617-009
COLUMN	19	.2169-008	.2051-008	-.9617-009
COLUMN	20	.7633-019	.6201-008	.0000
COLUMN	21	-.2169-008	.2051-008	.9617-009
COLUMN	22	-.2051-008	.2170-008	-.9617-009
COLUMN	23	-.6201-008	-.1018-018	.0000
COLUMN	24	-.2051-008	-.2170-008	.9617-009
COLUMN	25	-.2169-008	-.2051-008	-.9617-009
COLUMN	26	.1781-018	-.6201-008	.0000
COLUMN	27	.2169-008	-.2051-008	.9617-009
COLUMN	28	.2051-008	-.2170-008	-.9617-009

Figure B-2. Equilibrium Check for Total Element Stiffness Matrix

NQDOF = number of degrees of freedom for the quadrant element

NQHDOF = number of degrees of freedom on the hole boundary of the quadrant

NQEDOF = number of degrees of freedom on the outer boundaries of the quadrant

NTDOF = number of degrees of freedom for the total element

When executing a NASTRAN solution, there is a certain amount of computer core available for the orthotropic hole element code. If the available space is sufficient, the value of JMAX will give the number of memory locations necessary to provide for all the arrays used in the hole program. If the available space is not sufficient, a message will appear which gives the minimum number of additional storage locations which must be made available through the NASTRAN HICORE specification (it is recommended that this minimum number be increased by at least 2000 to supply a margin of safety); in this case, program execution is terminated.

The remaining information shown in Figure B-1 consists of the number of Gaussian integration points per interval for the boundary integration (NIPB), number of integration intervals per volume octant (NIO), and number of integration points per interval for the volume integration (NIPV).

Figure B-2 gives a typical final equilibrium check for the stiffness matrix of the total orthotropic hole element. The values have been normalized with respect to the diagonal element in each column of the stiffness matrix.

Figures B-1 and B-2 give the minimum hole element output currently furnished to the user. However, much other output can be obtained if desired by exercising the WRITE options discussed in the description of the CDUM7 data card. These options are further described as follows:

ITOTRT > 0	will print the total stiffness matrix [K] in Equation (111) and the total stress matrices R[S^j], with [S^j] given in Equation (115);
IQDTRT > 0	will print the quadrant stiffness matrices [KQ^j] in Equation (100) and the quadrant stress matrices R[BQ^j], with [BQ^j] given in Equation (94);
ICOND > 0	will result in transformed stiffness and stress matrices for quadrant elements with traction free hole boundaries; output will consist of intermediate steps in the transformation, the final modified stress and stiffness matrices, and stresses on the hole boundary due to unit values of the nodal displacements on the outer boundaries of the element.
IACHK > 0	will print the arrays [A^j] in Equation (109);
IBNDRT > 0	will print the boundary work arrays [G^j] in Equation (93);
IVOLRT > 0	will print the volume work arrays [H^j] in Equation (92);
IHINVS > 0	will print the products [H^j] [H^j]$^{-1}$ and provide some check on the accuracy of the inverse of [H^j].

This completes the description of the output which is associated with the development of the hole element stiffness and stress matrices. Final output, consisting of stress coefficients and values of stress components at specified locations, is discussed in the description of the PDUM7 data card.

REFERENCES

1. Timoshenko, S.P. and Goodier, J.N., Theory of Elasticity, Third Edition, McGraw-Hill Book Company, New York, 1970.

2. Coker, E.G. and Filon, L.N.G., A Treatise on Photo-Elasticity, Second Edition, Cambridge University Press, London, 1957.

3. Bickley, W.G., "The Distribution of Stress Round a Circular Hole in a Plate," Philosophical Transactions of the Royal Society of London, Series A, Vol. 227, 1928, pp. 383-415.

4. Hong, C.S. and Crews, J.H., "Stress Concentration Factors for Finite Orthotropic Laminates with a Circular Hole and Uniaxial Loading," NASA TP1469, May 1979.

5. Lekhnitskii, S.G., Anisotropic Plates, Second Edition, Gordon and Breach, New York, 1968.

6. Peterson, R.E., Stress Concentration Design Factors, John Wiley and Sons, New York, 1953.

7. The NASTRAN Programmers Manual, Level 17.5, NASA SP-223(05), December, 1980.

8. Rao, A.K., Raju, I.S., and Krishna Murty, A.V., "A Powerful Hybrid Method in Finite Element Analysis," International Journal of Numerical Methods in Engineering, Vol. 3, 1971, pp. 389-403.

9. Orringer, O. and Stalk, G., "A Hybrid Finite Element for Stress Analysis of Fastener Details," Engineering Fracture Mechanics, Vol. 8, 1976, pp. 719-729.

10. Robinson, J., "Stress Elements with Holes," Computer Methods in Applied Mechanics and Engineering, Vol. 11, 1977, pp. 309-318.

1. Report No.	2. Government Accession No.	3. Recipient's Catalog No.
NASA CR-165759		

4. Title and Subtitle	5. Report Date
DEVELOPMENT OF AN ORTHOTROPIC HOLE ELEMENT	August 1981
	6. Performing Organization Code

7. Author(s)	8. Performing Organization Report No.
C.V. Smith, J.W. Markham, J.W. Kelley and K. Kathiresan	LG81ER0159
	10. Work Unit No.

9. Performing Organization Name and Address	11. Contract or Grant No.
Lockheed-Georgia Company 86 South Cobb Drive Marietta, Georgia 30063	NAS1-15840
	13. Type of Report and Period Covered
12. Sponsoring Agency Name and Address National Aeronautics and Space Administration Langley Research Center Hampton, Virginia 23665	Contractor Report
	14. Sponsoring Agency Code

15. Supplementary Notes

Langley technical monitor: John H. Crews, Jr.

16. Abstract

A finite element has been developed which adequately represents the state of stress in the region around a circular hole in orthotropic material experiencing reasonably general loading. This was achieved with a complementary virtual work formulation of the stiffness and stress matrices for a square element with center circular hole. The assumed stress state provides zero shearing stress on the hole boundary, so the element is suitable for problems involving load transfer without friction. The element has been implemented in the NASTRAN computer program, and sample problem results are presented.

17. Key Words (Suggested by Author(s))	18. Distribution Statement
Finite element Orthotropic materials Load transfer	Unclassified

19. Security Classif. (of this report)	20. Security Classif. (of this page)	21. No. of Pages	22. Price
Unclassified	Unclassified	137	